Membrane based separation of nitrogen, tetrafluoromethane and hexafluoropropylene

HERTZOG BISSETT

Membrane based separation of nitrogen, tetrafluoromethane and hexafluoropropylene

HERTZOG BISSETT

(B.Sc., M.Sc.)

12181471

Thesis submitted in fulfillment of the requirements for the degree

Philosophiae Doctor

in Chemistry

at the School of Physical and Chemical Sciences of the North-West University

Promoter:	Prof. H.M. Krieg
Co-promoter:	Dr. J.T. Nel

Potchefstroom

March 2012

Declaration by Candidate

I hereby declare that the thesis submitted for the degree Philosophiae Doctor in Chemistry, at the North-West University, is my own original work and has not yet been submitted to any other institution of higher education. I further declare that all sources cited or quoted are indicated and acknowledged by means of a comprehensive list of references.

Hertzog Bissett

_____

Date

DEDICATION

With God all things are possible

This thesis is dedicated to my beloved family and
all my friends for their endless love and support

LIST OF PUBLICATIONS

The content of this thesis is based on the following papers:

1. H. Bissett, H.M. Krieg, H.J.W.P. Neomagus, Adsorption of tetrafluoromethane and hexafluoropropylene on MFI zeolite, Journal of Chemical and Engineering Data, *under review*.

2. H. Bissett, H.M. Krieg, Synthesis of a composite inorganic membrane for the separation of nitrogen, tetrafluoromethane and hexafluoropropylene, Separation and Purification Technology, *submitted*.

3. H. Bissett, H.M. Krieg, Zeolite based membrane separation of nitrogen, tetrafluoromethane and hexafluoropropylene binary gas mixtures, Separation and Purification Technology, *to be submitted*.

SUMMARY

Pure fluorocarbon gases can be sold for up to 30 USD/kg, if they were manufactured locally. Due to the absence of local demand, South Africa at present has less than 0.3 % of the fluorochemical market and most fluoro-products used in the South African industry are currently imported. The depolymerisation of waste polytetrafluoroethylene (PTFE or Teflon) filters in a nitrogen plasma reactor results in the mixture of gases which includes N_2, CF_4 and C_3F_6. An existing challenge entails the separation of these gases, which is currently attained by an energy intensive cryogenic distillation process. Both the small energy requirements as well as the small process streams required, make a membrane separation an ideal alternative to the current distillation process. Based on our research groups existing expertise in the field of zeolite membranes, it was decided to investigate the separation capability of zeolite (MFI, NaA, NaY, and hydroxysodalite) coated tubular ceramic membranes for the separation of the above mentioned gases. The separation study was subdivided into adsorption studies as well as single and binary component studies.

C_xF_y gas adsorption on MFI zeolites. Tetrafluoromethane (CF_4) and hexafluoropropylene (C_3F_6) were adsorbed on zeolite ZSM-5 and silicalite-1 to help explain permeation results through zeolite membranes. According to the obtained data, the separation of CF_4 and C_3F_6 would be possible using adsorption differences. The highest ideal selectivities (~ 15) were observed at higher temperatures (373 K). While the CF_4 adsorption data did not fit any isotherm, the heat of adsorption for C_3F_6 adsorbed on ZSM-5 and silicalite-1 was calculated as -17 and -33 kJ/mol respectively.

Single gas permeation. A composite ceramic membrane consisting of a ceramic support structure, a MFI intermediate zeolite layer and a Teflon AF 2400 top layer was developed for the separation of N_2, CF_4 and C_3F_6. The adsorption properties of the Teflon AF 2400 sealing layer was investigated. A theoretical selectivity, in terms of the molar amount of gas adsorbed, of 26 in favour of the C_3F_6 *vs* CF_4 was calculated, while the N_2 adsorption remained below the detection limit of the instrument. While the ideal N_2/CF_4 and N_2/C_3F_6 selectivities for the MFI coated support were either near or below Knudsen, it was 5 and 8 respectively for the Teflon coated support. Ideal selectivities improved to 86 and 71 for N_2/CF_4 and N_2/C_3F_6 when using the composite ceramic

membrane, while CF_4/C_3F_6 ideal selectivities ranged from 0.9 to 2, with C_3F_6 permeating faster though the composite ceramic membrane.

Zeolite based membrane separation. Inorganic membranes (α-alumina support, NaA, NaY, hydroxysodalite, MFI) and composite membranes (Teflon layered ceramic and composite ceramic membrane) were synthesized and characterized using the non-condensable gases N_2, CF_4 and C_3F_6. For the inorganic membranes either near or below Knudsen selectivities were obtained during single gas studies, while higher selectivities were obtained for the composite membranes. Subsequently, the MFI, hydroxysodalite and both composite membranes were chosen for binary mixture separation studies. The membranes exhibited binary mixture permeances in the order Teflon layered ceramic > hydroxysodalite > MFI > composite ceramic, which was comparable to the single gas permeation results. The highest separation for N_2/CF_4 (4) and N_2/C_3F_6 (2.4) was obtained with the composite ceramic membrane indicating that the Teflon layer was effective in sealing non-zeolitic pore in the intermediate zeolite layer.

The aim of this project was met successfully by investigating a method of fluorocarbon gas separation by zeolite based membranes using various inorganic and composite membranes with single and binary mixtures.

Keywords: Nitrogen, tetrafluoromethane, hexafluoropropylene, membrane separation, zeolite, AF 2400

OPSOMMING

Suiwer fluoorkoolstof gasse kan vir tot 30 VSD/kg verkoop indien dit plaaslik vervaardig sou word. Weens die afwesigheid van die plaaslike aanvraag verteenwoordig Suid-Afrika op die oomblik minder as 0.3% van die fluoor-chemiese mark en die meeste fluoor-produkte wat gebruik word in die Suid-Afrikaanse bedryf word tans ingevoer. Die depolimerisasie van afval politetrafluooretileen (PTFE of Teflon) filters in 'n stikstof plasmareaktor produseer 'n mengsel van gasse wat insluit N_2, CF_4 en C_3F_6. 'n Bestaande uitdaging behels die skeiding van hierdie gasse, wat tans deur 'n energie-intensiewe kriogene distillasie proses bewerkstellig word. Beide die klein energie vereistes, sowel as die klein proses strome wat nodig word, maak 'n membraanskeiding' n ideale alternatief vir die huidige distillasie proses. Gebaseer op ons navorsingsgroepe se bestaande kundigheid in die gebied van die seoliet membrane, is daar besluit om die skeidingsvermoë van seoliet (MFI, NaA, NaY, en hidroksiesodaliet) bedekte buisvormige keramiekmembrane vir die skeiding van die bogenoemde gasse te ondersoek. Die skeidingstudie is onderverdeel in adsorpsie studies sowel as enkel-en binêre komponent studies.

C_xF_y gas adsorpsie op MFI seoliete. Tetrafluoormetaan (CF_4) and hexafluoorpropeen (C_3F_6) is geadsorbeer op seoliet ZSM-5 en silikaliet-1 om resultate wat met die seoliet membrane verkry is, te verduidelik. Volgens die data sou die skeiding van CF_4 en C_3F_6 moontlik wees deur gebruikmakend van die adsorpsieverskille. Die hoogste ideale selektiwiteite (~ 15) is verkry by hoër temperature (373 K). Terwyl geen isoterm op die CF_4 adsorpsie data gepas kon word nie, was die berekende hitte van adsorpsie van C_3F_6 op ZSM-5 en silikaliet-1 onderskeidelik -17 en -33 kJ/mol.

Enkel gas permeasie. 'n Saamgestelde keramiekmembraan, bestaande uit 'n keramiek ondersteuningstruktuur, 'n MFI intermediêre seolietlaag en 'n Teflon AF 2400 bo-laag, is ontwikkel vir die skeiding van N_2, CF_4 en C_3F_6. Die adsorpsie eienskappe van die Teflon AF 2400 laag is ondersoek. 'n Teoretiese selektiwiteit, in terme van die molêre hoeveelheid gas geadsorbeer, van 26 ten gunste van die C_3F_6 teenoor CF_4 is bereken, terwyl die N_2 adsorpsie onder die deteksielimiet van die instrument gebly het. Terwyl

die ideale N_2/CF_4 en N_2/C_3F_6 selektiwiteite vir die MFI bedekte ondersteuners óf naby of onder die Knudsenselektiwiteit was, was dit 5 en 8 onderskeidelik vir die Teflon bedekte ondersteuner. Ideale selektiwiteite verbeter tot 86 en 71 vir N_2/CF_4 en N_2/C_3F_6 by die gebruik van die saamgestelde keramiekmembraan, terwyl die CF_4/C_3F_6 ideale selektiwiteite gewissel het tussen 0.9-2 ten gunste van C_3F_6.

Seoliet gebaseerde membraanskeiding. Anorganiese membrane (α-alumina ondersteuner, NaA, NaY, hidroksiesodaliet, MFI) en saamgestelde membrane (Teflon bedekte keramiek en saamgestelde keramiekmembraan) is gesintetiseer en gekarakteriseer met behulp van die nie-kondenseerbare gasse N_2, CF_4 en C_3F_6. Vir die anorganiese membrane was óf naby of onder Knudsenselektiwiteite tydens enkelgasstudies verkry, terwyl hoër selektiwiteite vir die saamgestelde membrane verkry is. Voorts is die MFI, hidroksisodaliet en beide saamgestelde membrane vir binêre mengsel skeidingstudies geselekteer.

Die membrane het binêre mengselpermeasies in die volgorde Teflon bedekte keramiek > hidroksiesodaliet > MFI > saamgestelde keramiek getoon, wat vergelykbaar is met die enkelgas permeasieresultate. Die hoogste skeiding vir N_2/CF_4 (4) en N_2/C_3F_6 (2.4) is met die saamgestelde keramiek membraan verkry wat daarop dui dat die Teflon laag effektief in die verseëling van nie-seoliet porieë in die intermediêre seolietlaag was.

Die doel van die projek is suksesvol bereik deur skeiding van C_xF_y gasse deur seoliet gebaseerde membrane met behulp van verskeie anorganiese en saamgestelde membrane met enkel- en binêre mengsels te illustreer.

Sleutelterme: Stikstof, tetrafluoormetaan, hexafluoropropylene, membrane separation, zeolite, AF 2400

TABLE OF CONTENTS

CHAPTER 1

INTRODUCTION

SUMMARY

Fluorocarbon gases have become important due to the phase-out of CFCs. Waste polytetrafluoroethylene (PTFE or Teflon) filters is an inexpensive source of fluorocarbon gases. The depolymerisation of the Teflon filters in a nitrogen plasma reactor results in a mixture of gases which includes N_2, CF_4 and C_3F_6. Purification of these gases can be achieved by means of composite zeolite based inorganic membranes which is an attractive alternative to the energy intensive cryogenic distillation process generally used for separation of fluorocarbon gases.

This chapter presents a basic overview of fundamental information on zeolites and zeolite membranes. A layout is given on the subjects investigated in this thesis including the adsorption of fluorocarbon gases on MFI zeolites, composite inorganic membrane synthesis and fluorocarbon gas mixture separation.

1.1 Introduction

1.1.1 BACKGROUND

Fluorocarbon gases are used in various sectors of industry. Tetrafluoromethane (CF_4) for example is used as a refrigerant coolant as a CFC alternative, whilst tetrafluoroethylene (C_2F_4) monomers are used for the synthesis of polymers and copolymers. Fluorocarbon (C_xF_y) gases are also applied in the manufacture of electronic gases and used in etching, solvent cleaning and fire extinguishers.[1] The industrially and thermodynamically most favourable method of producing C_xF_y gases is to first make HF, by reacting fluorspar (CaF_2) with H_2SO_4 and then producing fluorine by the electrolysis of the HF in a KF•HF electrolyte. The subsequent fluorination of carbon and/or hydrocarbons, results in the formation of the desired fluorocarbon gases.[2] The disadvantage of this process however is that hydrofluoric acid is used, which is extremely dangerous.[3] The depolymerisation of waste polytetrafluoroethylene (PTFE or Teflon) filters can be an inexpensive source of fluorocarbon gases. High temperature depolymerisation of PTFE results in a range of fluorocarbon gas species which is determined by the material feed rate, the reactor temperature, the reactor pressure and the rate at which the gas phase is cooled. Using a reactor with a nitrogen plasma torch as heating source, a range of gases can be synthesised which includes nitrogen, tetrafluoromethane (CF_4) and hexafluoropropylene (C_3F_6).

Separation is an integral part of any synthesis process. Products have to be separated from reagents or solvents after the synthesis process, whilst the separation of products from one another in most instances determines the purity and consequently the market price of a product. High purity gases for instance, are essential for the effective synthesis of target polymers. If the reagent purity is not adequate, the polymer synthesis can become difficult or even impossible. For gas separation of compounds, polymeric membranes are currently widely applied. For these polymeric membranes however, a trade-off exists between permeability and selectivity, with an “upper-bound” of separation performance. Inorganic membranes such as zeolites, are thermally, chemically and mechanically more stable and have been shown to exceed the

"upper-bound" performance of polymeric membranes.[4] Zeolite technology is a rapidly expanding sector of separation science, for which the most widely applied method of separation currently is adsorption. Zeolite membranes specifically, due to their unique crystallographic and physical properties, have the potential of separating mixtures that are traditionally difficult and expensive to separate.[5]

The most effective way of synthesizing a zeolite membrane, is to grow a continuous layer of zeolite crystals onto a ceramic support structure, such as α-alumina.[6] The support structure provides the mechanical stability for the thin zeolitic separation layer. A smooth support surface is required for synthesis of a thin, continuous zeolite to ensure both high permeabilities and selectivities. For gas separation, the use of inorganic membranes is hindered by the lack in technology to manufacture continuous and defect-free membranes.[7] The use of zeolites to date mostly still involves the separation of condensable gases due to the low selectivities experienced with non-condensable gas mixtures.[8,9] It has been shown that the presence of intercrystalline boundaries between zeolite crystals is pronounced by the Al-Al interactions of neighbouring crystals.[10] The intercrystalline boundaries as well as thermal cracks, as a result of template removal, are responsible for low separation selectivities experienced with non-condensable gases.[11] Avoiding the formation of defects or applying "defect repair" is required to increase selectivities. By applying a "sealing layer" onto the zeolite layer, the defects can be covered, resulting in increased gas separation factors.

1.1.2 ZEOLITE MEMBRANES

A zeolite crystal framework consists of alternating SiO_4 and AlO_4 tetrahedra. Depending on the amount of alumina present in the zeolite structure (Si/Al ratio), the hydrophilic/hydrophobic properties will differ, with the lowest Si/Al ratio equalling 1 (most hydrophilic), increasing to a Si/Al ratio approaching infinity (most hydrophobic). The synthesis method, template molecules used and Si/Al ratio exhibit different accessible aperture sizes to the three-dimensional pore network. The International Zeolite

Association (I.Z.A) assigned a three letter identification to each zeolite type with a specific structure (e.g. LTA, MFI, FAU) which can also differ according to chemical composition. For example silicalite-1 and ZSM-5 are both MFI type zeolites, but silicalite-1 is a pure siliceous framework (contains Si only) and ZSM-5 is an aluminosilicate framework (contains Si and Al). Zeolites can be divided into three general categories according to pore size. These are small, medium and large. The small size zeolites consist of 8-membered oxygen ring structures, such as LTA zeolites, with pore sizes in the range of 4 Å. An example of medium size zeolites is MFI, which has a 10-membered oxygen ring structure, with an aperture size of approximately 5.3 Å. The largest zeolite structures contain 12 oxygen atoms in the ring structure, for example NaY zeolite which has a pore size of 7.4 Å.[8]

The choice of the zeolite depends on the specific application. NaA zeolite for instance is ideally suited for the dehydration of water/organic mixtures due to the hydrophilic nature of the zeolite.[12] The charge on the individual zeolite crystals limits the use of these membranes in gas separation, due to the non-zeolitic (intercrystalline) pore regions present in the membrane structure.[10] For this reason the use of hydrophobic zeolites such as silicalite-1 (Si/Al ≈ infinity) are preferred, because the charge on the individual crystals is neutral. As a result the intergrowth of individual crystals has smaller intercrystalline regions. The support required for mechanical stability of a zeolite membrane can also influence the Si/Al ratio. Using α-alumina as a support membrane for example can result in alumina leaching into the zeolite structure during synthesis. For this reason even a zeolite such as silicalite-1 grown onto a ceramic support contains some alumina within its structure.

Methods to decrease the intercrystalline boundaries, such as advanced intergrowth synthesis of crystals,[11] repeated synthesis, post synthesis coking treatment,[13] chemical vapor deposition, and template-free synthesis[14] have been employed to decrease the effect of intercrystalline boundaries on selectivity. In many studies, the addition of a sealing layer, with a high permeability to plug imperfections, has been used to enhance selectivity, usually for polymeric membranes.[7]

1.2 Justification

Despite the industrial widespread application of the conventional fluorocarbon synthesis process, it remains a dangerous, complicated and expensive method. Another source of fluorocarbon gases which can be considered is waste PTFE. Depolymerization of waste PTFE in a nitrogen plasma torch results in the formation of a range of fluorocarbon gases depending on the reactor conditions such as pressure and temperature. The most important fluorocarbon gases produced from this method are nitrogen (N_2), tetrafluoromethane (CF_4), tetrafluoroethane (C_2F_4) hexafluoropropylene (C_3F_6) and cyclic-octafluorobuthane (c-C_4F_8). Since various products are likely to form, a separation of the gases is required. In this study on the separation of N_2, CF_4 and C_3F_6 would be considered. For this purpose, inorganic membranes, in particular zeolite membranes, can be used. The lack of adsorption data of fluorocarbon gases such as hexafluoropropylene (C_3F_6) on zeolites, requires an initial adsorption study to determine possible interactions between the gases and the membranes used in this study. The data can be used to help explain the separation capabilities of the various inorganic membranes. This study envisages addressing these requirements.

1.2.1 Adsorption of Nitrogen, Tetrafluoromethane and Hexafluoropropylene on zeolites

Data on the adsorption of fluorocarbon gases on zeolites is limited to CF_4 gas. As stated earlier it is likely that the plasma synthesis will result in the formation of various C_xF_y gases. At the South African Nuclear Energy Corporation (Necsa), it has become necessary to investigate the separation of nitrogen and various fluorocarbon gases including, CF_4, C_2F_4, C_2F_6, C_3F_6, and c-C_4F_8 which are formed during the depolymerization of polytetrafluoroethylene (PTFE). The presence of nitrogen is due to reactor preparation or plasma torch operation. For this study N_2, CF_4 and C_3F_6 were chosen as sample molecules. The absorption data of N_2, CF_4, and C_3F_6 on MFI zeolite

(silicalite-1 and ZSM-5) can be used to explain tendencies during membrane separation. The silicalite-1 was synthesized in-house and the ZSM-5 was purchased.

1.2.2 COMPOSITE INORGANIC MEMBRANE SYNTHESIS

The synthesis of an inorganic membrane was investigated for the separation of the gases. For the separation study the focus was on N_2, CF_4, and C_3F_6. For the initial characterization of inorganic membranes, single gas permeation studies of the ceramic support membrane and the various zeolite membranes (hydroxysodalite, NaA, NaY, and silicalite-1) was done. The obtained selectivities of the membranes could then be further enhanced by repairing defects, for example by applying a "sealing" layer, such as Teflon AF 2400 onto the zeolite layer. To help understand the separation of the composite ceramic membrane (zeolite membrane with Teflon AF 2400 layer) a single gas permeation study of both a Teflon® coated ceramic and the composite ceramic membrane was also conducted. Adsorption of the various gases onto the Teflon AF 2400 was subsequently included as part of the adsorption study. The Teflon AF 2400 was obtained from DuPont.

1.2.3 GAS MIXTURE SEPARATION

Once inorganic membranes with high single gas selectivities had been identified, the membranes were further characterized using binary gas permeation studies. Although single gas permeation studies are suitable to obtain some indication of membrane performance, mixture separations are however the only actual means of evaluating the efficiency of a membrane for a specific purpose.

1.3 Aim and Objectives

The aim of this study was to evaluate the separations of nitrogen and the fluorocarbons tetrafluoromethane (CF_4) and hexafluoropropylene (C_3F_6) using inorganic based composite membranes. The objectives of this study therefore were to:

- determine the adsorption of N_2, CF_4, and C_3F_6 onto MFI zeolites and fitting the data to suitable isotherms
- synthesize inorganic, as well as polymer coated inorganic membranes, for the separation of N_2, CF_4, and C_3F_6
- characterize various inorganic membranes according to single and binary mixture separation studies.

1.4 Outline of the Thesis

The various sections of the thesis are presented in article format. Chapters 2-4 are prepared in standard scientific format presenting specific subjects. The general layout of the thesis was structured as shown in Figure 1.1.

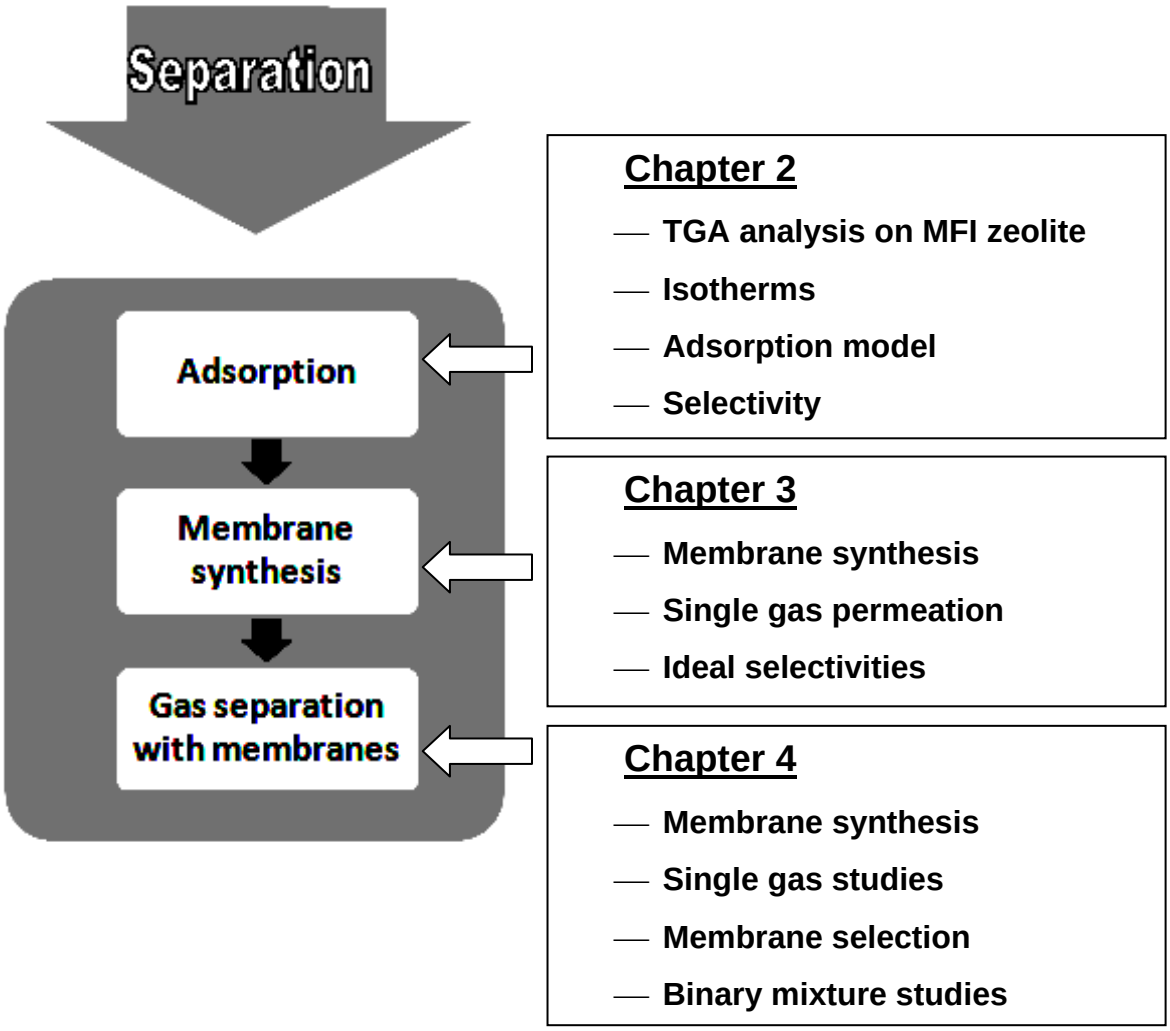

Figure 1.1 Basic layout of the study

Although CF_4, C_2F_6 C_3F_6 and c-C_4F_8 is formed in the plasma reactor during Teflon® (PTFE) depolymerization[15], CF_4 and C_3F_6 was chosen as the model molecules, due to the significant importance Necsa, who funded this project, attaches to the separation of

N_2, CF_4, C_3F_6 and c-C_4F_8 which are regarded as contaminants during the polymerization of C_2F_4 for PTFE synthesis. However, as mentioned previously, working with C_2F_4 is dangerous due to its explosive properties in the presence of oxygen, whilst the condensability of c-C_4F_8 makes a study with this gas difficult at moderate temperatures and higher pressures.

The separation study was initiated by determining the adsorption of N_2, CF_4, and C_3F_6 adsorption on ZSM-5 and silicalite-1 zeolites gravimetrically from 303 to 423 K, using various partial pressures of the adsorbed gas (**Chapter 2**). The Langmuir model was fitted to the experimental isotherm in order to determine the model parameter for sorption. Theoretical selectivity's were calculated to evaluate the possible separation of the gases by these zeolites.

Chapter 3 presents a study in which a composite zeolite membrane for the separation of N_2, CF_4, and C_3F_6 gases was synthesized. An α-alumina support was coated with an MFI intermediate layer and Teflon AF 2400 polymeric layer to manufacture the composite inorganic-polymer membrane. The composite inorganic-polymer membrane, α-alumina support, MFI zeolite membrane and a Teflon® layered alumina support were characterized according to single gas permeabilities and ideal selectivities were calculated. For the composite inorganic-polymer membrane, a significant selectivity improvement was observed, compared to the other membranes.

In **Chapter 4** the selectivity and permeance of the composite inorganic-polymer membrane (composite ceramic membrane) was compared to various inorganic membranes (α-alumina support, NaA, NaY, hydroxysodalite, MFI) and a Teflon® layered ceramic membrane using binary mixture permeation studies. The composite ceramic membrane compared favourably when ideal selectivities and mixture separations were investigated.

1.5 References

[1] The Economics of Fluorspar, 10th Edition, Rosskill Information Services Ltd., London (2009).

[2] I.N. Toumanov, Plasma and High Frequency Processes for Obtaining and Processing Materials in the Nuclear Fuel Cycle, Nova Science Publishers, Inc, New York, (2003), Chapter 8, p. 321.

[3] B.A. Kennedy, Surface Mining, 2nd Edition, Port City Press, Inc., Baltimore, Maryland, (1990) p. 163.

[4] A. Singh, W.J. Koros, Significance of entropic selectivity for advanced gas separation membranes, Industrial and Engineering Chemistry Research, 35, (1996) 1231.

[5] T.C. Bowen, R.D. Noble, J.L. Falconer, Fundamentals and applications of pervaporation through zeolite membranes, Journal of Membrane Science, 245, (2004) 1.

[6] M. Noack, J. Caro, Zeolite membranes, in F.Schüth. K.S.W. Sing, J. Weitkamp (Eds.), Handbook of Porous Solids, Vol. 4, Wiley-VCH, Weinheim, (2002) pp. 2433-2507.

[7] T. Chung, L.Y Jiang, Y. Li, S. Kulprathipanja, Mixed matrix membranes (MMMs) comprising organic polymers with dispersed inorganic fillers for gas separation, Progress in Polymer Science, 32, (2007) 483.

[8] S. Nair, M. Tsapatsis, Synthesis and properties of zeolitic membranes, in S.M. Auerbach, K.A. Carrado, P.K. Dutta (Eds.), Handbook of Zeolite Science and Technology, Marcel Dekker Inc., New York, Basel, (2003) pp. 867-919.

[9] A. van Niekerk, J. Zah, J.C. Breytenbach, H.M. Krieg, Direct crystallisation of a hydroxysodalite membrane without seeding using a conventional oven, Journal of Membrane Science, 300, (2007) 156.

[10] T. Sano, S. Ejiri, K. Yamada, Y. Kawakami, H. Yanagishita, Separation of acetic acid-water mixtures by pervaporation through silicalite membranes, Journal of Membrane Science, 123, (1997) 225.

[11] M. Noack, P. Kölsch, A. Dittmar, M. Stöhr, G. Georgi, R. Eckelt, J. Caro, Effect of crystal intergrowth supporting substance (ISS) on the permeation properties of MFI membranes with enhanced Al-content, Microporous and Mesoporous Materials, 97, (2006) 88.

[12] S. Furukawa, K. Goda, Y. Zhang, T. Nitta, Molecular simulation study on adsorption and diffusion behaviour of ethanol/water molecules in NaA zeolite crystal, Journal of Chemical Engineering of Japan, 37, (2004) 67.

[13] Y. Yan, M.E. Davis, G.R. Gavalas, Preparation of highly selective zeolite ZSM-5 membranes by a post-synthetic coking treatment, Journal of Membrane Science, 123, (1997) 95.

[14] M. Kanezashi, J. O'Brien, Y.S. Lin, Template-free synthesis of MFI-type zeolite membranes: Permeation characteristics and thermal stability improvement of membrane structure, Journal of Membrane Science, 286, (2006) 213.

[15] I.J. van der Walt, O.S.L. Briunsma, Depolymerization of clean unfilled PTFE waste in a continuous process, Journal of Applied Polymer Science, 102, (2006), 2752

CHAPTER 2

ADSORPTION OF TETRAFLUOROMETHANE AND HEXAFLUOROPROPYLENE ON MFI ZEOLITE

ABSTRACT

Adsorption data for the adsorption of tetrafluoromethane (CF_4) and hexafluoropropylene (C_3F_6) on ZSM-5 and silicalite-1 zeolite was obtained from temperatures ranging from 303 to 423 K by using a gravimetric method. The data was fitted to the Langmuir model to determine the model parameters for sorption. Theoretical ideal selectivities for separation of a binary mixture were calculated. Larger molar quantities of C_3F_6 than CF_4 adsorbed on ZSM-5 and silicalite-1. The CF_4 data did not fit the Langmuir isotherm. The heat of adsorption for C_3F_6 on ZSM-5 and silicalite-1 was -17 and -33 kJ/mol respectively. The highest ideal selectivities for separation of a binary gas mixture would be obtained at higher temperatures.

Keywords: CF_4, C_3F_6, ZSM-5, silicalite-1, zeolite, adsorption

2.1 Introduction

The use of zeolite technology as a separation technique is a rapidly expanding sector in industry and scientific research. Zeolites are microporous materials, possessing a network of pores with sizes in the order of nanometers. Unlike other microporous materials which can span a wide distribution of pore sizes; crystalline zeolites exhibit unique pore sizes for specific zeolite types. These distinct properties of zeolites offer an alternative to some of the current large-scale reaction and separation processes for gaseous and liquid mixtures. By tailoring the zeolite pore size and structure, control over reactions occurring in the pore interior can be achieved.[1,2] Current industrial separations involving zeolites are mainly performed by temperature swing adsorption using the zeolite in bulk forms such as granules, beads and pellets. Although this technique is an unsteady-state process, it enables large scale separation of gases.[3]

The development of new technologies depends largely on the production of chemicals of high purity and low cost, whilst limiting the impact of industrial activities on the surrounding environment. The depolymerisation of waste polytetrafluoroethylene (PTFE) at temperature from 873-1173 K at pressures between 5 and 80 kPa results in the formation of various C_xF_y product gases which have to be separated in order to isolate the monomers from which downstream fluoropolymers can also be manufactured.[4]

Pure fluorocarbon gases are stable and currently used in various industries. For example, tetrafluoromethane (CF_4) and hexafluoropropylene (C_3F_6) are used as low temperature refrigerants. In addition, CF_4 is used in the plasma etching of electronic microprocessors, while C_3F_6 is applied to surfaces to enhance the hydrophobic properties of the surface.[5] Currently cryogenic distillation is the most widely used technique to separate C_xF_y products. Cryogenic distillation is however an energy intensive process,[6] which makes exploring other separation techniques, such as adsorption, an attractive alternative.

This study focuses on the adsorption of CF_4 and C_3F_6 gas onto two MFI zeolite types namely silicalite-1 and ZSM-5. Measurements were performed at temperatures ranging from 303 to 423 K. The adsorption isotherms were obtained by gravimetry, using various partial pressures of the adsorbed gas. The Langmuir model was fitted to the experimental isotherm in order to determine the model parameter for sorption. Theoretical selectivities were calculated to evaluate the possible separation of the gases by these zeolites.

2.2 Experimental

2.2.1 MATERIALS

The adsorbents used were silicalite-1 and ZSM-5. The ZSM-5 was supplied by Süd-chemie SA (Pty) Ltd. and the silicalite-1 was synthesized in-house. For the silicalite-1, a zeolite precursor solution was prepared containing water, tetrapropylammonium hydroxide (TPAOH) and tetrapropylammonium bromide (TPABr). The precursor solution was aged for 10 min and then added drop-wise to a bottle containing tetraethylortosilicate (TEOS) under continuous stirring. The composition of the precursor and TEOS solutions are given in Table 2.1.

Table 2.1 Reactant mixture compositions for the MFI clear solution synthesis

Reactant mixture	TPAOH[a] (g)	TPABr[b](g)	TEOS (g)	H_2O (g)
Precursor solution	9.052	2.208	-	28.040
Silicate source	-	-	2.912	-

[a]TPAOH 20%, Fluka [b]TPABr 99%, Merck [c]TEOS 99%, Aldrich

The clear solution was aged for 1 h at 358 K and for a further hour at room temperature. A volume of 15 ml clear solution was poured into an autoclave and the reaction unit was sealed. Hydrothermal treatment was performed in a

preheated oven at a temperature of 443 K for 30 h, while the autoclave was rotated around the horizontal axis. Cooling of the reactor vessel under running water was commenced after the synthesis was completed.

The ZSM-5 had a Si/Al ratio of 90:1, while the molar oxide composition of the silicalite-1 crystals used in these experiments was as follows: 123 TPA : 100 SiO_2 : 63.7 OH : 14 200 H_2O. Topological features and average crystal size were investigated by scanning electron microscopy (SEM) with a FEI ESEM Quanta 200, OXFORD INCA 200 EDS SYSTEM. For SEM analysis, the dried samples were coated with Au/Pd (80/20). BET (Micrometric's ASAP 2010 system) analysis with nitrogen gas was used to determine the surface area and total pore volume. Nitrogen adsorption was performed at 77 K with 5 s equilibration intervals. Data was collected in a relative pressure (p/p_0) range of 0.03 to 0.99.

2.2.2 SORPTION STUDY BY GRAVIMETRIC ANALYSIS

2.2.2.1 GRAVIMETRIC APPARATUS

A TA Instrument TG was used for the thermal gravimetric analysis (TGA). Data was captured using a Compaq 800 MHz, 128 MB RAM with Microsoft Windows NT 4.0 as running platform. A zeolite sample 10-15 mg was weighed and placed in the sample cup and left for 24 h in the furnace at a temperature of 473 K in a helium flow of 50 ml/min to remove impurities. The oven temperature was controlled and recorded by a relayed controlled thermocouple (TC; Shinka GCS-300).

The sample was then cooled under helium to room temperature, and then set to the experimental temperature. A pre-determined mixture of helium and adsorbate gas was fed to the TGA instrument using mass flow controllers (MFC; Brooks Instruments B.V., Model 5850S) with the total gas flow rate equal to 50 ml/min. The weight of the sample was recorded until equilibrium was reached.

Subsequently, the composition of the gas mixture was adapted in order to measure the full isotherm in the 0-85 kPa range. Adsorption isotherms from 313 to 373 K and 303 to 423 K were recorded for CF_4 and C_3F_6 respectively.

2.2.2.2 ADSORPTION MODEL

When the design of an adsorber is considered, the equilibrium of adsorption is critical information that has to be obtained. To understand the process and accurately predict the separation of gas mixtures,[7] the interpretation and quantification of adsorption equilibrium isotherms is required. One method used to determine adsorption is gravimetry, where a sample is continuously weighed on a micro-balance. The increase in sample weight at various conditions is an indication of the amount of gas adsorbed. Once the free gas and the adsorbed gas are in equilibrium, the fractional coverage of the surface is dependent on the pressure of the free gas. This variation of surface coverage with pressure is described by the adsorption isotherm.

Various models can be applied to determine the adsorption parameters. The Langmuir model is one of the most frequently used and Equation 2.1 can be used to determine the isotherm by solving θ (-), where p is the partial pressure of the sorbate (10^2kPa), with rate constants k_a for adsorption and k_d for desorption (mol/kg.s^{-1}).

$$\theta = \frac{Kp}{1+Kp}, \text{where} \quad K = \frac{k_a}{k_d} \tag{2.1}$$

The adsorption isotherm can also be expressed by Equation 2.2,

$$\theta = \frac{q}{q_m} \tag{2.2}$$

where q is the amount absorbed (g/g$_{ads}$) and q_m is the maximum loading that can occur when complete coverage of the adsorbed gas takes place (g/g$_{ads}$).[8] The Langmuir model however excludes possible interactions between adsorbed

molecules. Martinez *et al.*[9] proposed a modified Langmuir isotherm taking adsorbate size, chemical dissociation and molecular interactions into account. The isotherm is given in Equation (2.3):

$$K_{eq} exp(\frac{nu\theta}{kT}) = \frac{1}{p}\frac{\theta^s}{(1-\theta)^n} \quad (2.3)$$

where s represents the dissociation parameter (-), K_{eq} an equilibrium constant (10^2kPa^{-1}), u is the interaction energy between the adsorbed molecules (J), k the Boltzmann constant (J/K), n the amount of active sites occupied by a single molecule (-) and T is the temperature (K). The equilibrium constant $K_{eq} = k_\infty exp(-\Delta H_{ads}/RT)$, with k_∞ a pre-exponential factor (g/g$_{ads}$·10^2kPa), R the universal gas constant (J/mol.K), T the temperature (K) and ΔH the heat of adsorption (J/mol). Equation 2.3 reduces to Equation 2.1 when there are no dissociation (s = 1), no interactions (u = 0) and a molecule occupies only one active site when it adsorbs (n = 1).

Experimental adsorption data of the CF_4 and C_3F_6 onto ZSM-5 and silicalite-1 zeolite was modelled using the modified Langmuir model given in Equation 2.3, based on the dynamic equilibrium between adsorbed and gas-phase species. In this study dissociation and interaction of molecules was ignored (thus s = 1 and u = 0). The model thus reduces to:

$$k_i e\left(\frac{-\Delta H_{abs}}{RT}\right) = \frac{1}{P_{C_xF_y}}\frac{\theta}{(1-\theta)^n} \quad (2.4)$$

where k_i is a pre-exponential factor (g/g$_{abs}$.10^2kPa), θ is equal to q/q_m and P_{CxFy} is the partial pressure of the gas adsorbed (10^2kPa). The maximum gas adsorption possible (q_m) was obtained by extrapolating the experimental data for each temperature. This approach differs from Silva and Rodriques,[7] but is consistent with the more recent paper of Ahn *et al.*[10] The best Langmuir model fit for each temperature and gas/zeolite system was used to obtain the k_o and n values. In all circumstances it was assumed that n was equal or larger than 1. The heat of adsorption was calculated using the following equation:

$$lnk_i = lnk_0 - \frac{\Delta H}{RT} \quad (2.5)$$

By fitting ln k_i against 1/T, the slope and intercept obtained is equal to $-\Delta H/R$ and ln k_0 respectively.

2.3 Results and Discussion

2.3.1 MATERIALS

Figures 2.1a and 2.1b shows the SEM images of silicalite-1 and ZSM-5 respectively, while the physical properties are listed in Table 2.2. No amorphous material was present in both zeolites according to the SEM images. The average crystal size of the silicalite-1 was 3-4 μm, while the average crystal size of the ZSM-5 was 2 μm. The surface area and pore volume presented in Table 2.2 were obtained with BET analysis, while the mean pore size was obtained from literature. The specific surface area for both zeolites is in a similar range than those obtained in literature. The contribution of the external surface to the total surface of the zeolite is minimal.[11] The slight differences in the surface area and the pore volume are due to the difference in crystal size and synthesis method of the zeolites. Although the Si/Al ratio of silicalite-1 and ZSM-5 differ, both have a similar structure. The mean pore size indicated in Table 2.2 is the diameter for MFI type zeolites as indicated by literature.[12]

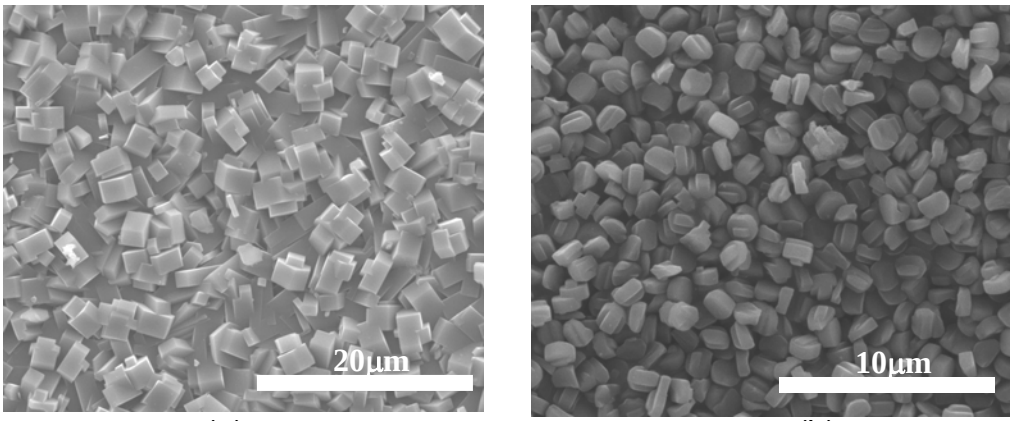

(a) (b)

Figure 2.1 SEM images of the (a) silicalite-1 and (b) ZSM-5.

Table 2.2 Physical properties of the Adsorbents

Adsorbents	BET surface area (m^2/g)	Total pore volume (cm^3/g)	Mean pore size (Å)
Silicalite-1	343.6	0.379	5.5
ZSM-5	347.5	0.342	5.5

2.3.2 SORPTION STUDY BY GRAVIMETRIC ANALYSIS

The adsorption isotherms of the CF_4 gas on ZSM-5 and silicalite-1 were measured at 313, 333, 353, and 373 K, while the adsorption isotherms of the C_3F_6 gas on ZSM-5 and silicalite-1 were measured at 303, 313, 333, 353, 373, and 423 K at relative pressures ranging from 0-85 kPa. Tables 2.3 to 2.6 list the data obtained. The experimental data are represented graphically in Figure 2.2 and 2.3 for the silicalite-1 and ZSM-5 respectively. The marks and lines indicate experimental data and fitting of the data to the modified Langmuir isotherm, respectively. Note the difference in the scale for Figure 2.2a and Figure 2.2b, as well as the scale for Figure 2.3a compared to Figure 2.3b.

Table 2.3 Adsorption data for CF_4 on silicalite-1

P (kPa)	q (mol/kg)			
	T = 313 K	T = 333 K	T = 353 K	T = 373 K
6.25	0.0733	0.0124	0.0034	0.0021
12.75	0.1078	0.0366	0.0062	0.0021
17.00	0.1216	0.0470	0.0227	0.0021
34.00	0.1444	0.0560	0.0282	0.0028
42.50	0.1686	0.0670	0.0371	0.0145
51.00	0.1901	0.0850	0.0488	0.0186
63.75	0.2232	0.0940	0.0605	0.0331
85.00	0.2329	0.0981	0.0660	0.0387

Table 2.4 Adsorption data for C_3F_6 on silicalite-1

P (kPa)	q (mol/kg)					
	T = 303 K	T = 313 K	T = 333 K	T = 353 K	T = 373 K	T = 423 K
6.25	0.8675	0.6330	0.5158	0.3576	0.2684	0.1311
12.75	1.1829	0.9176	0.7657	0.5906	0.4147	0.1751
17.00	1.2096	0.9486	0.7779	0.6102	0.4201	0.1868
34.00	1.2992	1.0451	0.8339	0.6621	0.4747	0.2431
42.50	1.3218	1.0749	0.8582	0.6752	0.4910	0.2716
51.00	1.3372	1.1076	0.8795	0.6895	0.5074	0.3186
63.75	1.3527	1.1240	0.9056	0.7264	0.5674	0.3817
85.00	1.3539	1.1240	0.9689	0.7300	0.5701	0.3848

Table 2.5 Adsorption data for CF_4 on ZSM-5

P (kPa)	q (mol/kg)			
	T = 313 K	T = 333 K	T = 353 K	T = 373 K
6.25	0.0502	0.0124	0.0055	0.0047
12.75	0.1051	0.0366	0.0082	0.0331
17.00	0.1766	0.0470	0.0123	0.0500
34.00	0.2302	0.0560	0.0300	0.0513
42.50	0.2502	0.1106	0.0593	0.0540
51.00	0.2721	0.1327	0.0695	0.0588
63.75	0.2996	0.1486	0.0743	0.0635
85.00	0.3038	0.1506	0.0764	0.0635

Table 2.6 Adsorption data for C_3F_6 on ZSM-5

P (kPa)	q (mol/kg)					
	T = 303 K	T = 313 K	T = 333 K	T = 353 K	T = 373 K	T = 423 K
6.25	0.4971	0.4181	0.3598	0.3243	0.2841	0.2274
12.75	0.8078	0.6893	0.5895	0.5746	0.4473	0.3748
17.00	0.8264	0.7006	0.6138	0.6030	0.4715	0.3871
34.00	0.8699	0.7289	0.6503	0.6087	0.5198	0.4363
42.50	0.8823	0.7345	0.6625	0.6371	0.5380	0.4486
51.00	0.8948	0.7402	0.6807	0.6485	0.5561	0.4732
63.75	0.9010	0.7458	0.7172	0.6599	0.6226	0.4916
85.00	0.9072	0.7515	0.7232	0.6656	0.6286	0.4977

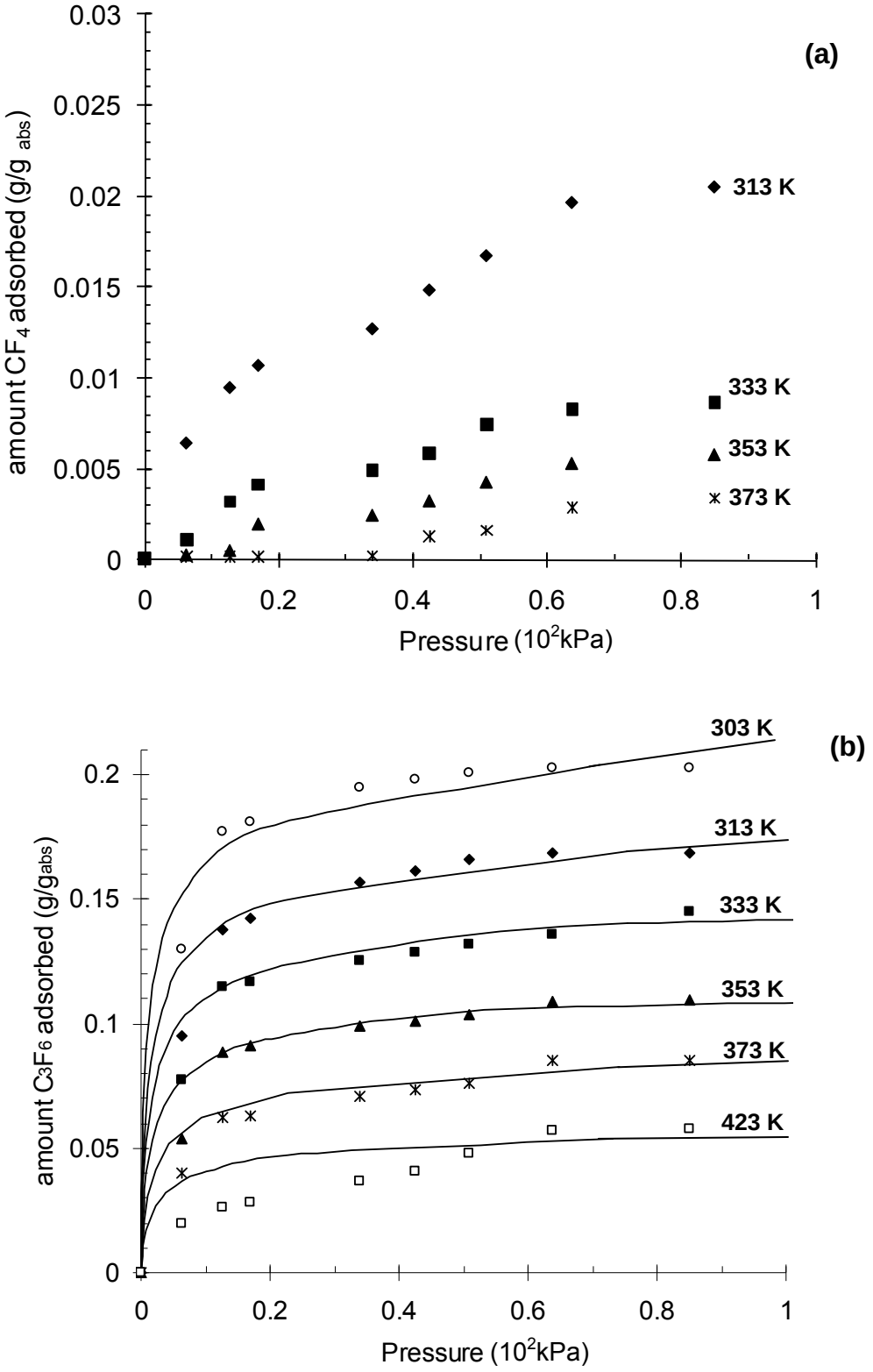

Figure 2.2 Adsorption isotherms of (a) CF_4 and (b) C_3F_6 on silicalite-1.

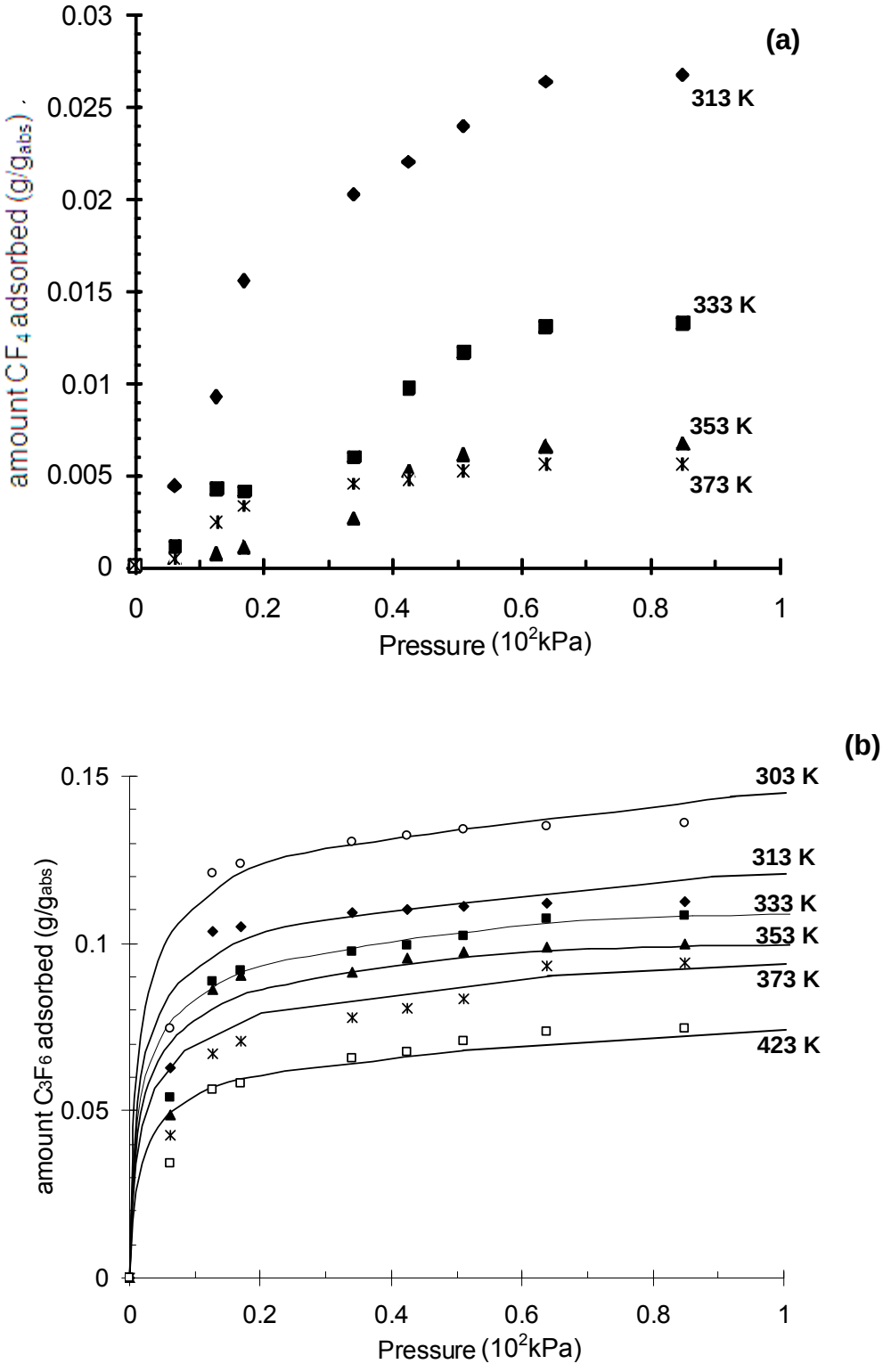

Figure 2.3 Adsorption isotherms of (a) CF_4 and (b) C_3F_6 on ZSM-5.

For all gases and zeolites tested, a decrease in the amount of gas adsorbed was found with increasing temperature. This was expected and correlates well with literature.[13,14,15] This phenomenon is due to the increased vibration energy associated with higher temperatures, which results in a decreased probability of molecular adsorption. From the adsorption of CF_4 and C_3F_6 on silicalite-1 (Fig. 2.2), it was clear that silicalite-1 adsorbed more C_3F_6 (~10 times) than CF_4 at similar temperatures over the whole temperature range. This trend was also observed for the ZSM-5 (Fig. 2.3). The higher amounts of C_3F_6 adsorbed, compared to CF_4 at similar pressures and temperatures, are in agreement with the study of Ahn *et al*.[10], where the compound with the longer carbon chain, namely C_2F_6, was adsorbed in larger amounts than CF_4 onto Zeolite 13X over the entire pressure and temperature range. Higher adsorption amounts for compounds with longer carbon chain lengths are commonly observed for hydrocarbons adsorbed onto molecular sieves.[3,16]

When comparing the adsorption of CF_4 onto silicate-1 and ZSM-5 respectively, it can be seen that a slightly higher amount adsorbed onto the ZSM-5, while the adsorption of C_3F_6 was also slightly higher for silicalite-1 compared to ZSM-5. The higher amount of C_3F_6 adsorbed onto the silicalite-1 can be attributed to the higher polarizability of the silicalite-1 lattice. The presence of Al^{3+} decreases polarizability and therefore the non-symmetrical C_3F_6 would be more prompted for attachment to the pure siliceous silicalite-1 than the aluminum containing ZSM-5 structure. This justification was given for alkane adsorption on Brønsted acid sites, but is a reasonable explanation for the observations made in this study.[17]

The average percentage deviation Δq of the Langmuir isotherm to the experimental points was calculated using the following equation,[10]

$$\Delta q = \frac{100}{k} \sum_{i=1}^{i=k} \left| \frac{q_i^{exp} - q_i^{cal}}{q_i^{exp}} \right| \qquad (2.6)$$

with k the number of data points, while q^{exp} and q^{cal} (g/g_{ads}) are the experimental and calculated adsorbed amounts respectively.

The experimental data for the CF_4 adsorbed onto silicalite-1 and ZSM-5 did not fit the Langmuir isotherm and therefore no Langmuir isotherm parameters were included. The average percentage deviation fit of the Langmuir isotherm for the CF_4 adsorbed onto silicalite-1 increased with increasing temperature from 8 to 79 %, while the average percentage deviation for the Langmuir isotherm for the CF_4 adsorbed onto ZSM-5 varied between 15 and 28 % over the temperature range. The estimated heat of adsorption values from these isotherms were -116 and -102 kJ/mol for CF_4 adsorbed onto silicalite-1 and ZSM-5 respectively which is more than 5 times larger than expected for hydrocarbons and fluorocarbons.[3,25] Although the heat of adsorption for hydrocarbons and fluorocarbons differ, it is expected that the heat of adsorption for CF_4 will be larger than the value for C_3F_6.

The parameters obtained from the best fit according to the modified Langmuir isotherm of the experimental data for the C_3F_6 adsorbed onto silicalite-1 and ZSM-5 are summarized in Table 2.7. For the C_3F_6 adsorbed onto the silicalite-1, it was observed that the Langmuir isotherm fits the experimental data to a higher degree at lower temperatures. Although it was not as clearly defined for ZSM-5, in general the trend seems to be observed. As expected, the q_m and n values were larger at lower temperatures due to the decreased vibrational energy of the adsorbed molecules, which results in an increased possibility of adsorption and occupation of active sites. The measured Henry constants (k_i) decrease with temperature increase for C_3F_6 adsorbed on both silicalite-1 and ZSM-5. The measured Henry constants are in the same order as those observed for alkanes adsorbed onto zeolite, which also yielded a decrease with increasing temperature.[18]

Table 2.7 Langmuir Isotherm Parameters Estimated for C_3F_6 on silicalite-1 and ZSM-5

Gas	Adsorbent	Temperature (K)	q_m (g/g_{abs})	n (-)	k_i ($g/g_{abs}.10^2kPa$))	Δq (%)
C_3F_6	silicalite-1	303	0.255	3.0	140.1	5.2
		313	0.212	2.9	120.2	5.4
		333	0.175	2.8	101.1	5.2
		353	0.133	2.6	87.5	6.6
		373	0.103	2.6	67.2	5.9
		423	0.067	2.5	65.0	26.7
C_3F_6	ZSM-5	303	0.180	3.0	108.0	6.2
		313	0.150	2.9	102.1	6.7
		333	0.135	2.9	101.0	2.9
		353	0.123	2.7	89.0	8.5
		373	0.113	2.6	75.7	7.9
		423	0.085	2.4	70.1	7.4

The calculated heat of adsorption and pre-exponential factor for C_3F_6 on silicalite-1 and ZSM-5, obtained using Equation 2.5, is shown in Table 2.8.

Table 2.8 Calculated heat of adsorption and pre-exponential factor for C_3F_6 on silicalite-1 and ZSM-5

Gas	Adsorbent	Heat of adsorption Δ*H* (kJ/mol)	k_o ($g/g_{abs}.10^2kPa$)
C_3F_6	silicalite-1	-33.05	7.6
C_3F_6	ZSM-5	-17.32	21.3

The calculated heat of adsorption values are in agreement with literature values of n-C_3 adsorbed onto Zeolite MCM-22,[18,19] which ranged from -30 to -49 kJ/mol. In general, the adsorption enthalpies increase with increasing length of the carbon chain for n-alkanes adsorbed onto zeolites. This trend is observed both in experimental[20,21,22] and molecular simulation studies for a wide range of

zeolites investigated.[23,24] The heat of adsorption values indicated in the study of Ndjaka *et al*.[25] for C_2H_6 and C_3H_8 adsorbed onto MFI zeolite were -40 and -31 kJ/mol respectively, while the heat of adsorption of CH_4 was -20 kJ/mol. Although the CF_4 in this study did not fit the Langmuir isotherm it should be expected that the heat of adsorption should be higher than the heat of adsorption calculated for C_3F_6, while the Henry constant of CF_4 should be smaller than C_3F_6 when the trend of C_xH_y gas adsorption is followed. In a study by Asanuma *et al*.[26] the heat of adsorption for CF_4 and C_2F_6 onto Na-mordenite was calculated as -25 and -36 kJ/mol. It has been shown for H-MFI that these hydrogen atoms give a negative contribution to the heat of adsorption of up to 10 kJ/mol and also results in a higher Henry coefficient. For each aluminium present there will be a hydrogen atom present resulting in an increase in the heat of adsorption. This trend is observed in Table 2.8 for the C_3F_6 adsorbed onto the silicalite-1 and ZSM-5. The ZSM-5 has aluminium present in its structure and therefore the heat of adsorption is larger than the adsorption of C_3F_6 onto silicalite-1. This is also the explanation for the higher pre-exponential factor observed for the C_3F_6 adsorbed onto ZSM-5.

For Langmuir type adsorption isotherms, the equilibrium separation factor is a constant and can be given by the ratio of the Henry Law's constants.[27,28] However, the ratio of the Henry constant is a definition of the adsorption selectivity in the low pressure region. In order to calculate selectivities we presume that the ideal selectivity for separation of a gas mixture containing CF_4 and C_3F_6 is determined by the amount of the pure gas adsorbed. The adsorption selectivies in this study were calculated according to:

$$S_{p,T} = q_{C3F6} / q_{CF4} \qquad (2.7)$$

where S is the molar selectivity with p the pressure (10^2kPa), T the temperature (K), q_{C3F6} the amount of C_3F_6 adsorbed (mol/g_{ads}) and q_{CF4} the amount of CF_4 adsorbed (mol/g_{ads}).

The molar selectivities were calculated at 0.85 (10^2kPa) and each temperature for both zeolites. The calculated theoretical selectivities are shown in Figure 2.4.

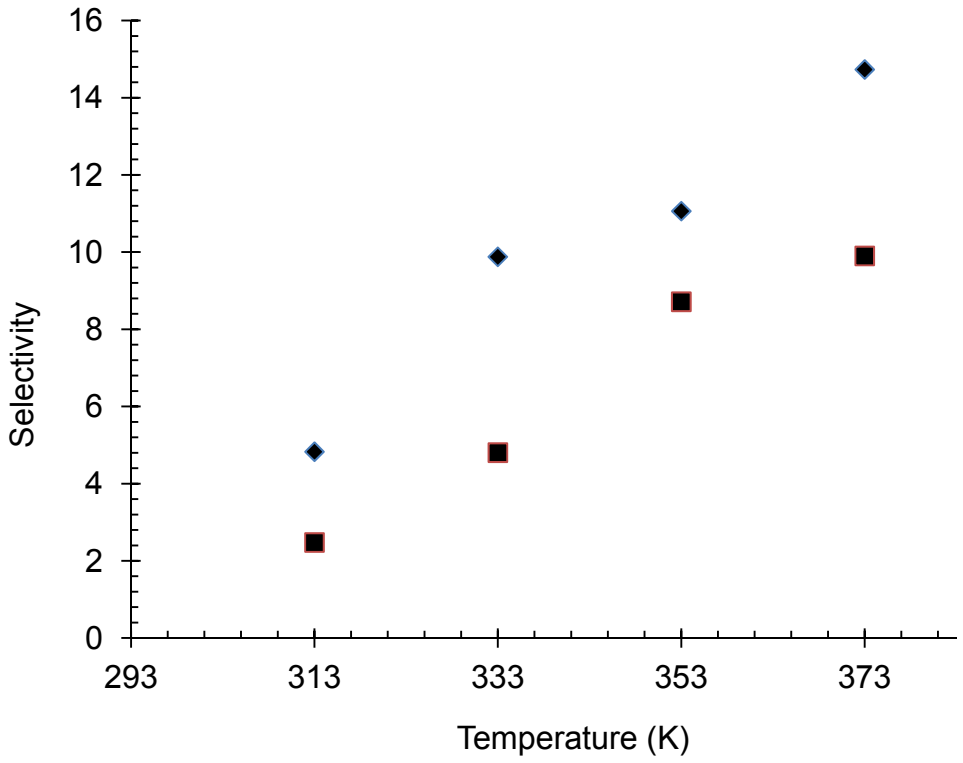

Figure 2.4 Theoretical selectivities of CF_4 and C_3F_6 on silicalite-1 (♦) and ZSM-5 (■) at 0.85 (10^2kPa) and various temperatures.

It seems that silicalite-1 yields a higher selectivity than ZSM-5. Silicalite-1 has a higher degree of polarizability as stated earlier and therefore this will increase the adsorption of the non-symmetrical C_3F_6, while this will have little effect on the symmetrical CF_4 molecule. Therefore the amount of CF_4 adsorbed for both silicalite-1 and ZSM-5 will be fairly similar, whilst the C_3F_6 amount difference will be larger explaining the larger overall selectivity observed for the silicalite-1. Furthermore, the ideal selectivities increase with increasing temperature. The increased selectivities at higher temperatures were due to the larger temperature dependence of CF_4 adsorption on both the silicalite-1 and ZSM-5 as observed

from the data. The CF_4 amount decreases more rapidly with temperature increase than the amount of C_3F_6 adsorbed. When ideal selectivities were calculated at lower pressures, a similar trend was observed with an overall increased selectivity at higher temperatures.

When considering molar selectivities at a constant temperature it was observed that calculated theoretical selectivities increased with decreasing pressure for both silicalite-1 and ZSM-5. In Figure 2.5 this effect is illustrated for the calculated theoretical selectivities of CF_4 and C_3F_6 on silicalite-1. Similar results were obtained for the selectivities of CF_4 and C_3F_6 on ZSM-5.

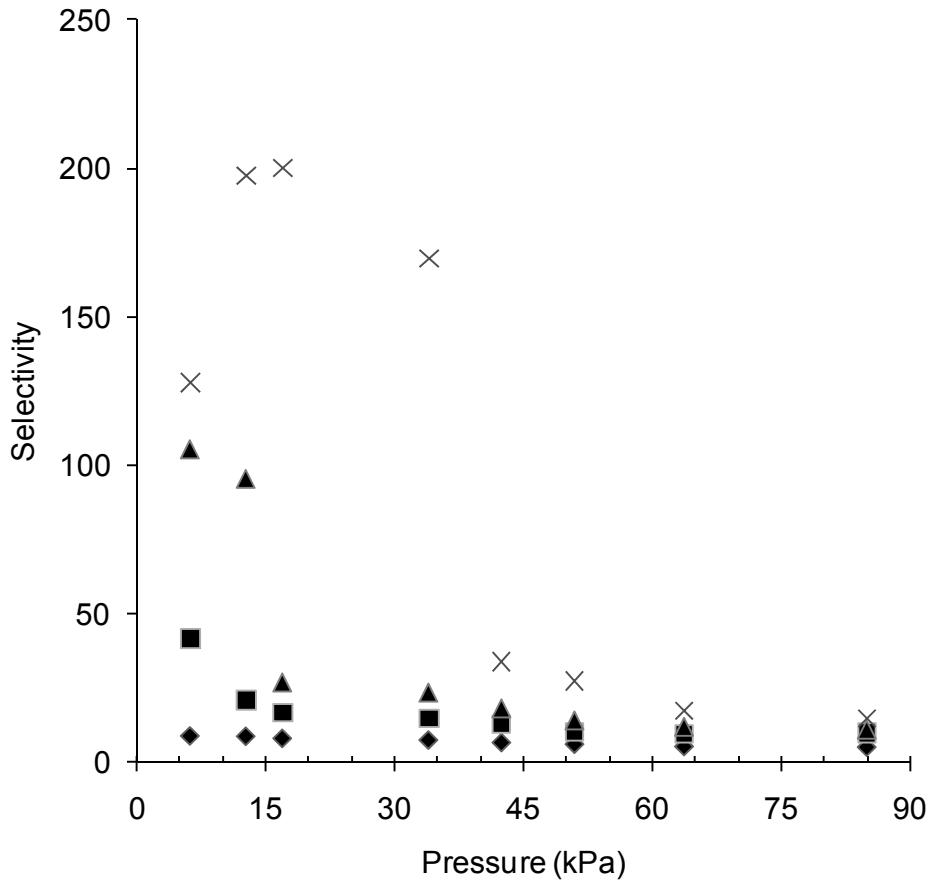

Figure 2.5 Theoretical selectivities of CF_4 and C_3F_6 on silicalite-1 at 313(♦), 333(■), 353(▲) and 373 K (X) at various relative pressures.

2.4 Conclusion

In this study the amounts of CF_4 and C_3F_6 adsorbed on zeolite ZSM-5 and silicalite-1 were measured experimentally using a gravimetrical method. Adsorption was determined at temperatures between 303 K and 423 K under normal atmospheric conditions (87 kPa). More C_3F_6 adsorbed on both silicalite-1 and ZSM-5 than CF_4. This effect could be explained due to the presence of aluminium in the ZSM-5 which decreases the polarizability of the zeolite structure. Experimental data was fitted to the Langmuir isotherm to determine the heats of adsorption for each component. The adsorption data indicated that separation of CF_4 and C_3F_6 would be possible by means of adsorption. The highest ideal selectivities for separation of this binary gas mixture would be obtained at higher temperatures and lower pressures.

2.5 Acknowledgement

The financial assistance of the Innovation Fund (IF), of South Africa (Project T50021), a separate business unit of the Department of Science and Technology (DST), is hereby acknowledged. The financial contribution of the South African Nuclear Energy Corporation (Necsa), towards this research is also acknowledged. The author wishes to thank Dr. L. Tiedt (NWU, South Africa) for the SEM images of the zeolites. The author also wants to acknowledge the contribution of Robbie Venderbosch (Netherlands) for his inputs during the research.

2.6 References

[1] S. Sircar, A.L. Myers, Gas separation by zeolites, in S.M. Auerbach, K.A. Carrado, P.K. Dutta (Eds.), Handbook of Zeolite Science and Technology, Machel Dekker Inc., New York, Bassel, (2003) pp. 1063-1104.

[2] R.M. Barrer, Zeolite and Clay minerals as sorbents and molecular sieves, Academic Press, London, (1978).

[3] R.W. Triebe, F.H. Tezel, K.C. Khulbe, Adsorption of methane, ethane, ethylene on molecular sieve zeolites, Gas separation and purification, 10, (1996) 81.

[4] I.J. van der Walt, O.S.L. Bruinsma, Depolymerization of clean unfilled PTFE waste in a continues process, Journal of Applied Polymer Science, 102, 3, (2006) 2752.

[5] S. Li, D. Jinjin, Improvement of hydrophobic properties of silk and cotton by hexafluoropropene plasma treatment, Applied Surface Science, 253, (2007) 5051.

[6] A.B. Hinchliffe, K.E. Porter, A comparison of membrane separation and distillation, Chemical Engineering Research and Design, 78, 2, (2000) 255.

[7] J.A.C. Silva, A.E. Rodrigues, Multisite Langmuir Model Applied to the Interpretation of Sorption of n-paraffins in 5A Zeolite, Industrial and Engineering Chemical Research, 38, (1999) 2438.

[8] J.D. Seader, E.J. Henley, Separation process principles, John Wiley & Sons, Inc., (1998) Chapter 15.

[9] G. Martinez, D. Basmaddjian, Towards a general gas adsorption isotherm, Chemical Engineering Science, 51, (1996) 1043.

[10] N. Ahn, S. Kang, B. Min, S. Suh, Adsorption Isotherms of Tetrafluoromethane and Hexafluoroethane on various adsorbents, Journal of Chemical Engineering Data, 51, (2006) 451.

[11] H. Kalipcilar, A. Culfaz, Synthesis of submicron silicalite-1 crystals from clear solutions, Crystal Research and Technology, 35, 8, (2000) 933.

[12] E.E. McLeary, J.C. Jansen, F. Kapteijn, Zeolite based films, membranes and membrane reactors: Progress and prospects, Microporous and Mesoporous Materials, 90, (2006) 198.

[13] I. Majchrzak-Kuceba, W. Nowak, A thermogravimetric study of the adsorption of CO_2 on zeolites synthesized from fly ash, Thermochimica Acta, 437, (2005) 67.

[14] C.M. Zimmerman, W.J. Koros, Comparison of gas transport and sorption in the ladder polymer BBL and some semi-ladder polymers, Polymer, 40, (1999) 5655.

[15] S. Himeno, T. Tomita, K. Suzuki, S. Yoshida, Characterization and selectivity for methane and carbon dioxide adsorption on the all-silica DD3R zeolite, Microporous and Mesoporous Materials, 98, (2007) 62.

[16] J. Peng, H. Ban, X. Zhang, L. Song, Z. Sun, Binary adsorption equilibrium of propylene and ethylene on silicalite-1: prediction and experiment, Chemical Physics Letters, 401, (2005) 94.

[17] F. Eder, J. A. Lercher, Alkane sorption in molecular sieves: The contribution of ordering intermolecular interactions, and sorption on Brønsted acid sites, Zeolites, 18, (1997) 75.

[18] J.F.M. Denayer, R.A. Ocakoglu, J. Thybaut, G. Marin, P.Jacobs, n- and Isoalkane Adsorption Mechanism on Zeolite MCM-22, Journal of Physical Chemistry B, 110, (2006) 8551.

[19], R.A. Ocakoglu, J.M.F. Denayer, G.B. Marin, J.A. Martens, G.V.J. Baron, Tracer Chromatographic Study of Pore and Pore Mouth Adsorption of Linear and Monobranched Alkanes on ZSM-22 Zeolite, Journal of Physical Chemistry B, 107, (2003) 398.

[20] S. Savitz, F. Siperstein, R.J. Gorte, A.L. Myers, Calorimetric Study of Adsorption of Alkanes in High-Silica Zeolites, Journal of Physical Chemistry B, 102, (1998) 6865.

[21] M.S. Sun, D.B. Shah, H.H. Xu, O. Talu, Adsorption of Equilibria of C1-C4 Alkanes, CO_2 and SF_6 on Silicalite, Journal of Physical, Chemistry,102, (1998) 1466.

[22] F. Eder, J. A. Lercher, On the Role of the Pore Size and Tortuosity for Sorption of Alkanes in Molecular Sieves, Journal of Physical Chemistry B, 101, (1997) 1273.

[23] H. Abdul-Rehman, M.A. Hasanain, and K.F. Loughlin, Quaternary, Ternary, Binary, and Pure Component Sorption on Crystallites: I Light Alkanes on Linde S115 Silicalites at Moderate to High Pressures, Industrial and Engineering Chemistry Research, 29, (1990) 1525.

[24] F. Eder, M. Stockenhuber, J.A. Lercher, Sorption of light alkanes on H-ZSM 5 and H-mordenite, Studies in Surface Science and Catalysis, 97, (1995), 495.

[25] J.B. Ndjaka, G. Zwanenburg, B. Smit, M. Schenk, Molecular simulations of adsorption isotherms of small alkanes in FER-, TON-, MTW- and DON-type zeolites, Microporous and Mesoporous Materials, 68, (2004) 37.

[26] T. Asanuma, H. Nakayama, T. Eguchi, N. Nakamura, ^{19}F NMR study on C_nF_{2n+2} (n=1 and 2) adsorbed in Na-mordenite: Dynamic behaviour and host–guest interaction, Journal of the Chemical Society, Faraday Transactions, 94, (1998) 3521.

[27] P. Li, Adsorption and separation for methane, carbon dioxide, nitrogen and oxygen gases, Ph.D. Thesis, University of Ottawa, Ottawa, Canada, (2007), p. 17.

[28] M. Noack, J. Caro, Zeolite membranes – Recent developments and progress, Microporous and Mesoporous Materials, 115, (2008) 215.

CHAPTER 3

SYNTHESIS OF A COMPOSITE INORGANIC MEMBRANE FOR THE SEPARATION OF NITROGEN, TETRAFLUOROMETHANE AND HEXAFLUOROPROPYLENE

ABSTRACT

Various zeolites were synthesized on the inner surface of α-alumina support tubes by a hydrothermal process. Gas permeation properties were investigated at 298 K for single component systems of N_2, CF_4, and C_3F_6. Ideal selectivities lower than Knudsen selectivities were obtained as a result of defects from intercrystalline slits and crack formation during synthesis and template removal. A composite ceramic membrane consisting of a ceramic support structure, an MFI intermediate zeolite layer and a Teflon AF 2400 top layer was developed to improve separation. The Teflon layer sealed possible defects present in the separation layer forcing the gas molecules to follow the path through the zeolite pores. Ideal selectivities of 88 and 71 were obtained for N_2/CF_4 and N_2/C_3F_6 respectively. Adsorption experiments performed on materials present in the membrane structure suggested that although adsorption of C_3F_6 onto Teflon AF 2400 compared to CF_4 results in a considerable contribution to permeation for the composite ceramic membrane, the sealing effect of the zeolite layer by the Teflon layer is however the reason for the large N_2/CF_4 and N_2/C_3F_6 selectivities obtained.

Keywords: N_2, CF_4, C_3F_6, zeolite, Teflon AF 2400, sealing layer, membrane

3.1 Introduction

While polymeric membranes are most suitable for water-related applications, many separation processes in industry require a membrane with high temperature and chemical stability. For polymeric materials a general trade-off exists between permeability and selectivity, with an "upper-bound" of separation performance predicted. Inorganic membranes such as zeolites, are thermally, chemically and mechanically more stable and have been shown to exceed the "upper-bound" performance of polymeric membranes.[1] Zeolite membranes specifically have, due to their unique crystallographic and physical properties, the potential of separating mixtures that are difficult and expensive to separate.[2] The advanced use of inorganic membranes however, including zeolites, in large scale industrial processes is hindered by the lack in technology to manufacture continuous and defect-free membranes.[3] While authors have increased selectivity by altering synthesis methods[4] or eliminating possible defects by pre- or post synthesis treatments,[5,6,7] the use of zeolites to date mostly involves the separation of condensable gases due to the low selectivities experienced with non-condensable gas mixtures.[8,9]

It has been shown that the presence of intercrystalline boundaries between zeolite crystals is caused by the Al-Al interactions in adjacent crystals.[10] However, while mainly Al-free MFI (silicalite-1) and DDR type zeolites are able to separate molecules by size, these membranes are still not effective due to residual defects remaining in the separation layer. Recently, it has been shown that intercrystalline defects are present even in alumina-free MFI membranes where the size of the defects was determined by adsorbing gas (i-butane, p-xylene, benzene) onto the membrane layer.[11] Various authors have introduced methods to enhance the crystal intergrowth for alumina containing zeolites to decease the intercrystalline boundaries which are significantly larger than the zeolite pores.[12] Repeated synthesis, chemical vapour deposition and template-free synthesis[13] have been employed to decrease the effect of intercrystalline boundaries on selectivity. The preparation of highly selective

zeolite membranes by a post-synthetic coking treatment has also been investigated.[14] In general, these techniques have resulted in a decrease in permeability. Recently, the application of Mixed-Matrix Membranes (MMMs) for gas separation has attracted interest due to their higher selectivity compared to polymeric membranes and their repeatability compared to zeolite composite membranes.[15] Much of the research concerning MMMs have been on molecular sieves introduced into a polymer matrix. Although some research on composite MMMs has been performed, such as thin MMMs deposited on porous ceramic supports, few studies have been done on the application of a polymer layer on a composite inorganic membrane.[3] In many studies, the addition of a sealing layer with a high permeability to plug imperfections has been used to enhance selectivity usually for polymeric membranes.[16, 17]

The aim of this study was to synthesize a composite zeolite membrane for the separation of non-condensable gas mixtures and to investigate whether it would be possible to enhance the separation capability of the composite membrane by the addition of a thin polymer layer. In the manufacturing of the composite inorganic-polymer membrane, an α-alumina support, MFI intermediate layer and a Teflon AF 2400 polymeric layer were used.

The non-condensable gases investigated in this study are N_2, CF_4, and C_3F_6. Tetrafluoromethane (CF_4) and hexafluoropropene (C_3F_6) are used as low temperature refrigerants. CF_4 is also used in the plasma etching of electronic microprocessors, while C_3F_6 is also applied to surfaces to enhance its hydrophobic properties.[18] Currently cryogenic distillation is the most widely used separation process for the separation of CF_4 and C_3F_6. Cryogenic distillation is an energy intensive process,[19] which makes exploring alternative separation methods, such as membrane separation, an attractive alternative.

3.2 Experimental

In the development and performance evaluation of a composite (inorganic-polymeric) membrane, a few combinations of membranes were synthesized. To determine the individual performances and influence of the Teflon AF 2400 polymer and the MFI zeolite membranes, a Teflon AF 2400 layer and an MFI layer was applied directly onto the α-alumina support respectively. During the synthesis of the composite membrane, an MFI layer was used as an intermediate layer coated with Teflon AF 2400 as the top separation layer. The various membranes were evaluated using SEM, XRD, as well as gas permeability and adsorption of N_2, CF_4, and C_3F_6.

3.2.1 MEMBRANE SYNTHESIS

3.2.1.1 α-ALUMINA SUPPORT

Tubular α-alumina supports were manufactured in-house from a commercial powder (AKP-15; Sumitomo Chemical Co. Ltd, Japan) by means of the centrifugal casting technique. The optimized manufacturing technique for the centrifugal casting of the ceramic membranes was used.[20] Green casts were sintered at 1473 K for 1 h. Prior to application of the selective layer (either zeolite or AF 2400) onto the inner-surface, the ceramic tubes were cut to a length of 0.055 m and sonicated for 3 x 10 min in deionised water to remove particle residues to ensure a clean surface for attachment of the subsequent layers.

A layer specific pre-synthesis treatment was done for each separation layer synthesis to enhance crystal growth or attachment as described in the subsequent synthesis section.

After each pre-synthesis treatment, the tubular support was thoroughly rinsed in deionised water and dried for 3 h at 473 K and subsequently wrapped with PTFE tape to leave only the inner surface exposed.

3.2.1.2 MFI COATED CERAMIC MEMBRANE

Although the zeolite that was synthesized in this study was a silicalite-1 zeolite (containing no aluminium), migration of alumina from the ceramic support occurs during zeolite synthesis resulting in the addition of small quantities of aluminium into the zeolite framework.[9] For this reason the zeolite will hence forth be referred to as MFI.

For the zeolite synthesis pre-treatment, the support was refluxed in nitric acid (HNO_3 55 %, F.C. Scientific) for 3 h. This was done to decrease the hydrophilic nature of the α-alumina surface which enhances attachment of the hydrophobic MFI crystals.[21]

A direct *in situ* crystallization from a clear solution was chosen for the synthesis of the MFI layer onto the inner surface of the tubular support.[22] A zeolite precursor solution was prepared containing water, tetrapropylammonium hydroxide (TPAOH) and tetrapropylammonium bromide (TPABr). The composition of the precursor and tetraethylorthosilicate (TEOS) solutions used is given in Table 3.1.

Table 3.1 Reactant mixture compositions for the MFI clear solution synthesis

	Mass (g)			
Reactant mixture	TPAOH[a]	TPABr[b]	TEOS[c]	H_2O
Precursor solution	9.052	2.208	-	28.040
Silicate source	-	-	2.912	-

[a]TPAOH 20%, Fluka [b]TPABr 99%, Merck [c]TEOS 99%, Aldrich

This optimized solution composition was chosen according to previous studies in our research group. The clear precursor solution with a molar oxide ratio of 100 SiO_2 : 123 TPA : 63.7 OH : 14 200 H_2O was aged for one hour at 358 K and a further hour at room temperature. The hydrothermal treatment was performed in a preheated oven at a temperature of 443 K for 30 h, while the autoclave was rotated around the horizontal axis. After synthesis, the membrane was neutralized by rinsing in water. A second layer was synthesized onto the first layer by performing an identical hydrothermal synthesis as described for the first MFI layer.

The dried double layered composite membrane was calcined for 20 h at 673 K with a heating rate of 0.3 K/min and cooling rate of 0.5 K/min in order to remove the TPA template from the zeolite pores.

3.2.1.3 TEFLON COATED CERAMIC MEMBRANE

A composite membrane was manufactured which consisted of a ceramic support on which a double and triple layer of Teflon AF 2400 was synthesized to evaluate the performance of the Teflon AF 2400 polymer.

The support for this synthesis required no additional pre-treatment. The synthesis procedure for the Teflon® layer was as follows:

- The ceramic tube was wrapped in PTFE tape.
- A 0.5 wt% mixture of Teflon AF 2400 (DuPont) and FC-77 (3M™ Fluorinert™ Electronic Liquid FC-77) with a total volume of ~ 25 ml was placed in a 50 ml PTFE (polytetrafluoroethylene) bottle and closed. The Teflon AF 2400 was dissolved in a preheated oven at 363 K, under continuous stirring for 1 h. The mixture was allowed to cool to room temperature and poured into a pollitop with a total volume of ~ 25 ml.
- The ceramic tube was dip-coated in the 0.5 wt% mixture of Teflon AF 2400 and FC-77. The tube was vertically submerged in the

mixture for 20 s and then removed at a rate of 0.135 m/s, and vertically placed on a paper towel for 2 min.

- The composite membrane was turned (180 °) and the dip-coating procedure repeated.
- The PTFE tape was removed and the Teflon® (PTFE) coated ceramic membrane was left to air-dry vertically at room temperature for 24 h in a desiccator.
- The ceramic tube was wrapped in PTFE tape and the dip-coating procedure as described above was repeated again. Removal of the PTFE tape and drying of the membrane was again repeated.
- Finally, the dry composite membrane was heat treated in an oven at 423 K for 1 h with a heating and cooling rate of 1 K/min to ensure optimum attachment of the Teflon® onto the ceramic surface. This temperature was chosen based on results obtained and described in Section 3.3.1.4.

For the triple Teflon® coated membrane the dip-coating procedure was repeated once more with the above prepared membrane (dip-coating and turning) followed by the heat treatment.

3.2.1.4 COMPOSITE CERAMIC MEMBRANE

The procedure outlined for the MFI coated ceramic membrane was followed for the support pretreatment and synthesis of a double layered MFI zeolite on the ceramic support. After calcination, the outer surface of the ceramic tube was again wrapped with PTFE tape to ensure that the Teflon AF 2400 layer was applied only on the inner-surface of the MFI coated ceramic membrane.

The MFI coated ceramic membrane was dip-coated in the Teflon® / FC-77 (0.5 wt%) mixture for 20 s and the coating procedure repeated as described in the previous section (3.2.1.3) for the double Teflon® coated membrane.

The dry composite membrane was heat treated in an oven at temperatures ranging from 373 K to 613 K for 1 h to ensure attachment of the Teflon AF 2400 onto the underlying zeolite structure.

3.2.2 CHARACTERIZATION

3.2.2.1 MORPHOLOGY

Topological features such as membrane thickness and continuity were determined by scanning electron microscopy (SEM) with an FEI ESEM Quanta 200, OXFORD INCA 200 EDS SYSTEM. Dried samples were coated with Au/Pd (80 : 20). Zeolite phase identification was determined by X-ray diffraction (XRD; Siemens D-501). CuK_{α} radiation at a tube voltage of 40 kV was applied, while the sample was rotated at 30 rpm. The 2θ ranged from 4 to 50°.

3.2.2.2 SINGLE GAS PERMEATION

Single gas permeation values were measured for N_2, CF_4, and C_3F_6, using a continuous flow method with the membrane sealed in a dead-end configuration as displayed in Figure 3.1.

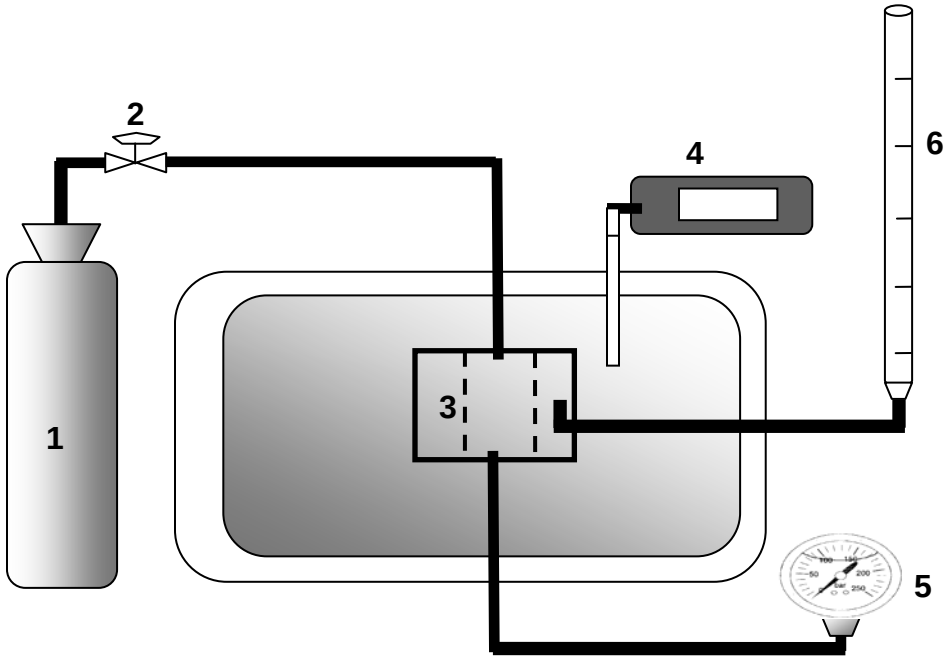

Figure 3.1 The experimental set-up for the single gas permeation.

The membranes were sealed with o-rings in a membrane module made from stainless steel (**3**, Fig. 3.1). The gas-tight permeation module was positioned vertically in an oven of which the temperature was electronically controlled by a relay-connected thermocouple (**4**). The transmembrane pressure was monitored by a pressure gauge (**5**) and gas feed (**1**) to the inner-tube side of the membrane was controlled by a pressure regulator (**2**). The permeate flow was measured by a soap flow meter (**6**) at atmospheric pressure (87 kPa in Potchefdstroom).

Membranes were conditioned beforehand by purging overnight at 373 K at a low transmembrane pressure (10 kPa) with helium to remove any residual moisture from the membrane. Subsequently, the membranes were purged for at least 3 h for each gas used to remove any He present and to allow a steady permeation rate to be reached for the specific gas.

The permeation flux ($mol.m^{-2}.s^{-1}$) from each experiment was recorded as an average of 5 measurements over a period of 60 min to ensure that a steady rate

had been reached. The permeance (mol.m^{-2}.s^{-1}Pa.$^{-1}$) was calculated as the straight line fit of the flux over the range of transmembrane pressures. Since the membrane modules for each membrane tested were similar, similar total membrane areas for each gas permeation experiment, due to the length (0.055 m) of the modules and the diameter of the tube (0.0177 m), were obtained. The total membrane surface area calculated was 3.06 x 10^{-3} m^2. This value was used for all calculations.

The ideal or permselectivity ($PS_{i/j}$) for gas *i* and gas *j* was defined as the single-component permeance ratio, at a given temperature and transmembrane pressure. The permselectivities were qualitatively compared to the Knudsen selectivities to evaluate the performance of each membrane. The Knudsen selectivities (PS_k) is obtained by,

$$PS_k\left(i/j\right) = \sqrt{\frac{M_j}{M_i}} \tag{3.1}$$

with *M* the molar weight (g/mol) of the gases *i* and *j*.

3.2.2.3 ADSORPTION

To investigate the adsorption of N_2, CF_4 and C_3F_6 on the various materials used in the membranes, gravimetry was employed. An isotherm accounting for adsorbate size, chemical dissociation, and molecular interactions is shown in Equation 3.2,

$$K_{eq}\exp(\frac{nu\theta}{kT}) = \frac{1}{p}\frac{\theta^s}{(1-\theta)^n} \tag{3.2}$$

where *s* represents the dissociation parameter (-), K_{eq} an equilibrium constant (10^2kPa^{-1}), *u* is the interaction energy between the adsorbed molecules (J), *k* the Boltzmann constant (J/K), *n* the amount of active sites occupied by a single molecule (-) and *T* is the temperature (K). The equilibrium constant $K_{eq} = k_\infty \exp(-\Delta H_{ads}/RT)$, with k_∞ a pre-exponential factor

($g/g_{ads}\cdot10^2kPa$), R the universal gas constant (J/mol·K), T the temperature (K) and ΔH the heat of adsorption (kJ/mol). In the equation

$$\theta = \frac{q}{q_m} \tag{3.3}$$

where q is the amount absorbed (g/g_{ads}) and q_m is the maximum loading that can occur when complete coverage of the absorbed gas takes place (g/g_{ads}). The experimental data was fitted to Equation 3.2 to determine the q_m for each gas/material combination. In this study the dissociation parameter and the interaction energy was ignored (s = 1 and u = 0 J).[23]

The TGA instrument was a TA Instruments TG and the data was captured by computer using a Compaq 800 MHz, 128 Mb RAM with Microsoft Windows NT 4.0 as running platform. A sample between 10-15 mg was placed in the sample cup and left for 24 h in the furnace at a temperature of 473 K in a helium flow of 50 ml/min to remove adsorbed water.

The sample was then cooled under helium to room temperature, and then set to the experimental temperature. A pre-determined mixture of helium and adsorbate gas were fed to the TGA using the calibrated mass flow controllers (MFC) with the total gas flow rate equal to 50 ml/min. The weight of the sample was recorded until equilibrium was reached. Subsequently, the composition of the gas mixture was adapted in order to measure the full isotherm in the 0 to 85 kPa range. The amount of gas adsorbed at each pressure was determined in order to obtain the isotherm.

Theoretical selectivities were calculated by the ratio of q_m values of the C_3F_6 and CF_4 adsorbed at each temperature according to:

$$S_T = qm_{C3F6} \Big/ qm_{CF4} \tag{3.4}$$

where S is the molar selectivity with T the temperature (K), qm_{C3F6} the amount of C_3F_6 adsorbed (mol/g_{ads}) and qm_{CF4} the amount of CF_4 adsorbed (mol/g_{ads}).

3.3 Results and Discussion

3.3.1 MORPHOLOGY

3.3.1.1 α-ALUMINA SUPPORT

The most important advantage of the centrifugal casting technique for the manufacturing of ceramic membranes compared to the more traditional extrusion method is the smooth inside surface with minimal surface defects obtained (Fig. 3.2), which is advantageous for the synthesis of a thin, continuous, defect free separation layer. [24]

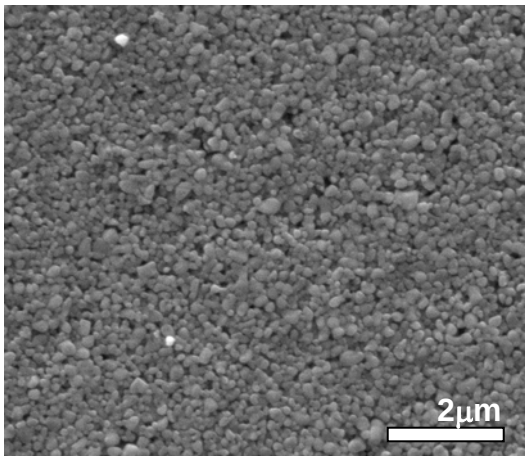

Figure 3.2 SEM image of the inner-surface of the AKP-15 α-alumina support sintered at 1473 K.

The sintered α-alumina tubes had an inner and outer diameter of 0.0177 m and 0.0207 m respectively. According to mercury porosimetry measurement, the porosity of the supports was 37 %, while the average pore size was 167 nm.

From the cross-section view (Fig. 3.3) it is clear that the smaller particles were situated near the inner-surface (Fig. 3.3a) while the larger particles settled at the outer surface (Fig. 3.3b) during the centrifugal casting process, which resulted in a graded ceramic support structure.

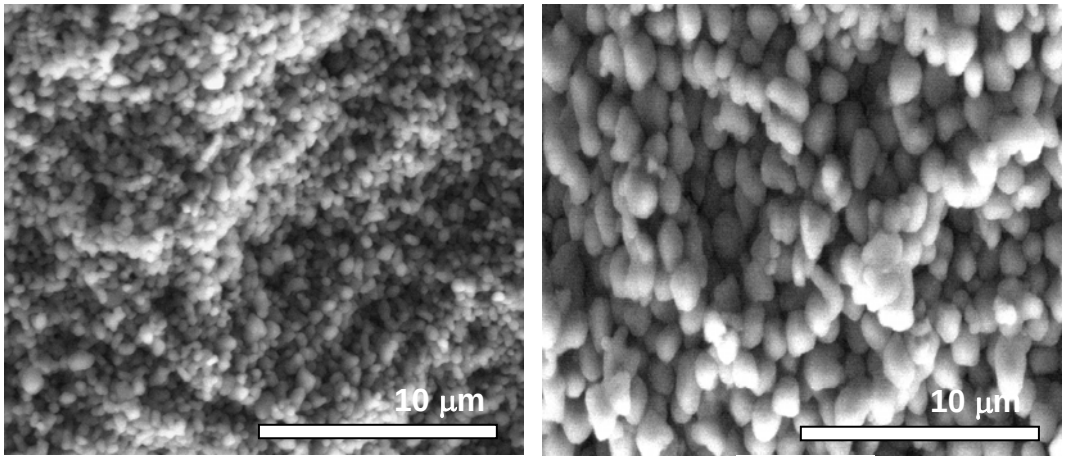

Figure 3.3 Cross-section SEM images of the α-alumina support near (a) the inner-surface and (b) the outer surface.

3.3.1.2 MFI COATED CERAMIC MEMBRANE

From the top-view (Fig. 3.4a), it is clear that the MFI had covered the support surface completely, while the cross-section view (Fig. 3.4b) shows that the MFI formed a closed, continuous zeolite layer of approximately 7 μm. The well-defined crystal edges signify a complete crystalline structure. The XRD spectrum (Fig. 3.5) confirmed the MFI zeolite structure according to the 2007 Relational Database.[25]

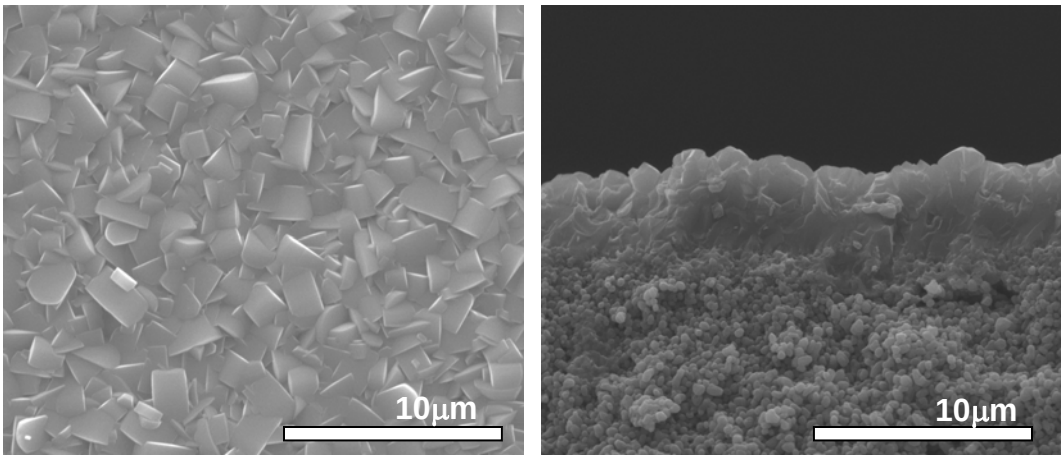

Figure 3.4 (a) Top and (b) cross-section SEM view of the double layered MFI membrane.

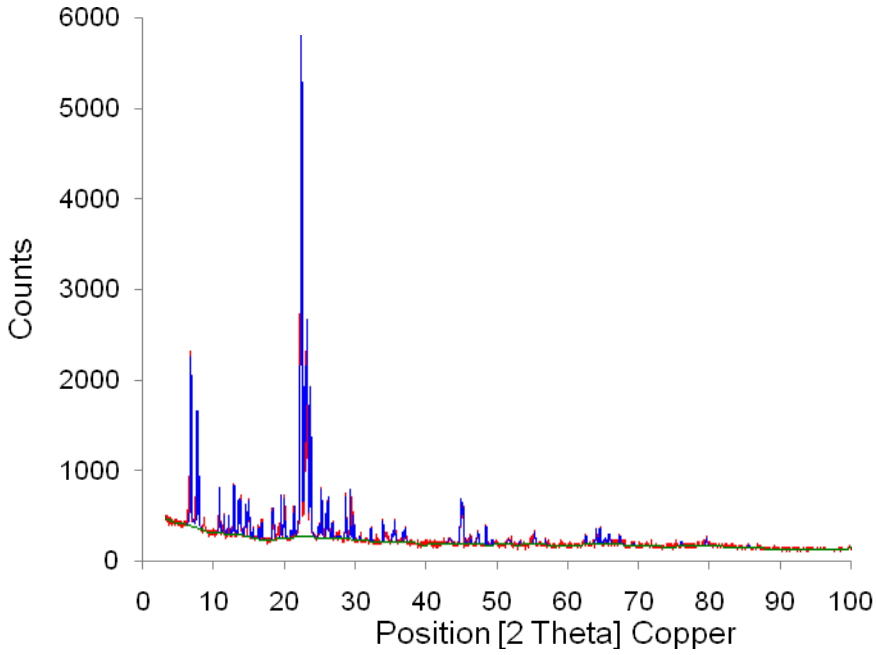

Figure 3.5 XRD of the MFI coated ceramic membrane.

While the support was completely covered (Fig. 3.4), due to thermal expansion mismatch between the bonded zeolite and the ceramic support, crack formation is frequently present with template removal during calcination, which is one of the

main causes of non-zeolite pores.[26] This phenomenon is clearly indicated in the SEM images of an MFI coated ceramic membrane before and after calcination, illustrated in Figures 3.6a and 3.6b respectively. Another important aspect of inorganic membrane synthesis is reproducibility. Poor reproducibility is a common problem encountered for zeolite membranes.[27]

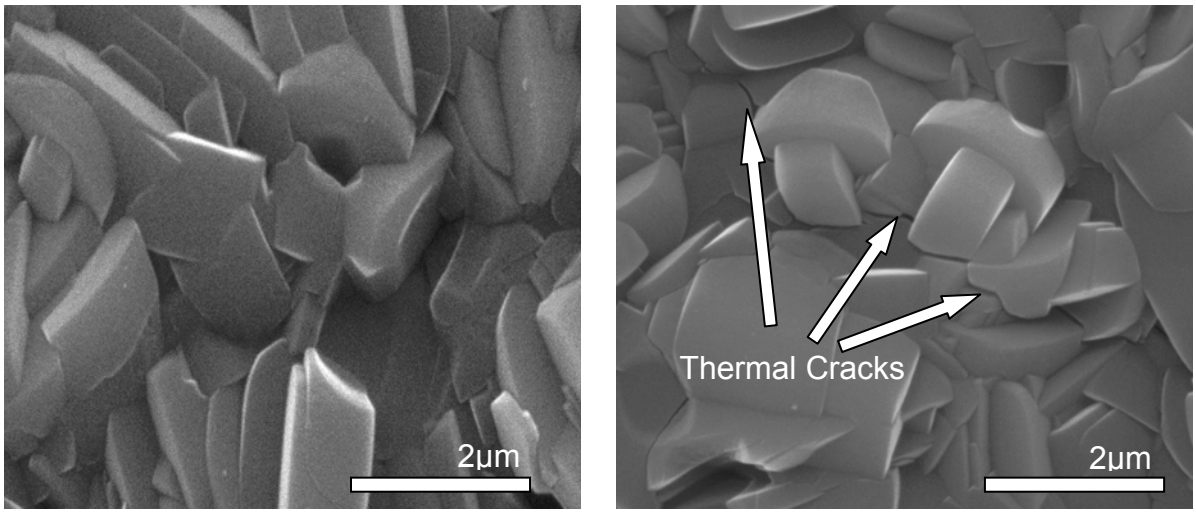

Figure 3.6 SEM images identifying the formation of cracks during template removal. Zeolite membrane (a) before and (b) after calcination.

3.3.1.3 TEFLON COATED CERAMIC MEMBRANE

The application of a polymer layer onto an inorganic support can be cumbersome when the polymer solution concentration and the dip-coating procedure are not optimized.

According to the supplier, the Teflon AF 2400 had to be dissolved in an electronic liquid at a temperature of 343 K or above. It was however important that no electronic liquid (FC-77) evaporated at elevated temperatures as this increases the concentration of the AF 2400 present in the mixture resulting in the deposition of AF 2400 onto the PTFE bottle.

To ensure the highest possible flux, it was decided to determine the lowest possible polymer concentration that yielded a closed continuous layer using the dip coating procedure described in Section 3.2.1.3. It was found that concentrations below 0.5 wt% Teflon AF 2400 resulted in non-continuous layers with defects (determined with SEM), concentrations at 0.5 wt% and above resulted in defect-free layers. For this reason 0.5 wt% was used for the synthesis of the Teflon® coated ceramic membrane as well as the composite ceramic membranes. The heat treatment which had been optimized to ensure attachment of the Teflon AF 2400 onto the inorganic material was used both for the composite ceramic membrane synthesis and the Teflon® coated ceramic membrane synthesis.

Another important aspect which had to be considered when applying the thin Teflon® layer was to ensure that the environment was dust free and that the ceramic surface contained no loose ceramic particles. The desiccator in which the membranes were dried after polymer dip-coating was subsequently kept dust free to avoid accumulation of dust during drying of the polymer.

The continuous double and triple Teflon® coated layer was approximately 2 µm and 2-3 µm (Fig. 3.7) thick respectively with limited penetration of the polymer phase into the underlying pores of the ceramic support membrane. From the top-view SEM images (not shown), it became clear that the Teflon® layer completely covered the smooth ceramic surface, with no visible defects present.

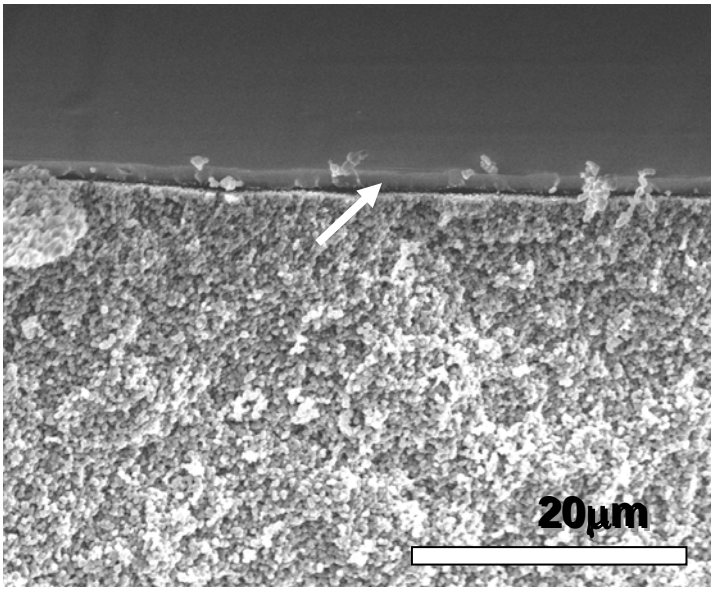

Figure 3.7 SEM images of the cross-section view of the triple Teflon coated ceramic membrane after temperature treatment at 423 K. The white arrow indicates the Teflon AF 2400 layer.

3.3.1.4 COMPOSITE CERAMIC MEMBRANE

The top view of the Teflon® layered MFI membrane after one hour treatments at various temperatures is shown in Fig. 3.8 a-d. The SEM assessments revealed that after treatment over a one hour period at 373 K slight attachment of the Teflon® layer onto the underlying MFI zeolite occurred, as is visible in Fig. 3.8a. Treatment at 423 K (Fig. 3.8a) resulted in improved penetration of the Teflon® in-between individual MFI crystals. Once the temperature was increased to 473 K (Fig. 3.8c), breaking of bonds within the polymer structure occurred which resulted in the appearance of the characteristic MFI zeolite shape underneath. This gave way to the appearance of a few pinholes and tears in the overlying Teflon® coating.[28]

The complete disintegration of the Teflon® layer is clearly visible at 573 K (Fig. 3.8d) as pronounced tearing is apparent. At 613 K no Teflon® was visible according to SEM (image not shown).

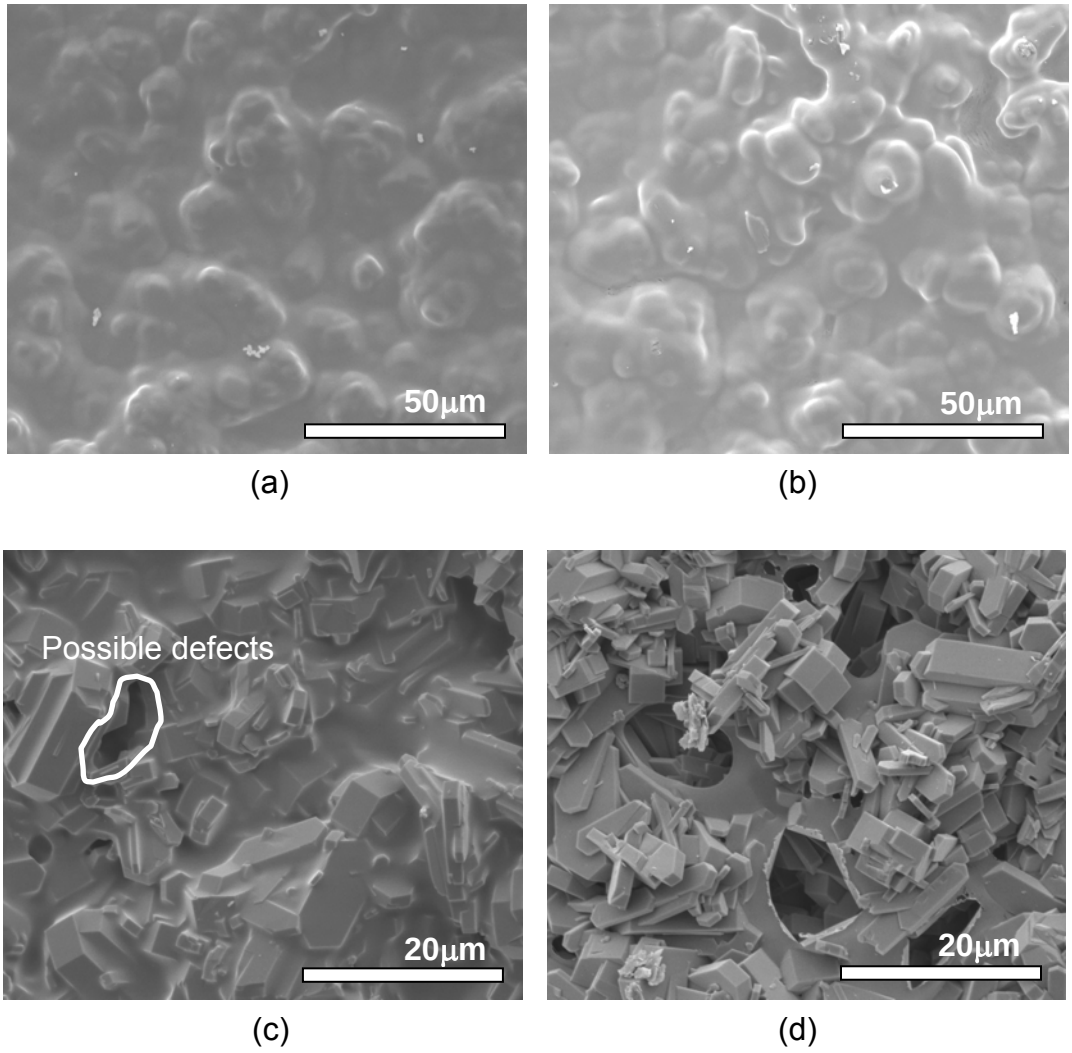

Figure 3.8 Top-view SEM images of the Teflon AF 2400 coatings over MFI after one hour temperature treatments at (a) 273 K, (b) 423 K, (c) 473 K and (d) 573 K.

According to SEM the attachment treatment at 423 K was optimal. A cross section of the 423 K treated membrane is shown in Figure 3.9, clearly showing the non-damaged Teflon® layer. The penetration of the 3-4 μm thick Teflon® layer in-between the zeolite crystals can be observed.

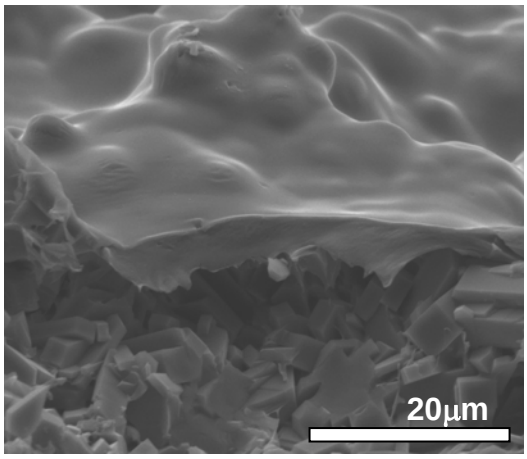

Figure 3.9 The cross-section view of the composite ceramic membrane after temperature treatment at 423 K.

3.3.2 SINGLE GAS PERMEATION

Before comparing the gas permeabilities of the various membrane types, the effect of the heat treatment used to attach the Teflon® layer onto the MFI zeolite in the composite membrane was evaluated in terms of gas permeances. The results are shown in Table 3.2. Standard deviations for permeance was approximately 5 % and in the range of 10 % for the ideal selectivities.

Table 3.2 Single gas permeances obtained for the Teflon coated MFI membranes at various temperature treatments. Permeances were obtained at 333 K and transmembrane pressures 1.5 - 2 (10^2kPa)

Treatment temperature	Permeance 10^{-8} (mol.s^{-1}.m^{-2}. Pa^{-1})			Ideal selectivities		
(ºC)	N_2	CF_4	C_3F_6	N_2/CF_4	N_2/C_3F_6	CF_4/C_3F_6
150	0.55	0.0064	0.0077	85.94	71.43	0.83
200	2.15	0.36	0.27	5.97	7.96	1.33
300	2.93	1.36	0.95	2.15	3.08	1.43

All membranes exhibited permeances in the order of $N_2 > CF_4 > C_3F_6$, which can be directly related to the kinetic diameter of the molecules (N_2 = 3.8 Å, CF_4 = 4.7 Å, $C_3F_6 \approx$ 6.6 Å) with the exception of the membrane treated at 423 K. The significant increase in permeances for all gases for membranes treated above 423 K is most likely as a result of the defects shown in the SEM images (Fig. 3.8), resulting in selectivity decrease with increasing temperature. This trend however was not observed for the ideal selectivities of CF_4/C_3F_6, where ideal selectivities increased with increasing temperature. For a probable explanation of this phenomenon see the discussion surrounding the results obtained for the five different membranes (Fig. 3.10 and Fig. 3.11).

For comparison to the other synthesized membranes, the Teflon® coated MFI membrane manufactured at 423 K was used. In Table 3.3 the single gas permeances for the various membranes synthesized in this study are summarized. Similar to Table 3.2 the results indicated had shown standard deviations in the range of 5 %.

Table 3.3 Summary of the single gas permeances for the various membranes

Membrane	Conditions			Permeance 10^{-8} (mol.s^{-1}.m^{-2}. Pa^{-1})		
	Membrane. No	Temp. (K)	Pressure range (10^2kPa)	N_2	CF_4	C_3F_6
Ceramic Support	1	298	0.5 – 2	130	84	75
Double Teflon coated ceramic	2a	298	0.5 – 2	5.37	1.12	0.56
Triple Teflon coated ceramic	2b	298	0.5 – 2	2.90	0.58	0.35
MFI coated ceramic	3	298	0.5 – 2	3.05	1.47	1.07
Composite ceramic	4	333	1.5 – 2	0.55	0.0064	0.0077

As expected, the ceramic support (membrane 1) without any layers yielded the highest permeances for N_2, followed by CF_4 with C_3F_6 permeance the lowest. This observation is expected considering the kinetic diameters of the gases and the pore size of the ceramic support. The calculated molar diameters of the gases according to molecular modelling were 0.168, 0.268 and 0.552 nm for N_2, CF_4 and C_3F_6 respectively which is small compared to the 167 nm pore diameter of the support. Kinetic diameter values of N_2[29] and CF_4[30] given in literature are 0.36 and 0.47 nm respectively. Permeance results were consistent with Knudsen diffusion.

The additional Teflon® layers applied onto the ceramic support (membrane 2a and 2b) resulted in an overall decrease in permeability compared to the ceramic support with the lowest permeability for the triple Teflon® coated ceramic as expected in the view of the increasing thickness of the triple coated Teflon® layer. Similar to the ceramic support, higher permeance for N_2 than for CF_4 and C_3F_6 was observed for both the double and triple Teflon® coated ceramic. As the N_2/CF_4 and N_2/C_3F_6 permselectivities were larger than the permselectivities for the ceramic support and above Knudsen (Fig. 3.10), the contribution of adsorption to the overall permeation through the membrane becomes more significant according to the solubility-diffusion model which is largely present when polymer membrane permeabilities are considered. The relation is given by

$$P = D \times S \tag{3.5}$$

where *P* is the permeability coefficient ($m^3.m/m^2.s.Pa$), *D* the diffusion coefficient (m^2/s) and *S* the solubility coefficient (Pa^{-1}).[31] The significant decrease in permeance due to Teflon® layers confirms that a Teflon® layer was obtained without significant defects.

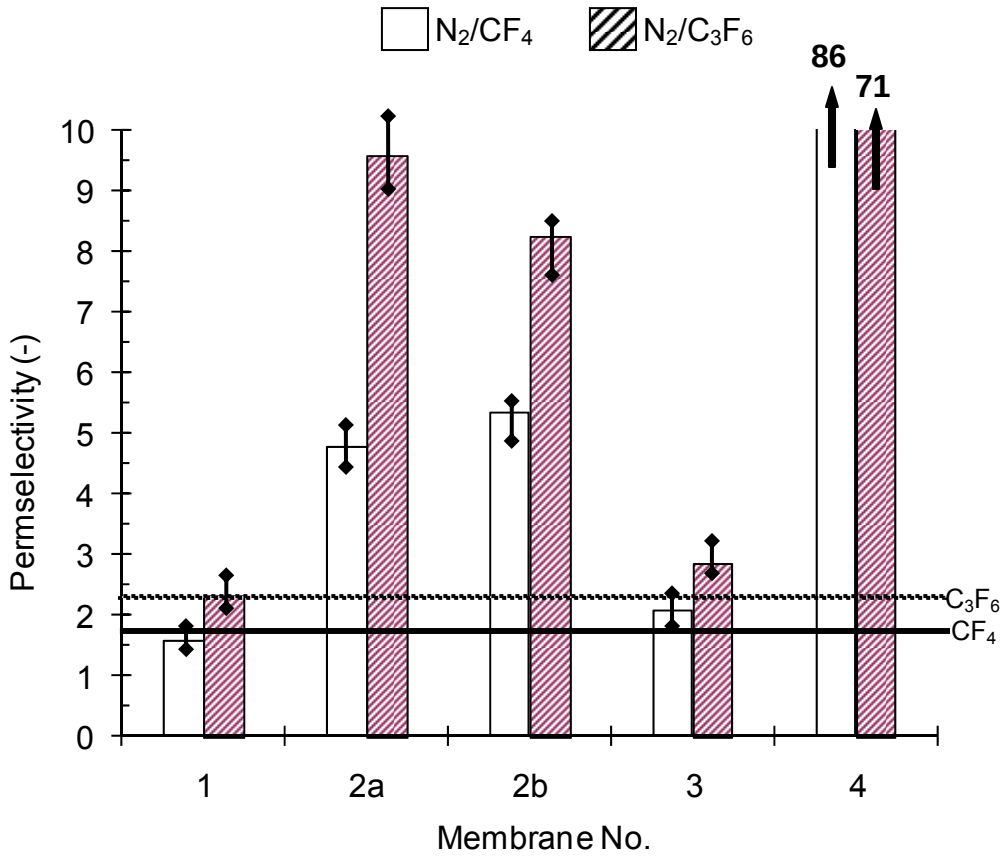

Figure 3.10 Permselectivity for N_2/CF_4 and N_2/C_3F_6 for the (1) ceramic support, (2a) double Teflon coated ceramic, (2b) triple Teflon coated ceramic, (3) MFI coated ceramic and (4) composite ceramic membrane. The respective Knudsen selectivity values are indicated by the cross bars and the deviations by the vertical lines on each respective bar.

The significant decrease in permeability of the MFI coated ceramic (membrane 3) compared to the ceramic support indicated the formation of an inter-grown MFI layer. The preferential permeation of N_2 compared to CF_4 and C_3F_6 was also observed for the MFI coated ceramic. The permselectivities for the CF_4/C_3F_6, although above Knudsen selectivity, is low when it is considered that the C_3F_6 molecule is larger than the MFI zeolite pore sizes. This confirms the existence of non-zeolite pores, since the total measured permeance through the MFI zeolite membrane was the summation of the zeolite and non-zeolite (intercrystalline)

permeances. The existence of non-zeolite pores were the result of non-perfect intergrowth between individual crystals during synthesis[5] and crack formation during template removal.

The considerable decrease in permeability of the composite ceramic membrane (membrane 4) compared to all manufactured membranes indicates that a dense, defect free membrane had been obtained. The N_2 permeation is the largest with the C_3F_6 permeation through the composite ceramic membrane larger than the CF_4. It is expected that the diffusion coefficient of CF_4 should be larger than C_3F_6 since the diffusion characteristics are usually determined by the membrane properties and the size of the permeant species. The considerable solubility of C_3F_6 compared to CF_4 in the Teflon® resulted in a larger overall C_3F_6 permeability, attributed to the interaction between the membrane and the permeant.[32] The larger gas permeation of C_3F_6 compared to CF_4 is consistent with explanations given by Wijmans and Baker for permeation of n-alkanes through silicone rubber membranes. According to the authors, the saturation vapour pressure and the diffusion coefficient both decrease with increasing molecular weight of the permeate creating competing effects on the permeability coefficient. The permeability coefficient is given as

$$P_i^G = \frac{D_i \gamma_i}{\gamma_{i(m)} p_{i(sat)}} \tag{3.6}$$

where P_i^G is the permeability coefficient, D_i the diffusion coefficient, γ_i the activity coefficient linking concentration with activity, $\gamma_{i(m)}$ the activity of component i in the membrane phase and $p_{i(sat)}$ the saturation vapour pressure. For molecules up to a weight of 100, permeability generally increases with increasing molecular weight because $p_{i(sat)}$ is the dominant term. Thus $p_{i(sat)}$ decreases which results in an increased permeability. For molecules with molecular weights above 100, the diffusion coefficient term becomes more dominant, and permeabilities decrease with increasing molecular weight of the permeate. This trend is clearly illustrated for permeation of simple alkanes in silicone rubber membranes. Permeation increased from CH_4 to C_5H_{12} and permeation decreased again as molecular

weight increased for molecules heavier than C_5H_{12}. The permeation of $C_{10}H_{22}$ was however still equivalent to C_3H_8. In our study the larger C_3F_6 permeability compared to CF_4 permeability is equivalent to the permeability increase from the CH_4 to C_5H_{12} in the study of Wiljmans and Baker.[31]

Let's now consider the ideal selectivities of the five different membranes. According to the ideal selectivity values (Fig. 3.10 and Fig. 3.11), the ceramic support (membrane 1) yielded selectivities in the range of the Knudsen selectivity for N_2/CF_4, N_2/C_3F_6 and CF_4/C_3F_6. This was expected for a typical microfiltration type membrane (pore size = 167 nm).

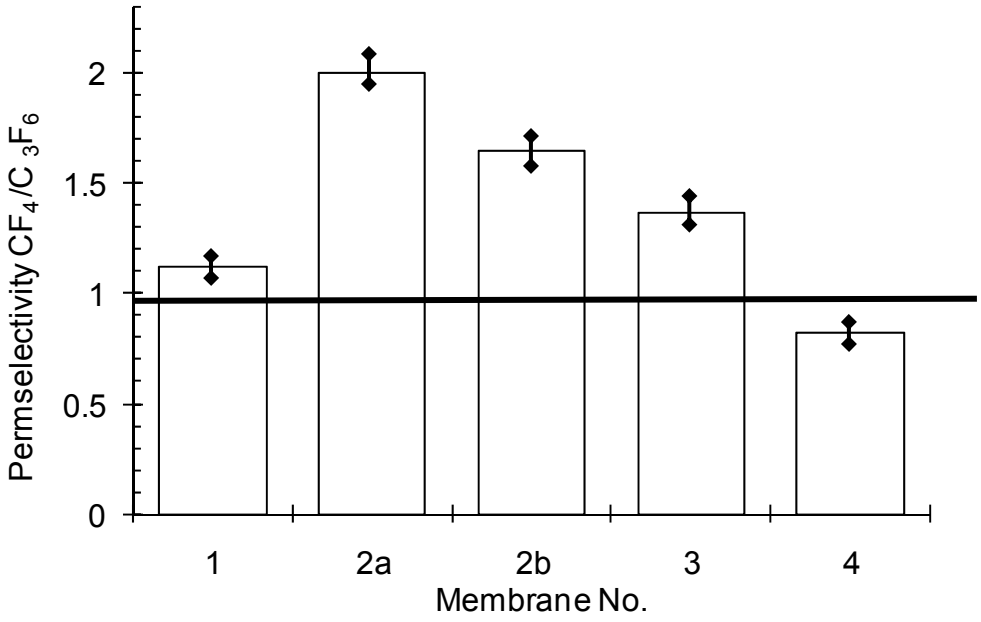

Figure 3.11 Permselectivity for CF_4/C_3F_6 for the (1) ceramic support, (2a) double Teflon coated ceramic, (2b) triple Teflon coated ceramic, (3) MFI coated ceramic and (4) composite ceramic membrane. The respective Knudsen selectivity value for CF_4/C_3F_6 is indicated by the cross bar and the deviations by the vertical lines on each respective bar.

The ideal selectivities for the double (membrane 2a) and triple Teflon® (membrane 2b) coated ceramic were above Knudsen selectivities for N_2/CF_4 and N_2/C_3F_6. The lower CF_4 and C_3F_6 permeabilities compared to N_2 were due to the

high saturation vapour pressure of CF_4 and C_3F_6 compared to N_2 according to Equation 3.6. According to Figure 3.11, CF_4/C_3F_6 ideal selectivities were above Knudsen with a preferential permeation of CF_4. This finding is in disagreement with those of Wijmans and Baker[31] for permeation of n-alkanes through silicone rubber membranes, where a higher permeation of C_3F_6 is expected.[31] It is assumed that this discrepancy was due to defects or cracks in the Teflon® layers not observed with the SEM analysis. In the presence of cracks, Knudsen diffusion, with a preferential transport of CF_4, is therefore the most likely mechanism of transport for the Teflon® coated ceramic.

The MFI coated ceramic (membrane 3) showed some degree of molecular sieving with selectivities slightly above Knudsen. When the size of the C_3F_6 molecule is considered with relation to the pore size of the MFI zeolite and the ideal selectivities obtained with only the ceramic support, it is evident that the contribution of non-zeolite pores to the total permeation is considerable.

The effect of combining a Teflon® layer and a MFI zeolite (membrane 4) is clearly seen as selectivities for N_2/CF_4 and N_2/C_3F_6 for the composite ceramic membrane increase dramatically compared to the Teflon® or zeolite only ceramic. The increased N_2/CF_4 and N_2/C_3F_6 selectivities were due to a dense defect-free Teflon® layer which effectively sealed the non-zeolite pores. The influence of the higher saturation pressures of CF_4 and C_3F_6 on the permeability coefficient was amplified by the defect-free Teflon® layer. The preferential permeation of C_3F_6 to CF_4 confirms this statement and is in agreement with the findings of Wijmans and Baker.[31] These results again confirm the existence of defects and/or cracks in both the Teflon® coated ceramic as well as the MFI coated ceramic membranes. This then also helps explain the results observed for the heat treatment variations of the composite membrane (Table 3.2). At 423 K the Teflon layer is defect free, hence increased solubility and permeance of C_3F_6. However at 473 K and above the Teflon layer tears resulting in gas permeation through the zeolite layer only and it has been shown (Fig. 3.10 and 3.11) that the zeolite layer on its own does also contain defects and hence the increase permeance of the smaller CF_4 at higher Teflon treatment temperatures.

In Table 3.4 some literature permeability values possibly relating to the gases evaluated in this study for polymer and zeolite membranes are presented. Since limited literature is available of C_xF_y, literature studies of C_xH_y were included for comparative purposes.

Table 3.4 Literature permeability values

Membrane	Reference	Gas	Permeance	
			Barrer[b]	10^{-8}mol.m^{-2}s.$^{-1}$Pa.$^{-1}$
AF 2400[a]	Pinnau *et al*.[33]	N_2	790	~ 1.47
		CH_4	600	~ 1.12
		C_2H_6	380	~ 0.71
		C_3H_8	200	~ 0.37
silicone Rubber	Hirayama *et al*.[34]	N_2	142	~ 0.047
		CF_4	73	~ 0.024
		C_2F_6	73	~ 0.024
		C_3F_8	108	~ 0.035
		C_4F_8	300	~ 0.097
		CH_4	480	~ 0.156
		C_2H_6	1420	~ 0.462
		C_3H_8	2950	~ 0.961
silicalite-1	Xiao *et al*.[35]	N_2		~ 8.7 – 81.9
silicalite-1	Arruebo *et al*.[36]	CH_4		~ 15
		C_2H_6		~ 8

[a] Obtained from the membrane with a 18 µm thickness. [b] Barrer = 10^{-10}cm^3(STP)cm/cm^{2}s.cmHg

Pinnau *et al*.[33] conducted permeability studies of gases including nitrogen and hydrocarbons through Teflon AF 2400 membranes. It is interesting to note that

the permeabilities deceased with increasing carbon chain length of the hydrocarbons, which is in disagreement with the predicted trend of Wiljmans and Baker.[31] A study by Hirayama *et al*.[34] on fluorocarbons and hydrocarbons through silicone rubber membranes (102 µm) however resulted in larger permeabilities for longer carbon chain length components, which again correlates with the study of Wijmans and Baker.[31] Hirayama *et al*.[34] stated that the reason for the increased permeability with increased molecular size was that a more condensable gas is more soluble in a polymer membrane. Apart from the difference in membrane material used, the permeances obtained in the study of Pinnau *et al*.[33] were notably higher than those obtained in the study by Hirayama *et al*.[34] which amongst others may be due to the thinner membrane thickness in the study by Pinnau *et al*.[33]

A decrease in permeability with increased gas molecular size was observed for the double and triple Teflon® coated ceramic membrane in this study similar to the AF 2400 membrane manufactured by Pinnau *et al*.[33] with permeabilities and selectivities comparable with the triple Teflon® coated ceramic membrane.

The silicon rubber membrane characterized with hydrocarbon and fluorocarbon gases by Hirayama *et al*.[34] showed similar permeability trends than the composite ceramic membrane synthesized in this study. The permeabilities increased with increased carbon chain length of the probe gas molecules. The composite ceramic membrane however had a superior permeability with regard to N_2, but a considerably lower CF_4 permeability resulting in a higher N_2/CF_4 permselectivity. Although C_3F_8 and not C_3F_6 was investigated by Hirayama *et al*., similar results are anticipated due to the number of carbons present in the molecules and therefore a lower N_2/C_3F_6 permselectivity is expected for silicon rubber membrane compared to the composite ceramic membrane in this study. The CF_4/C_3F_6 permselectivity in our study is comparable with the CF_4/C_3F_8 permselectivity in the study by Hirayama *et al*.[34]

According to the studies on silicalite-1 by Xioa *et al*.[35] and Arruebo *et al*.[36] the permeabilities of fluorocarbons through the MFI coated ceramic evaluated in this

study were low compared to the permeabilities of hydrocarbons using the same zeolite. However, similar to literature this study showed preferential permeation of the smaller molecules though the MFI membrane due to molecular sieving. The permselectivities obtained by Arruebo *et al*.[36] were however higher which is unexpected as an increased permselectivity is expected as permeability decreases. This observation again confirms the presence of defects in these membranes.

3.3.3 ADSORPTION

A comprehensive adsorption study has been conducted which has been discussed in Chapter 2 of this thesis. However to explain gas permeances through MFI (silicalite-1) and the composite membrane, it is essential to elaborate on the adsorption data.

The zeolite crystals used in the adsorption study were pure silicalite-1 crystals synthesized from a clear solution. The synthesis was conducted exactly as described for the MFI coated ceramic membrane without the addition of the α-alumina support.

The control adsorption study showed that no noticeable amounts of N_2, CF_4 or C_3F_6 adsorbed onto the α-alumina.

Adsorption of C_3F_6 onto silicalite-1 was higher than the adsorption of CF_4 (Figure 3.12), while N_2 adsorption was too low to measure. Higher adsorption amounts for longer carbon chain length compounds are commonly observed in literature[37,38] for hydrocarbons adsorbed onto molecular sieves. For fluorocarbon gases this was also observed in a study by Ahn *et al*.[39] where the longer chain carbon compound in their study, namely C_2F_6, was adsorbed in larger amounts than CF_4 onto Zeolite 13X over the entire pressure and temperature range.

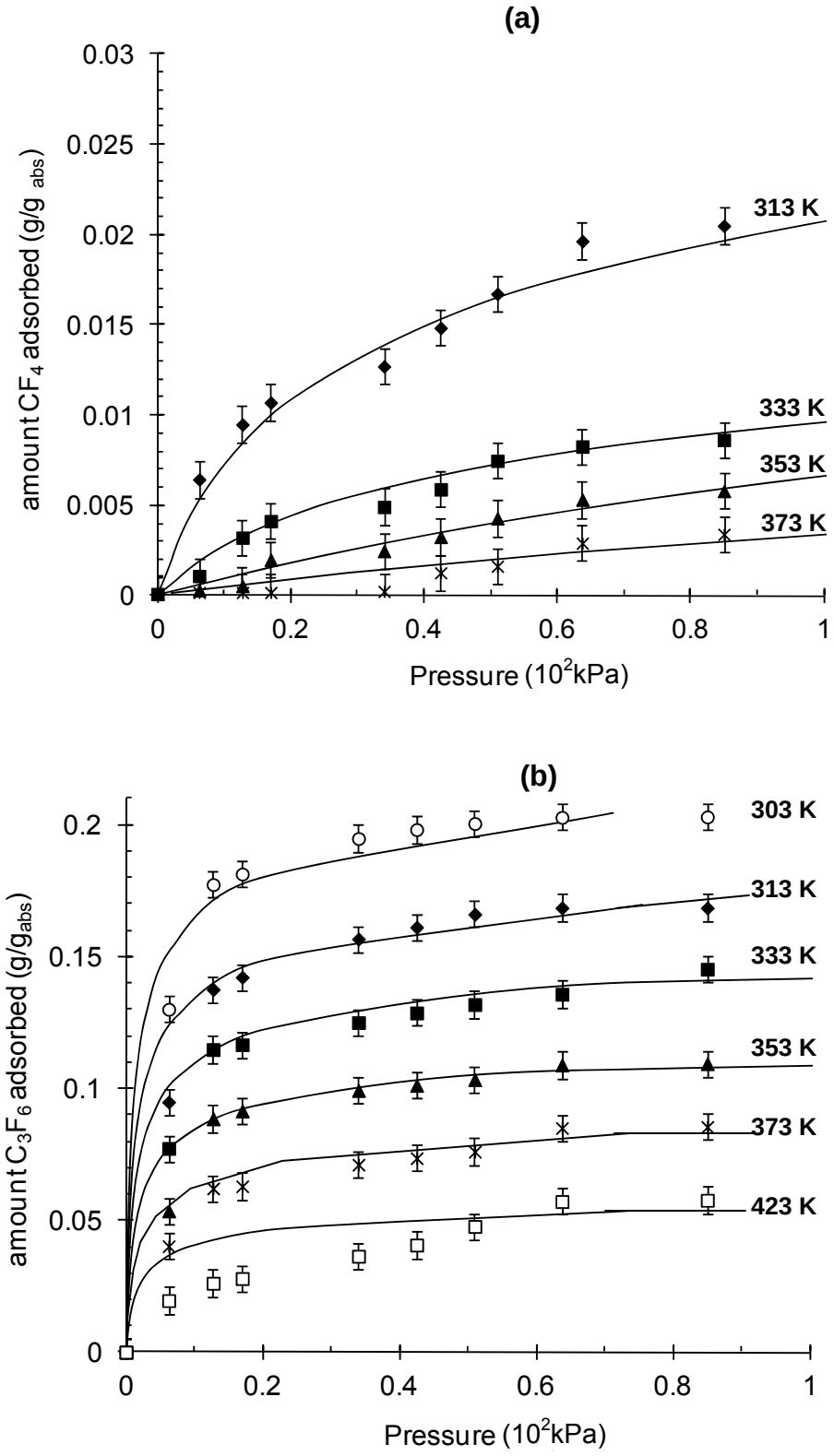

Figure 3.12 Adsorption isotherms of (a) CF_4 and (b) C_3F_6 on MFI (silicalite-1) at 303 (o), 313 (♦), 333 (■), 353 (▲), 373 (Ж) and 423 K (□).

The adsorption amount in this study decreased with increasing temperature as would be expected.[39] There was an increase in adsorption with increased pressure for both CF_4 and C_3F_6. Theoretical selectivities (based on adsorption) increase with increasing temperature. The calculated selectivities for example at 85 kPa were 5, 10, 11, and 15 at 313, 333, 353, and 373 K respectively. For the silicalite-1, the maximum theoretical selectivity of 15 (mol to mol ratio in favour of C_3F_6) was obtained at 373 K when the amounts of CF_4 and C_3F_6 adsorbed at 85 kPa was used in the calculation.

The only noticeable amount of CF_4 adsorption onto the Teflon® (results not shown) was observed at 293 K and 85 kPa. The maximum adsorbed amount recorded was 0.0024 g/g_{abs} (0.27 x 10^{-4}mol). The adsorption of N_2 onto Teflon AF 2400 was also investigated, but no noticeable adsorption was obtained. The adsorption isotherms of C_3F_6 on Teflon AF 2400 are shown in Figure 3.13.

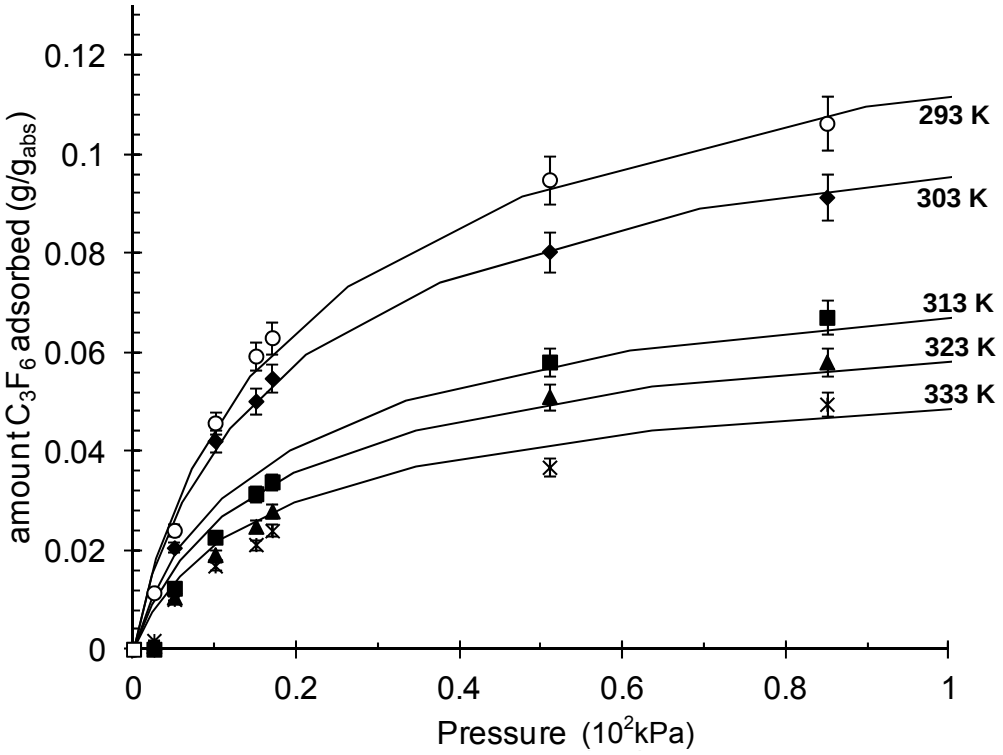

Figure 3.13 Adsorption isotherms of C_3F_6 on Teflon AF 2400 at 293 (o), 303 (♦), 313 (■), 323 (▲) and 333 (Ж).

Isotherms were obtained at temperatures ranging from 303 to 333 K. The amount of C_3F_6 adsorbed increased with increased pressure and decreased temperature. A theoretical selectivity of 26 in favour of C_3F_6 was calculated in terms of the maximum molar amount of gas adsorbed at 293 K for CF_4 and C_3F_6 onto Teflon®.

It is well known that the solubility of a gas in a polymer structure is related to the condensability of the gas. The condensability is a function of the critical temperature which is in turn related to the diameter of the gas molecule.[40] The critical temperature of N_2, CF_4 and C_3F_6 is 129.2 K[41], 227.65 K[42] and 359.35 K[41] respectively. It is obvious that the C_3F_6 molecule is larger than the CF_4[43] molecule, while the N_2 molecule is the smallest. The calculated diameters of the gases according to molecular modelling were 0.168, 0.268, and 0.552 nm for N_2, CF_4 and C_3F_6 respectively. The reason why C_3F_6 was preferentially adsorbed both for the zeolite and the Teflon AF 2400 is therefore due to the higher condensability and thus solubility of C_3F_6 in the Teflon®.

By fitting the Langmuir isotherm to the adsorption data, the maximum adsorption at each temperature was obtained (Fig. 3.12 and 3.13). The results are shown in Table 3.5.

The adsorption results explain why a higher permeability of C_3F_6 as compared to CF_4 was obtained through the composite ceramic membrane. The contribution of the solubility effect was however not significant enough when the Teflon® coated ceramic membrane was considered due to the presence of defects which favours the contribution of the diffusion coefficient term to the permeability according to Equation 3.6.

Table 3.5 Langmuir isotherm parameters estimated for CF_4 and C_3F_6 on silicalite-1 and Teflon AF 2400

Gas	Adsorbent	Temperature (K)	q_m (g/g_{abs})	q_m (mol_{gas}/g_{abs}) x 10^{-4}
CF_4	MFI	313	0.060	6.82
		333	0.029	3.30
		353	0.020	2.27
		373	0.011	1.25
C_3F_6	MFI	303	0.255	17.0
		313	0.212	14.1
		333	0.175	11.7
		353	0.133	8.87
		373	0.103	6.67
		423	0.067	4.47
C_3F_6	Teflon	293	0.172	11.5
		303	0.148	9.87
		313	0.113	7.53
		323	0.109	7.27
		333	0.094	6.27

3.4 Conclusions

One paramount factor that determines the performance of inorganic membranes for gas separation is the amount of defects present in the selective layer. For continuous layer zeolite membranes, defects result from intercrystalline slits[11] and crack formation[26] during synthesis and template removal. The prevention or "repair" of defects is essential to obtain high ideal selectivity values.

A composite ceramic membrane consisting of a ceramic support structure, an MFI intermediate zeolite layer and a Teflon AF 2400 top layer was developed for

separation of N_2, CF_4, and C_3F_6. The synthesis of the Teflon® layer is aimed at the closure of possible defects present in the separation layer forcing the gas molecules to follow the path through the zeolite pores. In the evaluation, the composite membrane was compared with a ceramic membrane, an MFI coated ceramic membrane and a Teflon® coated ceramic membrane using single gas permeation experiments. Adsorption experiments were performed on materials present in the membrane structures to clarify the results obtained.

The two best performing membranes according to N_2/CF_4 and N_2/C_3F_6 ideal selectivities was the Teflon® coated ceramic membrane and the composite ceramic membrane. Although the top layer in both membranes was similar, the presence of the MFI zeolite in the composite ceramic membrane resulted in higher permselectivities. For the composite ceramic membrane ideal selectivities of 86 and 71 were obtained for N_2/CF_4 and N_2/C_3F_6 respectively, compared to 5.5 and 8 for the Teflon® coated ceramic. CF_4/C_3F_6 selectivities ranged from 0.9 to 2 with C_3F_6 permeating faster though the composite ceramic membrane.

The high adsorption of C_3F_6 onto Teflon AF 2400 compared to CF_4 results in a considerable contribution to permeation for the composite ceramic membrane. The sealing effect of the zeolite layer by the Teflon® layer is however the reason for the large N_2/CF_4 and N_2/C_3F_6 selectivities obtained.

3.5 Acknowledgement

The financial assistance of the Innovation Fund (IF), of South Africa (Project T50021), a separate business unit of the Department of Science and Technology (DST), is hereby acknowledged. The financial assistance of the South African Nuclear Energy Corporation (Necsa), towards this research is hereby also acknowledged. The authors wish to thank Dr. L. Tiedt (NWU, South Africa) for the SEM images and Mr. J. Kroeze and Mr. A. Brock (Technical Advisory, NWU, South Africa) for the manufacture of the membrane reactors and the permeation setup. The authors also want to acknowledge the contribution of

Dr. Klaus-Victor Peinemann, (GKSS Research Centre, Germany) towards the application of a polymer layer for sealing of defects present in a zeolite membrane.

3.6 References

[1] A. Singh, W.J. Koros, Significance of entropic selectivity for advanced gas separation membranes, Industrial and Engineering Chemistry Research, 35, (1996) 1231.

[2] T.C. Bowen, R.D. Noble, J.L. Falconer, Fundamentals and applications of pervaporation through zeolite membranes, Journal of Membrane Science, 245, (2004) 1.

[3] T. Chung, L.Y Jiang, Y. Li, S. Kulprathipanja, Mixed matrix membranes (MMMs) comprising organic polymers with dispersed inorganic fillers for gas separation, Progress in Polymer Science, 32, (2007) 483.

[4] J. Caro, M. Noack, Zeolite membranes – Recent developments and progress, Microporous and Mesoporous Materials, 115, (2008) 215.

[5] Y. Yan, M.E. Davis, G.R. Gavalas, Preparation of highly selective zeolite ZSM-5 membranes by a post-synthetic coking treatment, Journal of Membrane Science, 123, (1997) 95.

[6] J. Hedlund, F. Jareman, A. Bons, M. Anthonis, A masking technique for high quality MFI membranes, Journal of Membrane Science, 222, (2003) 163.

[7] S. Miachon, E. Landrivon, M. Aouine, Y. Sun, I. Kumakiri, Y. Li, O. Pachtov´a Prokopov´a, Nanocomposite MFI-alumina membranes via pore-plugging synthesis: Preparation and morphological characterization, Journal of Membrane Science 281, (2006) 228.

[8] S. Nair, M. Tsapatsis, Synthesis and properties of zeolitic membranes, in S.M. Auerbach, K.A. Carrado, P.K. Dutta (Eds.), Handbook of Zeolite Science and Technology, Marcel Dekker Inc., New York, Basel, (2003) pp. 867 – 919.

[9] A. van Niekerk, J. Zah, J.C. Breytenbach, H.M. Krieg, Direct crystallisation of a hydroxysodalite membrane without seeding using a conventional oven, Journal of Membrane Science, 300, (2007) 156.

[10] T. Sano, S. Ejiri, K. Yamada, Y. Kawakami, H. Yanagishita, Separation of acetic acid-water mixtures by pervaporation through silicalite membranes, Journal of Membrane Science, 123, (1997) 225.

[11] J.B. Lee, H.H. Funke, R.D. Noble, J.L. Falconer, Adsorption-induced expansion of defects in MFI membranes, Journal of Membrane Science, 341, (2009) 238.

[12] M. Noack, P. Kölsch, A. Dittmar, M. Stöhr, G. Georgi, R. Eckelt, J. Caro, Effect of crystal intergrowth supporting substance (ISS) on the permeation properties of MFI membranes with enhanced Al-content, Microporous and Mesoporous Materials, 97, (2006) 88.

[13] M. Kanezashi, J. O'Brien, Y.S. Lin, Template-free synthesis of MFI-type zeolite membranes: Permeation characteristics and thermal stability improvement of membrane structure, Journal of Membrane Science, 286, (2006) 213.

[14] Y. Yan, M.E. Davis, G.R. Gavalas, Preparation of highly selective zeolite ZSM-5 membranes by a post synthetic coking treatment, Journal of Membrane Science, 123, (1997) 95.

[15] M. Noack, J. Caro, Zeolite membranes – Recent developments and progress, Microporous and Mesoporous Materials, 115, (2008) 215.

[16] J. Shieh, T. Chung, D.R. Paul, Study on multi-layer composite hollow fiber membranes for gas separation, Chemical Engineering Science, 54, (1999) 675.

[17] R.W. Baker, Membrane Technology and Applications, Second Edition, Wiley, (2004) p. 126 & p. 313.

[18] S. Li, D. Jinjin, Improvement of hydrophobic properties of silk and cotton by hexafluoropropene plasma treatment, Applied Surface Science, 253, (2007) 5051.

[19] A.B. Hinchliffe, K.E. Porter, A comparison of membrane separation and distillation, Chemical Engineering Research and Design, 78, 2, (2000) 255.

[20] H. Bissett, J. Zah, H.M. Krieg, Manufacture and Optimization of tubular ceramic membrane supports, Powder Technology, 181, (2008) 57.

[21] J. Hofman-Züter, Chemical and thermal stability of modified mesoporous ceramic membranes, Nerderlands, Twente, Ph.D. thesis, (2003) p. 211.

[22] A. Van Niekerk, Direct crystallization of hydroxysodalite and MFI membranes on α-alumina support, South Africa, Potchefstroom, M.Pharm, (2005) pp. 63-64.

[23] J.D. Seader, E.J. Henley, Separation process principles, John Wiley & Sons, Inc., (1998) Chapter 15.

[24] T. Zivkovic, Thin Supported Silica Membranes, Twente, The Netherlands, Ph.D., (2007) p. 5.

[25] M.M.J. Treacy, J.B. Higgins, Collection of Simulated XRD Power Patterns for Zeolites, 4th ed., Elsevier, Amsterdam, (2001).

[26] M. L. Gualtieri, C. Andersson, F. Jareman, J. Hedlund, A. F. Gualtieri, M. Leoni, C. Meneghini, Crack formation in α-alumina supported MFI zeolite membranes studied by in situ high temperature synchrotron powder diffraction, Journal of Membrane Science 290, (2007) 95.

[27] E.E. McLeary, J.C. Jansen, F. Kapteijn, Zeolite based films, membranes and membrane reactors: Progress and prospects, Microporous and Mesoporous Materials, 90, (2006) 198.

[28] N.N. Li, A.G. Fane, W.S.W. Ho, T. Matsuura, Advanced membrane technology, John Wiley and sons, New Jersey, 2008, Chapter 23, pp. 650.

[29] R.W. Baker, Membrane technology and applications, McGraw Hill, 2000, Appendix A, pp. 531.

[30] E. Albrecht, G. Baum, T. Bellunato, A. Bressan, S. D. Torre, C. D'Ambrosio, M. Davenport, M. Dragicevic, S. D. Pinto, P. Fauland, S. Ilie, G. Lenzen, P. Pagano, D. Piedigrossi, F. Tessarotto, O. Ullaland, VUV absorbing vapours in n-perfluorocarbons, Nuclear Instruments and Methods in Physics Research A, 510, (2003) 262.

[31] J.G. Wijmans, R.W. Baker, The solution-diffusion model: a review, Journal of Membrane Science, 107, (1995) 1.

[32] S.A. Stern, Polymers for Gas Separations: The Next Decade, Journal of Membrane Science, 94, (1994) 1.

[33] I. Pinnau, L.G. Toy, Gas and vapor transport properties of amorphous perfluorinated copolymer membranes based on 2,2-bistrifluoromethyl-4,5-difluoro-1,3-dioxole/tetrafluoroethylene, Journal of Membrane Science, 109, (1996) 125.

[34] Y. Hirayama, N. Tanihara, Y. Kusuki, Y. Kase, K. Haraya, K. Okamoto, Permeation properties to hydrocarbons, perfluorocarbons and chlorofluorocarbons of cross-linked membranes of polymethacrylates with poly(ethylene oxide) and perfluorononyl moieties, Journal of Membrane Science, 163, (1999) 373.

[35] W. Xiao, J. Yang, J. Lu, J. Wang, A novel method to synthesize high performance silicalite-1 membrane, Separation and Purification Technology, 67, (2009) 58.

[36] M. Arruebo, J. Coronas, M. Menendez, J. Santamarı´a, Separation of hydrocarbons from natural gas using silicalite membranes, Separation and Purification Technology, 25, (2001) 275.

[37] J. Peng, H. Ban, X. Zhang, L. Song, Z. Sun, Binary adsorption equilibrium of propylene and ethylene on silicalite-1: prediction and experiment, Chemical Physics Letters, 401, (2005) 94.

[38] R.W. Triebe, F.H. Tezel, K.C. Khulbe, Adsorption of methane, ethane and ethylene on molecular sieve zeolites, Gas Separation and Purification, 10, (1996) 81.

[39] N. Ahn, S. Kang, B. Min, S. Suh, Adsorption Isotherms of Tetrafluoromethane and hexafluoroethane on various adsorbents, Journal of Chemical Engineering Data, 51, 2006, 451.

[40] M. Dingemans, J. Dewulf, A. Kumar, H. van Langenhove, Solubility of volatile organic compounds in polymers: Effect of polymer type and processing, Journal of Membrane Science, 312, (2008) 107.

[41] MSDS.

[42] S. Stapf, S. Han, NMR Imaging in Chemical Engineering, Wiley-VCH, (2006) Chapter 3, p. 310.

[43] G. Grazian, On superhydrophobicity of tetrafluoromethane, Chemical Physical Letters, 460, (2008) 470.

CHAPTER 4

ZEOLITE BASED MEMBRANE SEPARATION OF NITROGEN, TETRAFLUOROMETHANE AND HEXAFLUOROPROPYLENE BINARY GAS MIXTURES

ABSTRACT

An existing challenge entails the separation of N_2, CF_4 and C_3F_6, currently attained by an energy intensive cryogenic distillation process. Based on our existing expertise in the field of zeolite membranes, the separation capability of zeolite (MFI, NaA, NaY and hydroxysodalite) coated tubular ceramic membranes for the separation of the above mentioned gases was investigated. During single gas studies, selectivities near or below Knudsen selectivities were obtained for all membranes due to non-zeolitic pore diffusion. To improve on the obtained ideal selectivities, a Teflon AF 2400 layer was applied to the tubular ceramic support and the MFI coated ceramic membrane yielding composite membranes. Based on these results, the hydroxysodalite (HS), MFI, Teflon layered ceramic and the composite ceramic membranes were chosen for binary gas mixture separation. Permeation varied between 1.08×10^{-8} $mol.s^{-1}.m^{-2}.Pa^{-1}$ and 0.82×10^{-8} $mol.s^{-1}.m^{-2}.Pa^{-1}$ for the MFI coated ceramic and the composite membrane respectively. In spite of the decrease in permeation in the presence of the Teflon layer, the selectivities for the N_2/CF_4 mixture increased from 1.2 to 4.0. The N_2/C_3F_6 selectivity increased from 2.0 to 2.4, with the CF_4/C_3F_6 selectivity decreasing from 1.8 to 1.2. This decrease in CF_4/C_3F_6 selectivity can be attributed to the higher solubility of the C_3F_6 molecule in the Teflon AF 2400 resulting in an increased competitive permeability of C_3F_6 compared to CF_4.

Keywords: N_2, CF_4, C_3F_6, zeolite, MFI, Teflon AF 2400

4.1 Introduction

Membrane separation processes provide several advantages over other conventional separation techniques. For example, no phase transformation is required for membrane separation, increasing the energy efficiency of the process. Equipment used in membrane separation is compact, which simplifies the operation.[1]

Membranes have been widely used in industry for the past two decades and an annual growth rate of about 10 percent has been forecast. Currently polymeric membranes dominate industrial applications, but recently research and application of inorganic membranes has gained momentum in new fields, such as fuel cells and high temperature separations.[2]

In the field of gas separation the use of inorganic membranes is hindered by the lack of technology to manufacture continuous and defect-free membranes.[3] Thus far for zeolites, only silicalite and ZSM-5 membranes have been prepared with adequate selectivities for gas separation.[4] Although the literature shows that increased selectivity can be achieved by altering synthesis methods,[5] or by elimination of possible defects by pre- or post synthesis treatment,[6,7,8] the use of zeolites to date is still largely restricted to the separation of condensable gases, due to the low selectivities experienced with non-condensable gas mixtures.[9,10]

The application of cross linked mixed matrix membranes for gas separation has attracted attention recently. Polymer membrane performance experiences the so called “upper bound” trade-off and new types of materials are needed to exceed this barrier. A major problem with mixed matrix membranes is the poor adhesion of the polymer-zeolite interface, which can result in non-selective voids and subsequent reduction in apparent selectivity.[11] In composite multi-layer membranes, where the selective layer is a polymer, the application of a highly permeable material such as silicone rubber over the polymer as a sealing or protective layer, generally increases selectivity.[12] Although some research on composite mixed matrix membranes (MMM) has been performed (such as thin

MMM deposited on porous ceramic supports) few studies have been done on the application of a highly permeable polymer layer on a composite inorganic membrane with a zeolite selective layer.[13]

Cryogenic distillation is currently the most widely used technique for the separation of C_xF_y gases. It is, however, an energy intensive process[14] which makes the exploration of alternative separation techniques, such as a membrane process, an attractive option.

The synthesis of a composite zeolite membrane and the application of a thin, highly permeable sealing layer over the zeolite layer for the separation of non-condensable C_xF_y gas mixtures (N_2, CF_4 and C_3F_6) was the subject of the current study. The composite inorganic-polymer membrane consisted of a α-alumina support, various zeolite layers and a Teflon AF 2400 polymeric sealing layer. Teflon AF 2400 (copolymer of 2,2-bis-trifluoromethyle-4,5-difluorodioxole and tetrafluoroethylene) was chosen due to its high gas permeability[15] and the nature of the non-condensable gases (fluorocarbons) investigated.

4.2 Experimental

4.2.1 MEMBRANE SYNTHESIS

In this study α-alumina supports, MFI coated ceramic membranes, Teflon® (PTFE) coated ceramic membranes and composite ceramic membranes were synthesized for the separation of the non-condensable gases investigated.

4.2.1.1 α-ALUMINA SUPPORT

Tubular α-alumina supports were manufactured in-house from a commercial powder (AKP-15; Sumitomo Chemical Co. Ltd, Japan) by centrifugal casting as described by Bissett *et al*.[16] The powder compact was sintered at 1473 K for 1 h. Tubes were cut to a length of 0.055 m and sonication in deionised water was conducted for 3 x 10 min to remove particle residues ensuring a clean surface for attachment of subsequent layers.

A layer specific pre-synthesis treatment was used for each separation layer to enhance crystal growth or attachment as described in the subsequent sections.

4.2.1.2 NAA COATED CERAMIC MEMBRANE

For the NaA coated ceramic membrane, the support was pretreated with UV radiation from a 400 Watt UV high pressure mercury vapour lamp (HOK 4/120, UV+IR Engineering). The tube was vertically submerged in deionised water and continuously irradiated for 10 h, inverted (180 °) and irradiated for a further 10 h.

A single step direct *in situ* crystallization from a clear solution was employed to deposit the NaA zeolite layer onto the ceramic tubular support, using the procedure of Zah *et al*.[17] The molar oxide ratio of the clear solution was $48.9Na_2O$: $1Al_2O_3$: $5.08SiO_2$: $979.2H_2O$. The two reactant mixtures (silicate and aluminate) were prepared and aged separately for one hour at room temperature after which the aluminate solution was added drop-wise to the silicate solution under continuous stirring. The compositions of the reactant mixtures are given in Table 4.1.

Table 4.1 Reactant mixture compositions for the NaA clear solution synthesis

Reactant mixture	$Na_2SiO_3 \bullet 5H_2O$[a] (g)	$NaAlO_2$[b](g)	NaOH (g)	H_2O (g)
Silicalite solution	2.628	-	3.481	20
Aluminate solution	-	0.452	4.807	20

[a] 28% Na_2O, 27% SiO_2; BDH, technical grade [b] 41% Na_2O, 54% Al_2O_3, Riedel-de Haën/Fluka [c] NaOH, Merck

The clear silicate/aluminate solution was aged for a further hour at room temperature. The support was wrapped in PTFE tape and placed in a 25 ml Teflon-lined tubular stainless steel autoclave. 15 ml clear solution was poured into the autoclave and the reaction unit sealed. Crystallization proceeded for 4 h at 358 K, while the autoclave was rotated at 25 rotations per minute around the horizontal axis. After the synthesis, the oven was switched off and the reactor allowed to cool for 3 h, while rotation continued.

The membrane was removed from the autoclave and neutralised by ultrasonic treatment in deionised water for 6 x 10 min. After neutralization was achieved, the membrane was dried overnight at 393 K, using a slow heating and cooling rate (~ 0.5 K/min).

A second layer was then deposited resulting in a double layered zeolite membrane.

4.2.1.3 HYDROXYSODALITE COATED CERAMIC MEMBRANE

The support used for the hydroxysodalite (HS) layer was pretreated with UV radiation, similarly to the NaA coated membrane.

For the direct *in situ* crystallization, two zeolite precursor solutions were prepared consisting of a silicate and an aluminate species. The compositions of the precursor mixtures (which differ for the 1st and 2nd layer synthesis) are given in Table 4.2.

Table 4.2 Reactant mixture compositions for the HS clear solution synthesis

Reactant mixture	$Na_2SiO_3 \bullet 5H_2O$[a] (g)		$NaAlO_2$[b](g)		NaOH[c] (g)		H_2O (g)	
	1st layer	2nd Layer	1st layer	2nd layer	1st layer	2nd layer	1st layer	2nd layer
Silicalite	6.18	5.46	-	-	8.56	7.57	20	20
Aluminate	-	-	1.10	0.97	11.82	10.45	20	20

[a] 28% Na_2O, 27% SiO_2; BDH, technical grade [b] 41% Na_2O, 54% Al_2O_3, Riedel-de Haën/Fluka [c] NaOH, Merck

For both the reactant mixtures the NaOH was firstly completely dissolved in water and the respective aluminate or silicate subsequently added. Both solutions were aged separately for 1 h in a water bath at 303 K (1st ageing period). Thereafter the aluminate solution was added drop-wise to the silicate under continuous stirring. The clear solution for the 1st layer hydrothermal synthesis (molar oxide ratio : $50Na_2O$: $1Al_2O_3$: $5SiO_2$: $450H_2O$) was aged in the water bath for 6 h (2nd ageing period). After ageing, 25 ml of this solution was poured into the reactor, containing the pre-treated, PTFE wrapped, ceramic support. Synthesis for the first zeolite layer was initiated in a conventional oven by ramping up the temperature at 3 K/min to a final temperature of 363 K and maintaining this temperature for 6 h. Upon completion, the reactor was allowed to cool. The membrane was removed from the vessel and rinsed with deionised water and then ultrasonically treated for 6 x10 min. After every 10 min, fresh deionised water was used in order to neutralise the membrane. The membrane was dried overnight at 393 K.

The procedure above was repeated, but with the reactant mixture compositions as indicated in Table 4.2 for the 2nd layer synthesis. The ageing period for the second layer synthesis was 4 h, while the duration of hydrothermal treatment was 5 h.

4.2.1.4 NaY COATED CERAMIC MEMBRANE

The support for the NaY synthesis required no additional pre-treatment.

For the direct *in situ* crystallization, two zeolite precursor solutions were prepared consisting of a silicate and an aluminate species. The composition of the precursor mixtures is given in Table 4.3.

Table 4.3 Reactant mixture compositions for the NaY clear solution synthesis

Reactant mixture	$Na_2SiO_3 \bullet 5H_2O$[a] (g)	$NaAlO_2$[b](g)	NaOH[c] (g)	H_2O (g)
Silicalite solution	1.706	-	1.568	20
Aluminate solution	-	0.152	1.568	20

[a] 28% Na_2O, 27% SiO_2; BDH, technical grade [b] 41% Na_2O, 54% Al_2O_3, Riedel-de Haën/Fluka [c] NaOH, Merck

The NaOH was weighed into separate dry PTFE bottles for both the aluminate and silicate species, after which the appropriate amount of deionised water was added. The sodium aluminate and sodium metasilicate were weighed into separate dry PTFE bottles and then sodium hydroxide solutions were added quantitatively to the sodium aluminate and sodium metasilicate, respectively. Subsequently, the two bottles were sealed and aged in a water bath at 25 ºC for 1 h under continuous stirring. After this (first ageing step) the aluminate solution was rapidly and quantitatively added to the silicate solution. The aluminate-silicate solution was aged in a water bath at 25 ºC for another 24 h under continuous stirring. After the completion of the second aging step, 25 ml of the solution was placed in a Teflon lined stainless steel autoclave with an α-alumina support. The autoclave was sealed and fastened in the rotator, situated in the conventional oven, pre-heated to 90 ºC. The synthesis for the first zeolite layer was achieved in 12 h. After completion the reactor was allowed to cool. The membrane was removed from the vessel and rinsed with deionised water and then ultrasonically treated for 6 x 10 min. After each 10 min period,

fresh deionised water was used to neutralise the membrane. The composite membrane was dried overnight at 393 K.

A second layer was then deposited by following the same procedure as described above.

4.2.1.5 MFI COATED CERAMIC MEMBRANE

Synthesis of the MFI coated ceramic membrane was conducted as described by Bissett and Krieg.[18]

4.2.1.6 TEFLON COATED CERAMIC MEMBRANE

Synthesis of the Teflon® coated ceramic membrane was conducted as described by Bissett and Krieg.[18]

4.2.1.7 COMPOSITE CERAMIC MEMBRANE

The composite ceramic membrane, consisting of a ceramic support, an MFI zeolite layer coated with Teflon AF 2400, was synthesized as described by Bissett and Krieg.[18] The heat treatment was done at 423 K for optimum attachment of the Teflon® onto the MFI layer.

4.2.2 MEMBRANE CHARACTERIZATION

Membranes were characterized according to morphology, single gas permeability and binary mixture permeability. Ideal selectivities and binary mixture separation selectivities were also obtained.

4.2.2.1 MORPHOLOGY AND ELEMENTAL ANALYSIS

Features such as membrane thickness and layer continuity were investigated by scanning electron microscopy (SEM - FEI ESEM Quanta 200, OXFORD INCA 200 EDS SYSTEM). Dried samples were coated with Au/Pd (80/20) prior to analysis

The identity of the zeolite phases was determined using X-Ray diffraction (XRD) analysis. This was done by applying CuKα radiation (λ_k = 1.5418 Å) at 40 kV with a Röntgen PW3040/60 X'Pert Pro diffractometer system. Spectra were interpreted using the 2007 Relational Database (International Centre for Diffraction Data).

4.2.2.2 SINGLE GAS PERMEATION

Single gas permeation values were measured for N_2, CF_4 and C_3F_6, the feed gas system to be evaluated in this study. The continuous flow method was used with the membrane sealed in a dead-end configuration (Fig. 4.1).

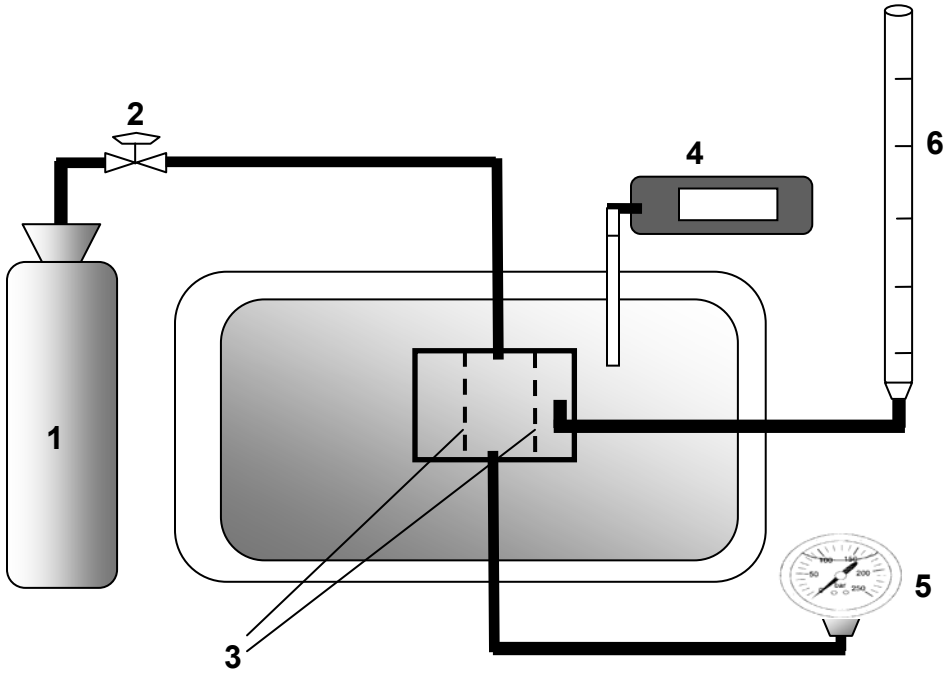

Figure 4.1 The experimental set-up for the single gas permeation

The membranes (**3**) were sealed in a gas tight permeation module. The module was positioned vertically in an oven. The temperature was electronically controlled (**4**) to ± 2 K of the set-point. The transmembrane pressure was monitored by a pressure gauge (**5**) and the gas feed (**1**) to the inner-tube side of the membrane was controlled by a pressure regulator (**2**). The permeate flow was measure by a soap bubble flow meter (**6**) at atmospheric pressure (87 kPa).

Due to the nature of the membranes, (especially the hydrophilic zeolite layers) the membranes were conditioned prior to measurements. Each membrane was purged at a transmembrane pressure of 20 kPa with He overnight at 373 K to remove any residual moisture. The membranes were purged subsequently with each gas for at least 3 h to remove any He present and to allow a steady permeation state to be reached.

The permeation flux ($mol.m^{-2}.s^{-1}$) in each experiment was recorded as an average of 5 measurements over a period of 60 min to ensure that a steady rate

had been reached. The permeance (mol.m^{-2}.s^{-1}Pa.$^{-1}$) was calculated from the flux divided by the transmembrane pressure. The same membrane reactor was used in all cases. Accordingly, the total membrane area for the gas permeation experiments was based on the length (0.055 m) of the membrane and the diameter of the tube (0.0177 m). The calculated total membrane surface was 3.06 x 10^{-3} m^2. This value was used in all subsequent calculations.

The ideal or permselectivity ($PS_{i/j}$) for gas *i* and gas *j* was defined as the single-component permeance ratio at a given temperature and transmembrane pressure. The permselectivities were qualitatively compared to the Knudsen selectivities to evaluate the performance of each membrane. The Knudsen selectivities (α_k) were obtained by :

$$\alpha_k \left(\frac{i}{j}\right) = \sqrt{\frac{M_j}{M_i}} \qquad (4.1)$$

with *M* the molar weight (g/mol) of the gas.[19]

4.2.2.3 BINARY MIXTURE SEPARATION

All the membranes screened during the C_xF_y single gas permeation experiments were evaluated and those membranes with promising results were chosen for the binary mixture separation. The experimental set-up is shown in Figure 4.2.

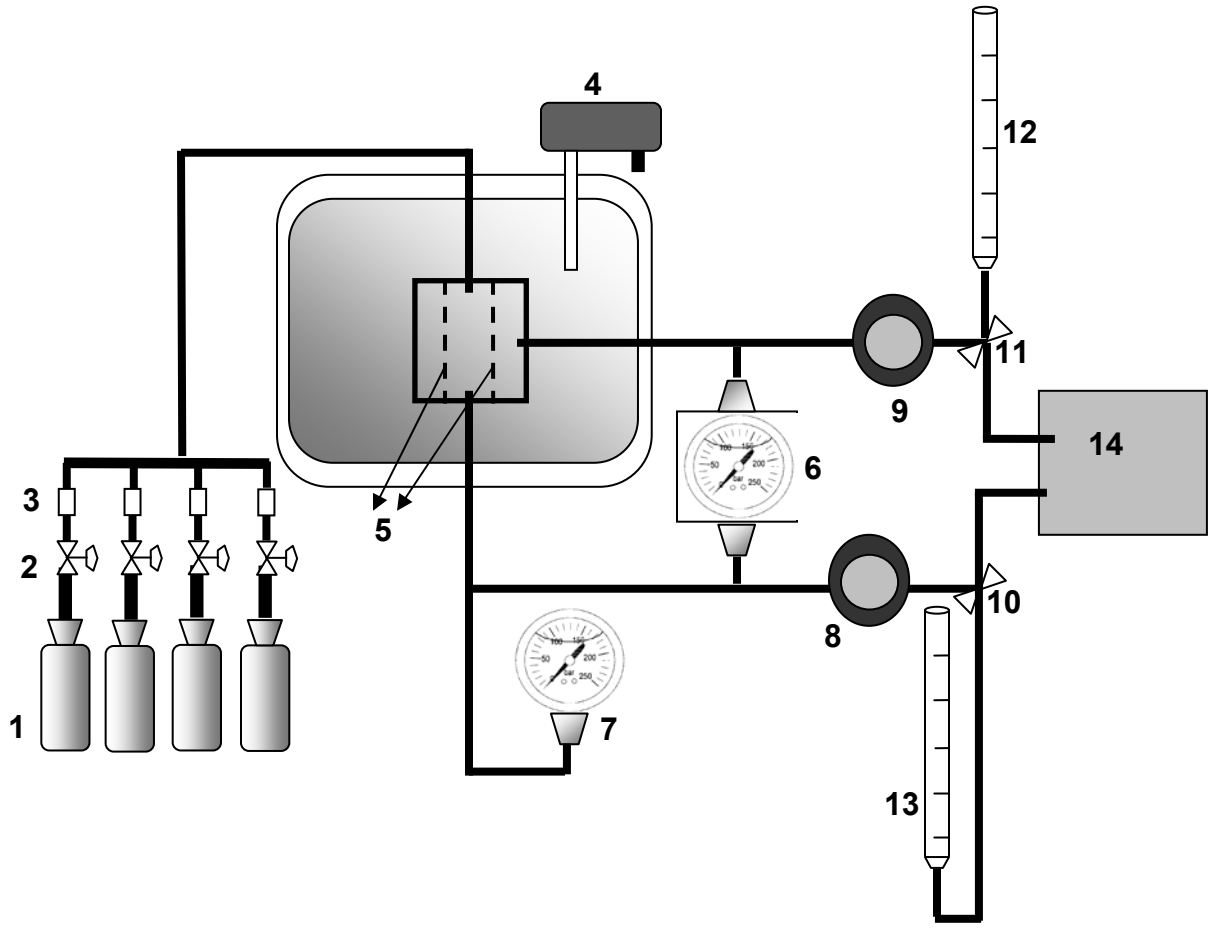

Figure 4.2 Experimental set-up for the binary mixture separation

The membranes (**5**) were sealed into a gas-tight module in the continuous flow configuration. The module was positioned vertically in an oven of which the temperature was controlled by a relay-connected thermocouple (**4**, Shinka GCS-300). He, N_2, CF_4 and C_3F_6 (**1**; N_2 and helium obtained from Afrox, SA; CF_4 and C_3F_6 obtained from Necsa) were fitted with stainless-steel pressure regulators (**2**; TESCOM Europe, 35 bar max.outlet) and set 100 kPa. Pre-calibrated mass flow controllers (**3**; Brooks Instruments B.V., Model 5850S) were used to regulate the gas feed rate from the respective gas bottles into the tube side of the tubular membrane. The binary mixture used was obtained by feeding pre-determined fractions of two chosen gases through the mass flow controllers. For all experiments an approximate 50/50 volume percentage of the two gases

were investigated with a total feed rate in all experiments of 100 ml/min. The absolute pressure in the tube was monitored by an electronic pressure gauge (**7**; WIKA Transmitter UT10) and controlled with a back-pressure regulator (**8**; Swagelok Inlet 0 - 250 psig) both of which were connected to the retentate outlet. A differential pressure gauge (**6**; WIKA Delta-Trans Differential pressure transmitter, Model 891.34.2189) monitored the pressure difference between the retentate and permeate lines. A back-pressure regulator connected to the permeate outlet (**9**; Swagelok Inlet 0-250 psig) was used to adjust the transmembrane pressure. The permeate and retentate flows were measured by downstream soap bubble flow meters (**12** & **13** respectively) under local atmospheric conditions (87 kPa). Analyses of the permeate or retentate stream were individually performed by switching the outlets towards a gas chromatograph (**14**) by means of 3-way valves (**10** & **11** respectively).

4.2.2.3.1 GAS CHROMATOGRAPH CALIBRATION

The gas chromatograph (GC) used in this study was a Carlo Erba GC 6000 Vega Series 2 equipped with a Carlo Erba HWD 450 thermal conductive detector (TCD). The attenuation was set to 128 with an amplification of 10. The gas sample was analyzed online via a sample loop with the detector and filament temperatures set to 393 K and 423 K respectively. Helium sweep gas was purged though the separation column (2x2 m Super Q packed 1/8" s steel tubing, Hayesep, Mesh range - 100/120) and reference column at a rate of 50 ml/min.

The temperature program for analysis was as follows: Once the sample was injected through the sample loop, the GC oven was initially kept at 323 K for 2 min. The temperature was then increased at a rate of 10 K/min to 433 K and kept at this temperature for 2 min. At the end of this program the sample had passed completely through the column. The GC oven temperature was then

returned to 323 K at a rate of 10 K/min. The data was captured on a PC with Clarity Chromatography Station for Windows Software.

Separation calculation required the analysis of various concentrations of N_2, CF_4 and C_3F_6 (mixture gas) diluted with He. A pre-determined mixture of He and mixture gas was fed to the sample loop using the mass flow controllers, at a total flow rate of 100 ml/min. Subsequently, the peak area versus volume percentage (from 0 % to 100 %) was plotted for each gas mixture, to obtain a calibration curve which was then used to determine a 100 % peak. The composition of the permeate and retentate during membrane separation was established by taking the area of each peak as a fraction of the 100 % peak and normalising the sum of the components.

4.2.2.3.2 MEMBRANE SEPARATION

During single gas permeation experiments, the following membranes had shown the most promising results for separation of the gas mixtures (N_2, CF_4 and C_3F_6):

- Hydroxysodalite coated ceramic
- MFI coated ceramic
- Teflon® coated ceramic
- composite ceramic

Subsequently, these membranes were chosen for the separation of the following binary mixtures:

- N_2/CF_4,
- CF_4/C_3F_6
- N_2/C_3F_6

The hydroxysodalite and MFI coated ceramic membranes were characterized at 298 K and 353 K and various transmembrane pressures (100, 150 and 200 kPa), whilst the Teflon® coated ceramic membrane was characterized at

transmembrane pressures of 50 and 100 kPa at 293 K and 333 K due to the nature of the membrane. The composite ceramic membrane was characterized at transmembrane pressures of 200 and 220 kPa at 333 and 353 K.

4.3 Results and Discussion

4.3.1 MORPHOLOGY AND ELEMENTAL ANALYSIS

4.3.1.1 SUPPORT

The properties of the centrifugally casted ceramic tubes were addressed in a previous paper by Bissett *et al*.[16] The α-alumina tubes used in this study had an inner and other diameter of 0.0177 m and 0.0207 m respectively, whilst the porosity and average pore diameter of the supports were 37 % and 167 nm respectively. According to the SEM images, the ceramic membrane had a graded structure with a smooth inner-surface and a rough outer surface as a result of the centrifugal casting process, which deposits the smallest particles nearest to the radial axis and the larger particles further away.

4.3.1.2 NAA COATED CERAMIC

Figures 4.3a and 4.3b clearly show that the NaA zeolite had formed a continuous, closed layer (approximate thickness 7 μm) on the smooth inner-surface of the α-alumina support.

The XRD spectra (not shown) confirmed that the zeolite layer consisted of a NaA crystalline phase without any preferred orientation or contaminants present.

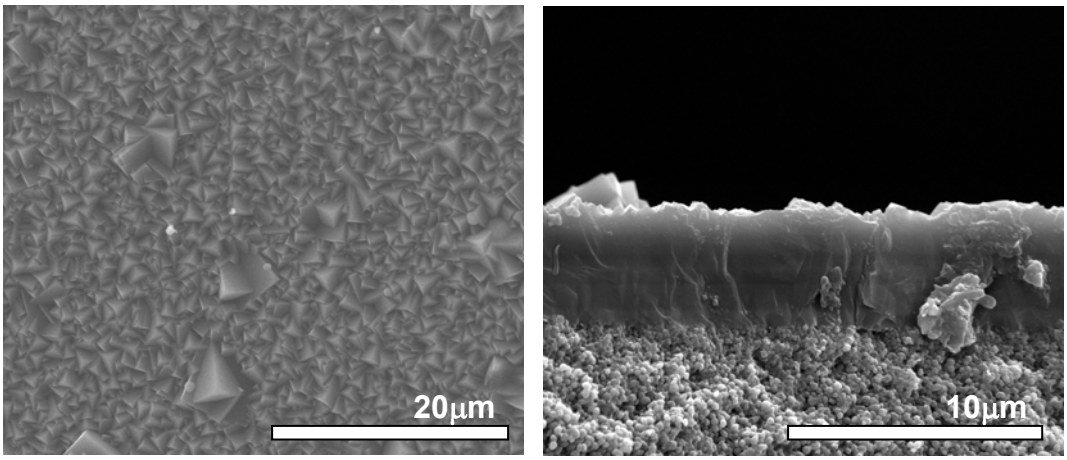

Figure 4.3 (a) Top and (b) cross-section SEM views of a double layered NaA coated ceramic membrane.

4.3.1.3 HYDROXYSODALITE COATED CERAMIC MEMBRANE

According to the SEM images of the double layered hydroxysodalite (HS) coated ceramic membrane, the zeolite layer was approximately 5 μm thick (Fig. 4.4b), while it was noticeable from the top-view (Fig. 4.4a) that a homogeneous hydroxysodalite was present without visual evidence of a contaminating phase (presence of crystals other than hydroxysodalite). The purity of the hydroxysodalite was confirmed by XRD analysis.

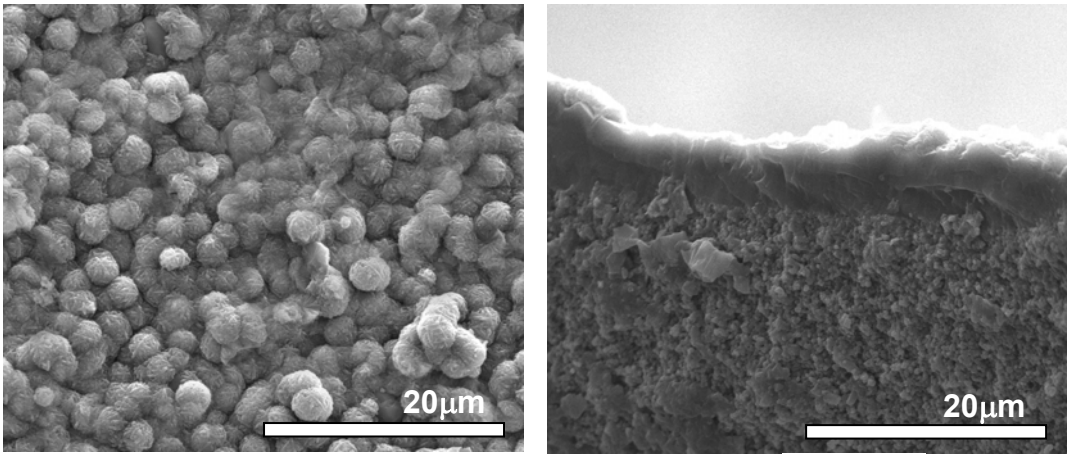

(a) (b)

Figure 4.4 SEM images of the (a) top and (b) cross-section double layered hydroxysodalite coated ceramic membrane.

4.3.1.4 NaY COATED CERAMIC MEMBRANE

The double layered zeolite NaY coated ceramic membrane had a layer thickness of 4-5 μm (Fig. 4.5b). The zeolite NaY crystals (3-5 μm) completely covered the α-alumina support surface (Fig. 4.5a).

The XRD spectrum obtained for the double layered NaY membrane is presented in Figure 4.6. Due to the interference of the support structure, the α-alumina peaks are indicated by α-signs. The XRD pattern confirmed the FAU structure. The prominent peaks observed could be correlated with literature values.[20]

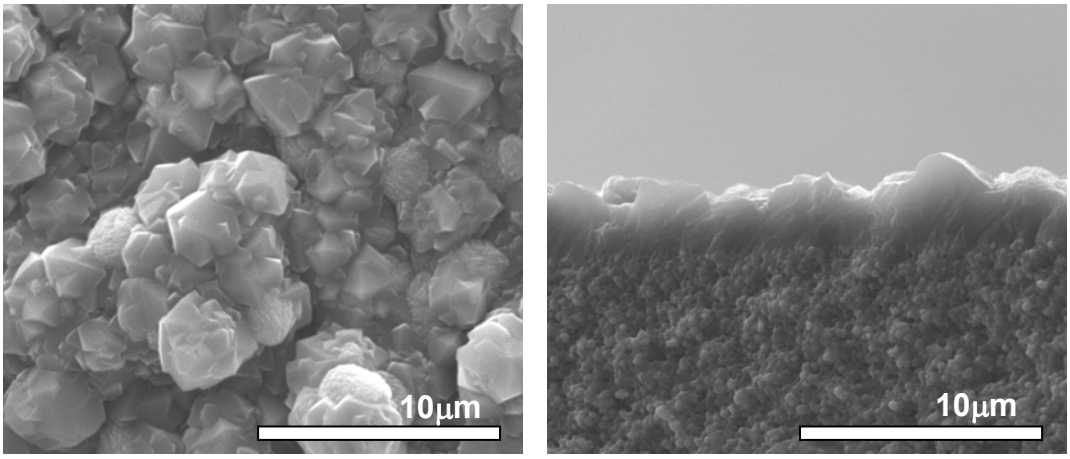

Figure 4.5 SEM images of the (a) top and (b) cross-section views of the zeolite NaY coated ceramic membrane after a double synthesis.

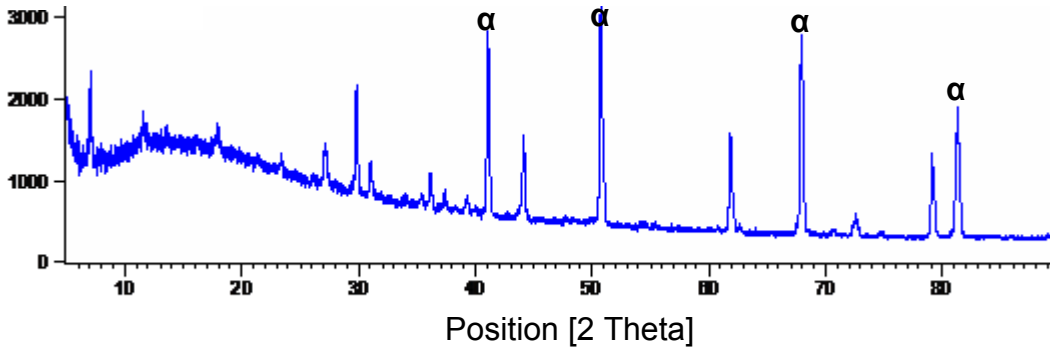

Figure 4.6 XRD pattern of the NaY coated membrane (α = reflections of the α-alumina support).

4.3.1.5 MFI COATED CERAMIC MEMBRANE

The results obtained for the MFI coated membrane corresponded to those published in a previous paper.[18] A closed layer was obtained (Fig. 4.7a), while the zeolite layer was approximately 7 μm thick (Fig. 4.7b).

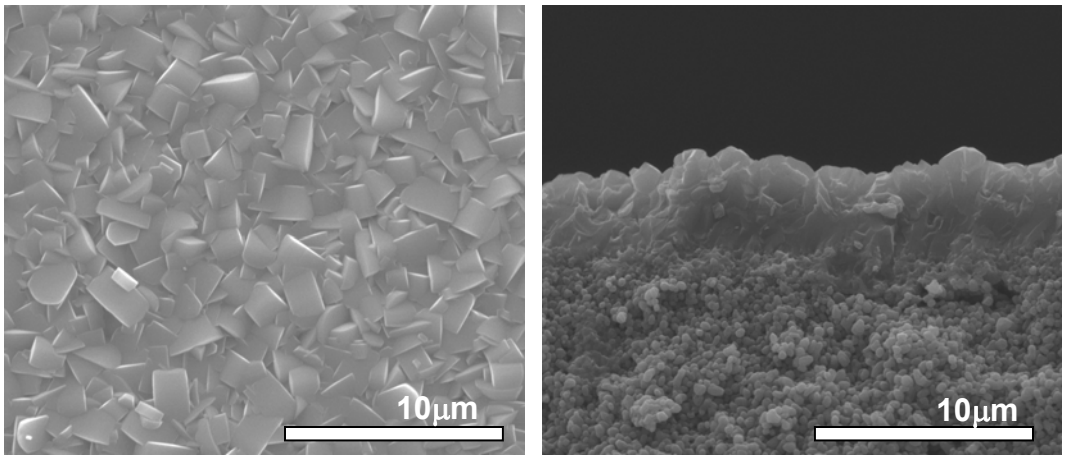

(a) (b)

Figure 4.7 (a) Top and (b) cross-section SEM views of the double layered MFI coated ceramic membrane.

4.3.1.6 TEFLON COATED CERAMIC MEMBRANE

The results obtained for the Teflon® coated ceramic membrane, corresponded to the results previously published.[18] The triple layer coated Teflon AF 2400 ceramic membrane is presented in Figure 4.8. The continuous defect-free Teflon® layer was approximately 2-3 μm thick, with limited penetration of the polymer phase into the underlying pores of the ceramic support.

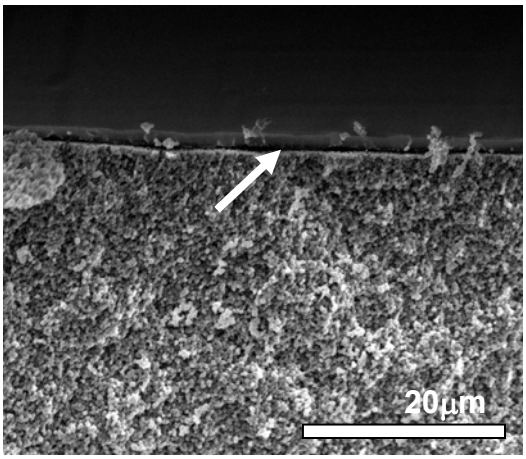

Figure 4.8 Cross-sectional view of the triple Teflon layered (arrow) membrane after temperature treatment at 423 K.

4.3.1.7 COMPOSITE CERAMIC MEMBRANE

The influence of the temperature treatment on the Teflon® layer deposition onto a zeolite layer was investigated in a previous study.[18] It was shown that at 423 K, optimal attachment and penetration was obtained as can be seen in the top view SEM image (Fig. 4.9). The 3-4 μm thick Teflon® layer shows slight penetration in-between the zeolite crystals.

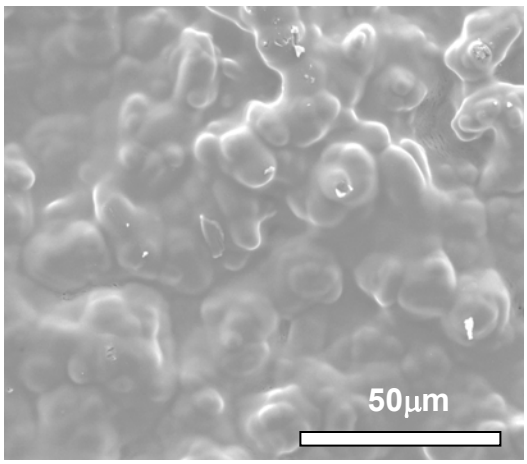

Figure 4.9 Top-view SEM image of the Teflon AF 2400 coating over MFI after one hour temperature treatments at 423 K.

4.3.2 SINGLE GAS PERMEATION

The average single gas permeances of the various membranes are summarised in Table 4.4. The values indicated are averages over the pressure range investigated as all membranes exhibited a linear permeance increase with pressure increase. The approximate error for each permeance measurement was in the range of 5 %.

Table 4.4 Summary of single gas permeances

Membrane	Conditions		Average Permeance 10^{-8} (mol.s^{-1}.m^{-2}. Pa^{-1})		
	Temp. (K)	Pressure range (10^2kPa)	N_2	CF_4	C_3F_6
Ceramic Support (1)	298	0.5 - 2	130	84	75
NaA (2)	298	0.5 - 2	1.47	1.40	1.30
Hydroxysodalite (3)	298	0.5 - 2	4.60	2.75	2.10
NaY (4)	298	0.5 - 2	1.40	0.71	0.69
MFI (5)	298	0.5 - 2	3.05	1.47	1.07
Teflon® layered ceramic (6)	298	0.5 - 2	2.90	0.58	0.35
Composite ceramic membrane (7)	333	1.5 - 2	0.55	0.0064	0.0077

All membranes, except the composite ceramic membrane, exhibited permeances in the order of N_2 > CF_4 > C_3F_6, which can be directly related to the kinetic diameter of the molecules (N_2 = 3.8 Å, CF_4 = 4.7 Å, C_3F_6 ≈ 6.6 Å). However, for the composite ceramic membrane, the C_3F_6 permeance was higher than the permeance of CF_4. This discrepancy can be attributed to the difference in the permeation mechanism of inorganic compared to polymeric membranes. Since

the Teflon® layered ceramic showed the same permeance preference as the purely inorganic membranes, it follows that the transport mechanism for this membrane was similar to that of the purely inorganic membranes. This implies the presence of some minor *cracks* in the Teflon® layer, with the result that selectivity was purely based on size preference and not on the solubility-diffusion model. For the composite ceramic membrane however, the solubility-diffusion model, as applied to polymeric membranes, can be used. According to this model the permeability coefficient (P in mol.s.$^{-1}$m.$^{-2}$Pa.$^{-1}$) can be expressed as

$$P = D \times S \tag{4.2}$$

where D (mol.s.$^{-1}$m.$^{-2}$) is the diffusion coefficient and S (Pa.$^{-1}$) the solubility coefficient. It would be expected that the diffusion coefficient of the smaller CF_4 was larger than the C_3F_6 diffusion. However, a considerable solubility of C_3F_6 in the Teflon® would result in a larger overall permeability. A significantly higher adsorption of C_3F_6 compared to CF_4 in Teflon AF 2400 was observed in an earlier study by Bissett *et al*.[18]

Permeances through the inorganic membranes in this study are governed by activated gaseous diffusion, while surface diffusion is negligible.[21] Surface diffusion is applicable to strong adsorbable gases and conditions where adsorbate loadings on zeolites are high. The relative inertness of the gases in this study and the low pressures used, decreased the probability of gas adsorption. For this reason the single gas permeances for the inorganic membranes are largely determined by molecular size as was observed.

The permeances of the ceramic supports were clearly higher than the zeolite membranes (NaA, HS, NaY, MFI). The permeance through the relatively large pores of the ceramic support structure (167 nm), is mainly attributed to Knudsen and Poiseuille flow contributions,[17] while activated gaseous diffusion was responsible for the permeances through the zeolite membranes. For this reason the ceramic support permeance was the highest, while all the zeolite membranes had permeances of similar magnitude. The low permeability of the composite

ceramic membrane is mainly due to the combined action of the MFI zeolite and the Teflon® coating sealing possible defects in the zeolite layer.

The single gas permeances of the membranes were in the order HS > MFI > NaA > NaY. Taking into account the pore sizes of the various zeolites, it would be expected that the NaY (≈ 6.7 Å) would show the largest permeance, followed by the MFI (5.5 Å), HS (2.8 Å[10]) and NaA (4.1 Å[17]).

The low Si/Al ratio of the NaA (1), NaY (1.5) and HS (4) resulted in unspecific intercrystalline permeances[22] due to imperfect growth of neighbouring negatively charged zeolite crystals during synthesis.[23] The low permeability of the NaY membrane, compared to the NaA and HS, was surprising when it was considered that the pore size of the NaY zeolite was larger and the thickness of the selective layer was the smallest of these three membranes. It is possible that the HS and NaA membranes contained a larger number of non-zeolite pores or defects than the NaY membrane. Although the MFI membrane contained no Al in its structure, dissolution of Al from the support would cause some incorporation of Al in the zeolite, resulting in intercrystalline boundary formation.[23,24] Another disadvantage of the MFI membrane synthesis was that calcination was required for template removal. The thermal expansion mismatch between the support and zeolite could have caused crack formation during membrane calcination.[25] The trends for the zeolite membranes in this study also depended largely on the reproducibility of the membrane synthesis. Although HS had the largest permeance, followed by the MFI, the results of the NaA and NaY for N_2 permeance were in the same order when considering that the reproducibility of the zeolite membranes synthesized under similar conditions, showed variations of up to 13 % in terms of permeances. Therefore this is an acceptable variation since variations of around 20 % are usual for zeolite synthesis.[26,27]

In Figure 4.10 the relationship of the N_2 permselectivities to CF_4 and C_3F_6 respectively is illustrated for all the membranes.

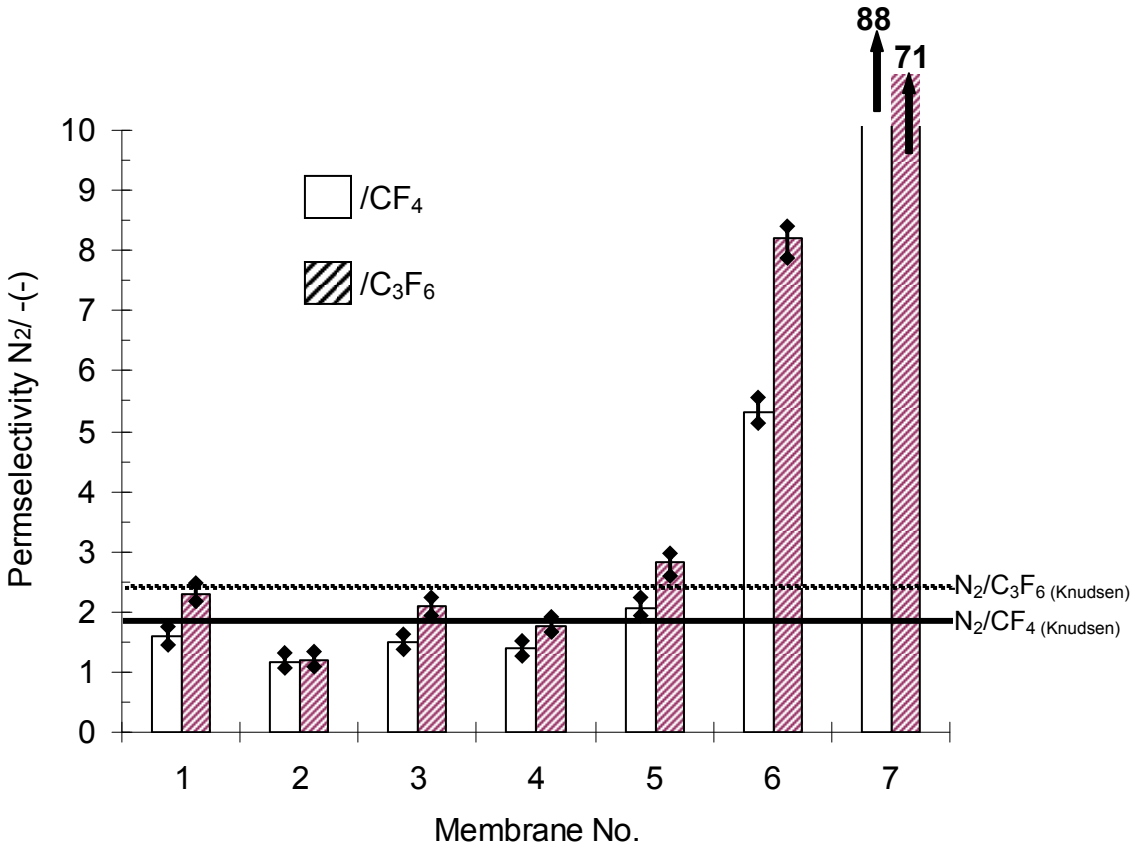

Figure 4.10 Permselectivity for N_2/CF_4 and N_2/C_3F_6 for the (1) ceramic support, (2) NaA, (3) hydroxysodalite, (4) NaY, (5) MFI, (6) Teflon layered ceramic and (7) composite ceramic. The respective Knudsen selectivity values are indicated by the cross bars.

The N_2/C_3F_6 ideal selectivities for membranes 1-7 were all larger than the N_2/CF_4 ideal selectivities. The only exception was for the composite ceramic membrane. As discussed previously this can be attributed to the separation mechanism for the dense Teflon AF 2400 sealing layer in the composite ceramic membrane. The dense polymer layer resulted in an increased solubility of the C_3F_6 molecule, resulting in an increased permeability compared to CF_4. The solubility is usually a function of gas condensability, gas interactions with the polymer and the free volume of the polymer.[28] The general rule is that solubility increases with critical temperature.[29,30,31] According to this rule C_3F_6 (T_c = 359.2 K) will be more soluble in the polymer than CF_4 (T_c = -227.5 K). Although the diffusion of the

smaller CF_4 might still be larger, the solubility effect seems to dominate, manifested by a higher N_2/C_3F_6 ideal selectivity for the composite ceramic membranes. This outcome was not observed for the Teflon® layered ceramic membrane which can probably be ascribed to cracks as previously discussed.

Both the ceramic support and the inorganic membranes (NaA, HS, NaY, MFI) displayed N_2/ CF_4 and N_2/C_3F_6 selectivities in the range of Knudsen selectivity. Higher selectivities were obtained for both Teflon® coated membranes.

Knudsen selectivities were anticipated for the relatively large pore size of the ceramic support as the support permeance equals the sum of the Knudsen and Poiseuille permeances, while gas adsorption did not affect permeance. Molecular sieving was not likely due to the size of the gas molecules, compared to the large pore sizes of the ceramic support structure. Permeance was thus determined by support and gas properties. Support properties included porosity, tortuosity, pore radius and support thickness, whilst the gas properties entailed the average molecular velocity and gas viscosity.

According to the kinetic diameter of the experimental gases higher N_2/C_3F_6 selectivities were expected for the inorganic membranes; NaA, HS and MFI. Since the aperture window of all these zeolites was smaller than 5.6 Å, only N_2 and CF_4 should have migrated through these membranes, while C_3F_6 should be rejected. Only for the NaY membrane C_3F_6 permeance would have been expected. This was clearly not the case, since all selectivities, with the exception of MFI, were lower than Knudsen.

The effect of increased gas solubility in a polymer matrix, with increased molecular size, is again highlighted for the Teflon® layered ceramic and the composite ceramic membrane as seen from the N_2/CF_4 and N_2/C_3F_6 permselectivity results. A dense polymer matrix would decrease the diffusion of both large and small molecules to a comparable degree, whilst the solubility of a larger molecule would become larger relative to that of a smaller gas molecule. However, it would be expected, that the N_2/CF_4 selectivity for the Teflon® layered ceramic and composite ceramic membrane would be larger than the N_2/C_3F_6

selectivity. This was however not observed for the Teflon® layered ceramic membrane. This indicated either a thin, highly permeable polymer layer or a cracked polymer layer resulting in an increased diffusion of the CF_4 molecule.

For the composite ceramic membrane however, the effect of the Teflon® sealing layer applied onto the MFI zeolite, was significant. The selectivities increased drastically, with the N_2/CF_4 selectivity slightly higher (88) than the N_2/C_3F_6 selectivity (71), signifying the increased solubility of the C_3F_6 gas molecule in a dense polymer matrix, resulting in an increased C_3F_6 permeability compared to the smaller CF_4 molecule. The purpose of the Teflon® layer to seal defects in the composite ceramic membrane was therefore largely successful. It did, however, not completely eliminate intercrystalline boundary diffusion.

Results for the composite ceramic membrane indicated that although the Teflon® "plugged" possible defects present in the zeolite layer, a defect-free Teflon® layer would have forced the gases to follow the path through the MFI zeolite. This would restrict the permeance of C_3F_6 even further, since the thickness of the Teflon® layer within the defects is the largest, resulting in low gas permeability through the non-zeolitic pores and a higher permeability through zeolitic pores. The permeance of the various gases would therefore be determined to a large degree by molecular size, with the smallest molecule permeating faster. The C_3F_6 permeance through the composite ceramic membrane was, however, larger than the CF_4 as described by the solubility-diffusion model for polymer membranes.

The CF_4/C_3F_6 permselectivities for all the membranes are illustrated in Figure 4.11. Permselectivies larger than 1 were obtained for membranes 1-6, indicating preferential CF_4 permeation. The composite ceramic membrane (7) was the exception. As discussed earlier for the ceramic support and the inorganic membranes (NaA, HS, NaY and MFI), this could be expected due to the higher diffusitivity of smaller molecules.

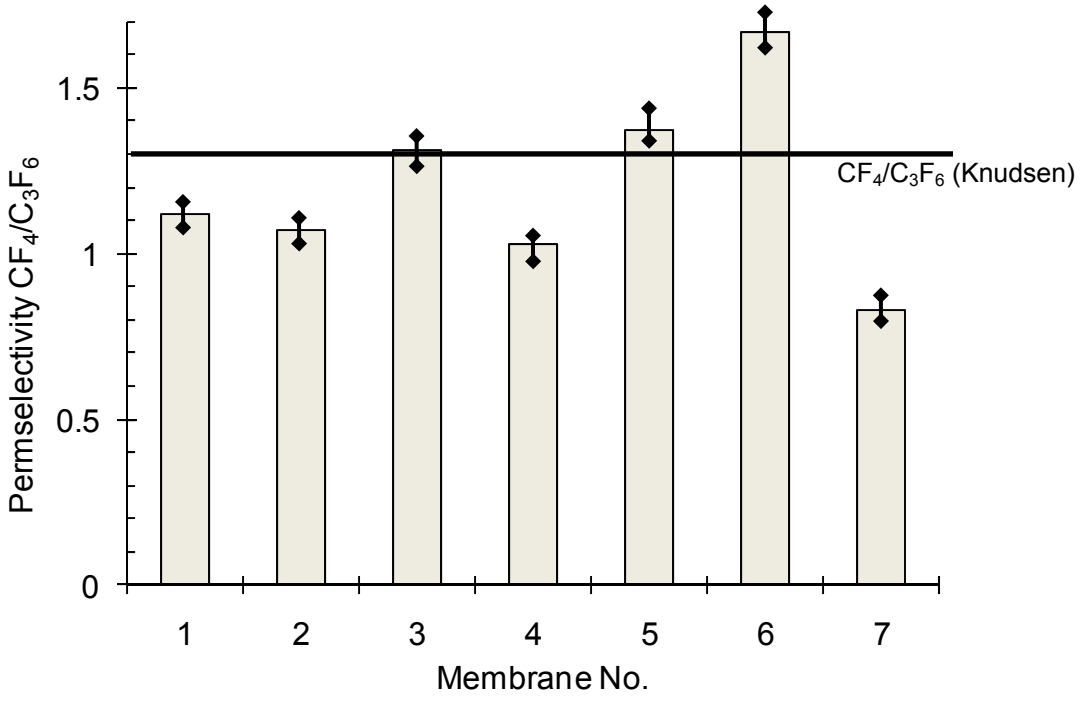

Figure 4.11 Permselectivity for CF_4/C_3F_6 for the (1) ceramic support, (2) NaA, (3) hydroxysodalite, (4) NaY, (5) MFI, (6) Teflon layered ceramic and (7) composite ceramic. Knudsen selectivity is indicated by the solid cross bar.

The relatively high CF_4/C_3F_6 permselectivity of the Teflon® layered ceramic was unexpected. This could imply that the defects in the Teflon® layer were such that they favoured the CF_4 permeance, while restricting the permeance of the C_3F_6 molecules through these defects. Furthermore, solubility contributions for both gases were fairly low due to the low density of the Teflon® matrix, thus favouring a higher CF_4 permeation. A dense matrix would result in a higher solubility contribution, increasing C_3F_6 permeation according to Equation 4.2. This explanation is confirmed by the < 1 CF_4/C_3F_6 permselectivity obtained for the composite ceramic membrane. The deposition of the Teflon® sealing layer onto the MFI zeolite resulted in a dense continuous polymer matrix, resulting in a greater C_3F_6 permeance compared to CF_4.

Only the MFI and the Teflon® layered ceramic membrane had CF_4/C_3F_6 permselectivity values greater than the Knudsen selectivities (solid cross bar, Fig. 4.11). This result was important for the MFI) when it is considered that the MFI membrane had the highest permeance, second only to hydroxysodalite. Therefore, a greater CF_4/C_3F_6 permselectivity signifies a zeolite layer with less, or smaller, intercrystalline defects compared to the other membranes (NaA, NaY and HS) - as found in previous studies and related to the low Al content.[22]

4.3.3 BINARY MIXTURE SEPARATION

The GC calibration curves obtained for the N_2, CF_4 and C_3F_6 diluted with He are shown in Figure 4.12. The straight line fit through the origin resulted in a R^2 value of 0.94 for both the CF_4 and C_3F_6, while a R^2 value of 0.96 was obtained for the N_2. The 100 % peak areas estimated from the straight lines and used for further calculations of component concentrations were as follows: N_2 - 6306, CF_4 - 10619 and C_3F_6 – 5905.

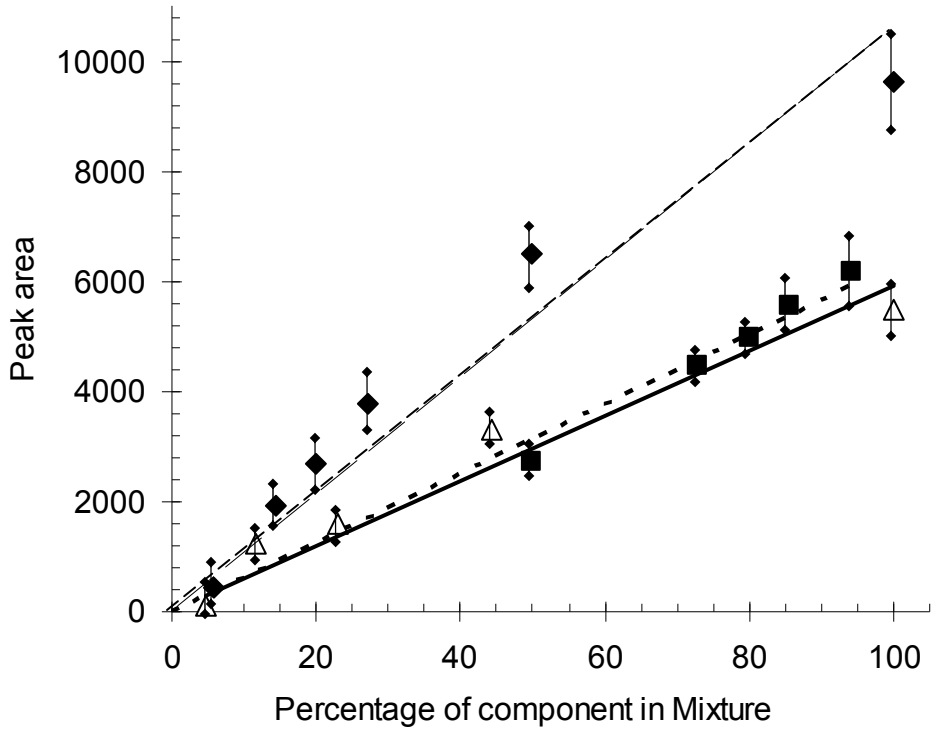

Figure 4.12 Gas chromatograph calibration curves obtained by helium dilution for CF_4 (– –♦– –), N_2 (- - ■ - -) and C_3F_6 (—Δ—).

The hydroxysodalite, MFI, Teflon® layered ceramic and the composite ceramic membranes had shown the most promising results in single gas studies and were consequently chosen for the binary mixture studies. Due to the large deviations associated with zeolite membrane synthesis, a single membrane which had shown promising results during single gas permeability experiments was characterized. Permeance and selectivities are given as an average of at least three measurements taken at each specific condition. Experimental deviations obtain was around 5 % for each data point. The values indicated are averages over the pressure range investigated as all membranes exhibited a linear permeance increase with pressure increase.

The binary mixture results for the hydroxysodalite (3), MFI (5) and Teflon® layered ceramic (6) and composite ceramic (7) membranes are shown in

Table 4.5. Due to the nature of the composite ceramic membrane (polymer layer properties), the binary studies were done at 333 K and not at room temperature as in the case of the other membranes. The approximate deviation for permeances were in the range of 5 %, while deviations of 10 % were obtained for the selectivities.

Table 4.5 Binary mixture membrane permeance and selectivity.

Membrane	Permeance[a] 10^{-8} (mol.s^{-1}.m^{-2}. Pa^{-1})			Selectivity[b]		
	N_2/CF_4	N_2/C_3F_6	CF_4/C_3F_6	N_2/CF_4	N_2/C_3F_6	CF_4/C_3F_6
Knudsen				*1.77*	*2.31*	*1.31*
Hydroxysodalite (3)	3.77	3.67	3.43	1.62	1.45	1.34
MFI (5)	1.15	1.26	0.97	1.24	1.55	1.73
Teflon layered ceramic (6)	6.38	6.11	6.00	1.71	1.37	1.13
Composite ceramic (7)	0.89	0.81	0.76	3.94	2.36	1.19

[a]Permeances were calculated from the linear regression of permeability (mol.s^{-1}.m^{-2}) against pressure (Pa^{-1}) over the experimental pressure range investigated

[b]Selectivities were calculated as the average values over the experimental pressure range investigated

Since the permeances for membranes were very similar, any discussion of tendencies is probably speculative, when considering, that variations of ± 20 % are not uncommon for identical zeolite membranes.[26] Having said this, it seems as if membranes 3, 6 and 7 exhibited binary mixture permeances in the order $N_2/CF_4 > N_2/C_3F_6 > CF_4/C_3F_6$. The only exception was for the MFI membrane, where the N_2/C_3F_6 permeance was higher than the N_2/CF_4 permeance. This trend can be correlated with the size of the gas molecules. A higher diffusivity is expected for smaller molecules. Therefore the sum of the diffusion rates of the individual molecules, will determine the diffusivity of the mixture.

For the hydroxysodalite (3) and MFI (5) this explanation applies since surface diffusion (where solubility is a factor) is negligible[21] and permeability is solely governed by activated gaseous diffusion.

For the Teflon® layered ceramic (6) and the composite ceramic membrane (7), gas solubility in the Teflon® matrix influenced permeability. The single gas permeability studies indicated that cracks may have been present in the polymer matrix of the Teflon® layered ceramic. Therefore permeation of smaller molecules was higher, due to diffusion, rather than solubility dominating.

The results for the composite ceramic membrane (7) were interesting, especially when compared to the single gas permeability studies. When considering only the single gas permeability results, the N_2/CF_4 permeance would be expected to be lower than for N_2/C_3F_6. During binary transport, the relatively high adsorption of the C_3F_6 most likely affected the N_2 permeance negatively, resulting in a lower overall mixture permeance. It should, however, be stressed that the permeance results for the composite ceramic membrane were very similar (variation 15 %) and therefore the trends observed could be a result of experimental deviations.

The membranes exhibited binary mixture permeances in the order 6 > 3 > 5 > 7, similar to the single gas permeation results with the exception of the Teflon® layered ceramic membrane (6). The hydroxysodalite (3) as previously stated, contained larger intercrystalline defects (due to the low Si/Al ratio) compared to the MFI membrane (5), resulting in a higher permeance. The combined zeolite and Teflon® layer effect, as well as membrane thickness of the composite ceramic membrane (7), was largely responsible for its low permeance. The relatively high permeance of the Teflon® layered ceramic membrane (6) was unexpected, as it was higher than the permeances obtained for single gas studies. No reasonable explanation for this result can be given. For the other membranes (3, 5, 7), the binary mixture permeances were slightly lower than the permeances observed for single gases.

A noticeable exception was the low single gas permeances of CF_4 and C_3F_6 compared to the high binary CF_4/C_3F_6 mixture permeances for the composite

ceramic membrane (7). A possible reason for this is the difference in diffusion and solubility of the CF_4 and C_3F_6. As indicated earlier, the solubility of C_3F_6 is larger than that of CF_4, while the CF_4 diffusivity was larger than that of C_3F_6. During mixture permeation these molecules compete for adsorption sites in the Teflon® matrix, with the C_3F_6 dominating. Once all sites are occupied, the interactions between the CF_4 and C_3F_6 molecules become overriding. Therefore the permeance shifts from a diffusion/adsorption driven mechanism to a diffusion driven mechanism only, resulting in an increased permeance through especially the cracks present in the Teflon® matrix as discussed earlier.

According to ideal selectivities obtained in this study, actual selectivities in the order of $N_2/C_3F_6 > N_2/CF_4 > CF_4/C_3F_6$ were expected, specifically for the zeolite membranes. However, the adsorption (occupancy) and condensability of gas molecules in pores or membrane media, can significantly affect the permeance of components during mixture separation.[21] Binary selectivities in the order $N_2/CF_4 > N_2/C_3F_6 > CF_4/C_3F_6$ were obtained for membranes 3, 6 and 7. These results differ from the single gas permeability studies. The C_3F_6 molecule probably has the greatest possibility of interaction (adsorption) with the membrane medium (greatest molecular size). Although the adsorption contribution may be small, it does contribute, especially to mixture permeances. This could explain the higher C_3F_6 permeance obtained for the hydroxysodalite (3) and the Teflon® layered ceramic membrane (6), resulting in the lower N_2/C_3F_6 selectivity. This was also observed for the composite ceramic membrane (7), where the adsorption of C_3F_6 was higher than the CF_4 adsorption.

It seems that smaller intercrystalline boundaries present in the MFI zeolite membrane (5) had an opposite effect, i.e. due to the pores of the MFI (5.5 Å) molecular sieving occurred. Consequently, the N_2 permeation was the largest, followed by CF_4, with C_3F_6 permeance the lowest; hence the N_2/C_3F_6 selectivity was larger than the N_2/CF_4 selectivity. As the pore size of the MFI zeolite (5.5 Å) was located between the kinetic diameter of the molecules CF_4 (4.7 Å) and C_3F_6 (6.6 Å), it resulted in the largest selectivity for the MFI membrane for the CF_4/C_3F_6 mixture. This result however also indicated the presence of

non-zeolitic pores, including intercrystalline boundaries and cracks, since a *perfect* MFI layer would not have allowed any permeability of the larger C_3F_6 molecule.

The performance of the composite membrane (7) for N_2/CF_4 separation was satisfactory (selectivity = 4). The N_2/C_3F_6 selectivity on the other hand, although higher than Knudsen selectivity, was unsatisfactory. These results were disappointing, especially when compared with the ideal selectivities (N_2/CF_4 = 88 and N_2/C_3F_6 = 71) obtained from the single gas permeability experiments. The Teflon® sealing layer successfully improved the N_2/CF_4 selectivity, forcing the molecules to rather permeate through the zeolite pores. The sections containing the thick Teflon® layer, however contributed to CF_4 and C_3F_6 permeance as larger molecules were preferably adsorbed in the polymer layer.

From Figure 4.13 it is clear that temperature had a small effect on the permeance of the binary mixtures for all the membranes tested. The largest effect was observed for the hydroxysodalite membrane (3). However, no particular trend was observed for the pure inorganic membranes (hydroxysodalite and MFI). Both surface diffusion and activated gaseous diffusion contribute to the total flux through zeolite pores. For adsorbable gases, surface diffusion is dominant, while activated gaseous diffusion is dominant for non-adsorbable gases. Therefore, at higher temperatures, gaseous diffusion becomes more dominant as gas adsorption decreases. For larger defects on the other hand, Knudsen diffusion and viscous flow become more pronounced. A decreasing flux is expected with increasing temperature in this instance. Therefore when considering that no particular trend was observed, it is clear that permeance occurred through both zeolite pores and defects.

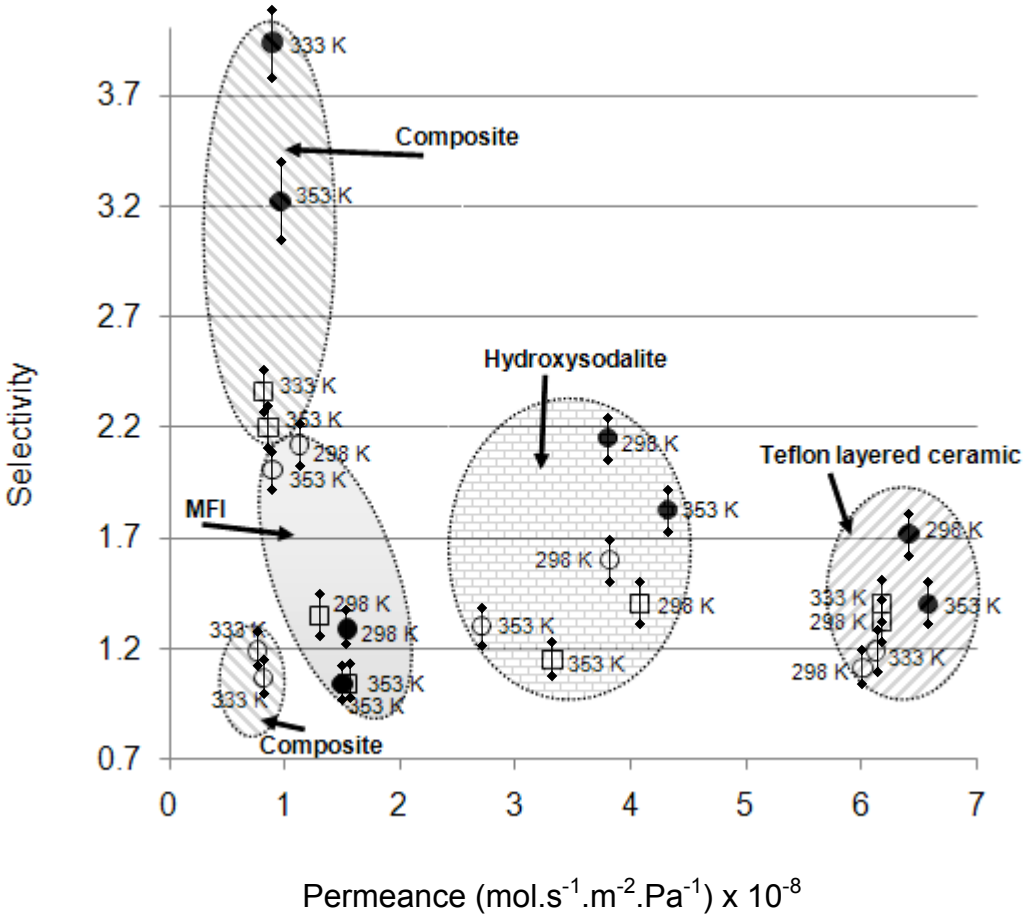

Figure 4.13 N_2/CF_4(●), N_2/C_3F_6(□), CF_4/C_3F_6(○) selectivities at various temperatures as a function of permeance for the various membranes.

The effect of temperature on the selectivity was however more pronounced for most of the membranes investigated, especially when studying the N_2/CF_4 mixture. In 9 of 11 experiments, a lower temperature yielded a higher selectivity. It therefore seemed that higher temperatures favoured the larger molecules, or as stated above, the effect of the membrane defects increased in terms of an increased Knudsen diffusion or viscous flow.

In the case of the composite ceramic membrane (7), a small increase (≈ 5.5 %) in permeance with increasing temperature can clearly be seen for all binary mixtures (Fig. 4.14). Gas permeance through zeolite membranes generally

decreases with increased temperature due to the increased vibration of the gas molecules. This result correlates with Equation 4.3 for flux due to Knudsen diffusion where the permeance decreases with increasing temperature.[21] Equation 4.3 is given by :

$$\Pi_{Kn} = \frac{2.g_{Kn}v.r_p}{3RT\delta} \qquad (4.3)$$

where g_{Kn} is a geometrical factor, v is the average molecular velocity ($m.s^{-1}$), r_p is the pore radius of the membrane (m), R the universal gas constant (8.314 $J.K^{-1}.mol^{-1}$), T the temperature (K) and δ is the membrane thickness (m).

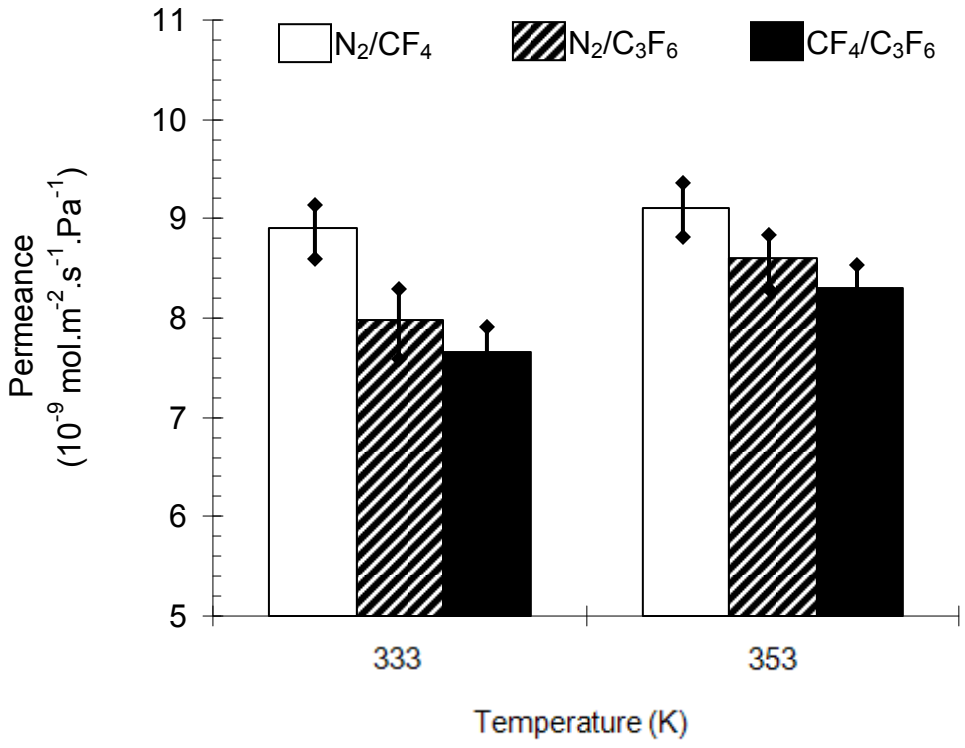

Figure 4.14 Binary mixture permeances for the composite ceramic membrane at 333 K and 353 K.

For the composite membrane however the permeance increase which could also be attributed to the Teflon® layer applied to the zeolite. Although the Teflon® layer forces the gas molecules to predominantly flow through the zeolite pores, the presence of defects in the Teflon®, plugging the non-zeolite pores, is enlarged when the temperature is increased. This results in an increased permeance through the composite membrane for all the gas mixtures. Since permeance through defects increases with increasing temperature, the molecular sieving of the zeolite layer decreases, resulting in a selectivity decrease.

This is confirmed by Figure 4.15 where the selectivity is presented as a function of temperature for the composite ceramic membrane, showing a corresponding decrease in selectivities with increasing temperature.

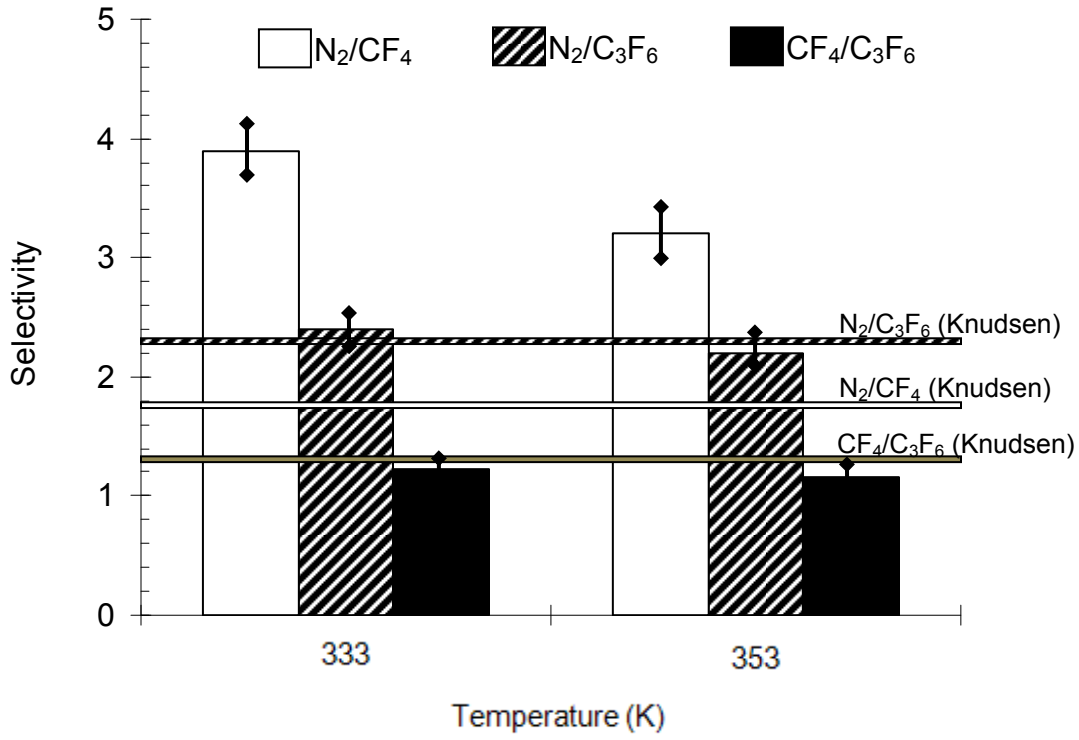

Figure 4.15 Binary mixture selectivities for the composite ceramic membrane at 333 K and 353 K including Knudsen selectivities for the three binary mixtures.

For polymer membranes, a temperature decrease often results in the more condensable gas (more soluble gas) permeating faster than the less soluble gas.[31] Since CF_4 has a lower solubility than C_3F_6, increasing the temperature should result in increased selectivity, because the relative permeation of the C_3F_6 would decrease. This explanation is also valid for the N_2/CF_4 selectivity where the solubility of N_2 is lower than that of CF_4. However, it is clear from Figure 4.15 that the opposite was observed in this work. This again confirms that, although the Teflon® layer covered the zeolite layer, it was not exclusively responsible for the separation mechanism.

4.4 Conclusion

The application of inorganic membranes is currently limited in a large degree to the separation of gases, where one of the gases is condensable. Low selectivities obtained during gas separation involving zeolite membranes are a consequence of defects resulting from intercrystalline slits and crack formation during synthesis and template removal.

Inorganic membranes (α-alumina support, NaA, NaY, hydroxysodalite, MFI) and composite membranes (Teflon® layered ceramic and composite ceramic membrane) were synthesized and characterized using non-condensable gases (N_2, CF_4 and C_3F_6) according to single gas and binary mixture separations. The composite ceramic membrane consisted of a ceramic support structure, a MFI intermediate zeolite layer and a Teflon AF 2400 top layer. The Teflon® layer was aimed at the closure of possible defects present in the separation layer, forcing the gas molecules to follow the path through the zeolite pores.

During single gas permeation studies, the selectivities obtained using the inorganic membrane, were in most instances, slightly lower than Knudsen selectivities for all three gases. The highest selectivities were obtained with the two Teflon® coated membranes, with ideal selectivities of 88 and 71 for N_2/CF_4 and N_2/C_3F_6 for the composite ceramic membrane. Based on these results, the

hydroxysodalite, MFI, Teflon® layered ceramic and the composite ceramic membrane were consequently chosen to study binary gas mixture separation.

The membranes exhibited binary mixture permeances in the order Teflon® layered ceramic > HS > MFI >composite ceramic, similar to the single gas permeation trends. The composite ceramic membrane showed the highest selectivity for N_2/CF_4 and N_2/C_3F_6 with selectivities of 3.9 and 2.4 respectively. The selectivities were however achieved at a permeance of $\approx 0.8 \times 10^{-8}$ mol.s^{-1}.m^{-2}. Pa^{-1} for all mixtures, which were 2 to 3 times lower than for the MFI and hydroxysodalite. The highest selectivity (1.7) for CF_4/C_3F_6 was obtained using the MFI membrane. The effect of temperature on permeance was not as pronounced as the effect on selectivity. In 9 of 11 experiments the lower temperature yielded a higher selectivity.

The study has shown that the composite ceramic membrane could be capable of separating N_2/CF_4 and N_2/C_3F_6 mixtures using a cascade system. The Teflon® sealing layer, for both the Teflon® coated and the composite ceramic membrane, probably had structural defects, which resulted in lower selectivity, whilst the adsorption of CF_4 and C_3F_6 contributed to the low binary CF_4/C_3F_6 selectivities.

4.5 Acknowledgements

The financial assistance of the Innovation Fund (IF), of South Africa (Project T50021), a separate business unit of the Department of Science and Technology (DST), is hereby acknowledged. The financial assistance of the South African Nuclear Energy Corporation (Necsa), towards this research is hereby also acknowledged. The authors also wish to thank Dr. L. Tiedt (NWU, South Africa) for the SEM images and Mr. J. Kroeze and Mr. A. Brock (Technical Advisor, NWU, South Africa) for the manufacture of the experimental set-up.

4.6 References

[1] S.A. Stern, Polymers for Gas Separations: The Next Decade, Journal of Membrane Science, 94, (1994) 1.

[2] J. Caro, M. Noack, P. Kolsch, R. Schafer, Zeolite Membranes – State of Their Development and Perspective, Microporous and Mesoporous Materials, 38, (2000) 3.

[3] T. Chung, L.Y Jiang, Y. Li, S. Kulprathipanja, Mixed matrix membranes (MMMs) comprising organic polymers with dispersed inorganic fillers for gas separation, Progress in Polymer Science, 32, (2007) 483.

[4] H.W. Deckman, A.J. Jacobson, J.A. McHenry, K. Keizer, A.J. Burggraff, Z.A.E.P. Vroon, L.R. Czarnetzki, F. Lai, A.J. Bons, W.J. Mortier, J.P. Verduun, E.W. Corcoran Jr., Molecular sieve layers and processes for their manufacture, Patent PCT/EP 9401301, (1994).

[5] J. Caro, M. Noack, Zeolite membranes – Recent developments and progress, Microporous and Mesoporous Materials, 115, (2008) 215.

[6] Y. Yan, M.E. Davis, G.R. Gavalas, Preparation of highly selective zeolite ZSM-5 membranes by a post-synthetic coking treatment, Journal of Membrane Science, 123, (1997) 95.

[7] J. Hedlund, F. Jareman, A. Bons, M. Anthonis, A masking technique for high quality MFI membranes, Journal of Membrane Science, 222, (2003) 163.

[8] S. Miachon, E. Landrivon, M. Aouine, Y. Sun, I. Kumakiri, Y. Li, O. Pachtov´a Prokopov´a, Nanocomposite MFI-alumina membranes via pore-plugging synthesis: Preparation and morphological characterization, Journal of Membrane Science, 281, (2006) 228.

[9] S. Nair, M. Tsapatsis, Synthesis and properties of zeolitic membranes, in S.M. Auerbach, K.A. Carrado, P.K. Dutta (Eds.), Handbook of Zeolite Science and Technology, Marcel Dekker Inc., New York, Basel, (2003) pp. 867 – 919.

[10] A. van Niekerk, J. Zah, J.C. Breytenbach, H.M. Krieg, Direct crystallisation of a hydroxysodalite membrane without seeding using a conventional oven, Journal of Membrane Science, 300, (2007) 156.

[11] A.M.W. Hillock, S.J. Miller, W.J. Koros, Crosslinked mixed matrix membranes for the purification of natural gas: Effects of sieve surface modification, Journal of Membrane Science, 314, (2008) 193.

[12] T. Chung, J. Shieha, W.W.Y. Laua, M.P. Srinivasana, D.R. Paul, Fabrication of multi-layer composite hollow fiber membranes for gas separation, Journal of Membrane Science, 152, (1999) 211.

[13] T. Chung, L.Y Jiang, Y. Li, S. Kulprathipanja, Mixed matrix membranes (MMMs) comprising organic polymers with dispersed inorganic fillers for gas separation, Progress in Polymer Science, 32, (2007) 483.

[14] A.B. Hinchliffe, K.E. Porter, A comparison of membrane separation and distillation, Chemical Engineering Research and Design, 78, 2, (2000) 255.

[15] A. Polyakov, G. Bondarenko, A. Tokarev, Y. Yampolskii, Intermolecular interactions in target organophilic pervaporation through the films of amorphous Teflon AF2400, Journal of Membrane Science, 277, (2006) 108.

[16] H. Bissett, J. Zah, H.M. Krieg, Manufacture and optimization of tubular ceramic membrane supports, Powder Technology, 181, (2008) 57.

[17] J. Zah, H.M. Krieg, J.C. Breytenbach, Single gas permeation through compositionally different zeolite NaA membranes: Observations on the intercrystalline porosity in an unconventional, semicrystalline layer, Journal of Membrane Science, 287, (2007) 300.

[18] H. Bissett, H.M. Krieg, Synthesis of a composite inorganic membrane for the separation of nitrogen, tetrafluoromethane and hexafluoropropylene, Submitted.

[19] B. Freeman, Y. Yampolskii, Membrane Gas separation, John Wiley & Sons Ltd., West Sussex, United Kingdom, (2010) p. 90.

[20] M.M.J. Treacy, J.B. Higgins, Collection of simulated XRD powder patterns for zeolites, 4th edition, Elsevier, Amsterdam, (2001).

[21] N. Nishiyama, L. Gora, V. Teplyakov, F. Kapteijn, J.A. Moulijn, Evaluation of reproducible high flux silicalite-1 membranes: gas permeation and separation, Separation and Purification Technology, 22-23, (2001) 295.

[22] M. Noack, G.T.P. Mabande, J. Caro, G. Georgi, W. Schwieger, P. Kölsch, A. Avhale, Influence of Si/Al ratio, pretreatment and measurement conditions on permeation properties on MFI membranes on metallic and ceramic supports, Microporous and Mesoporous Materials, 82, (2005) 147.

[23] M. Noack, P. Kölsch, V. Seefeld, P. Toussaint, G. Georgi, J. Caro, Influence of the Si/Al-ratio on the permeation properties of MFI-membranes, Microporous and Mesoporous Materials, 79, (2005) 329.

[24] J. Caro, D. Albrechta, M. Noack, Why is it so extremely difficult to prepare shape-selective Al-rich zeolite membranes like LTA and FAU for gas separation?, Separation and Purification Technology, 66, (2009) 143.

[25] M. Noack, M. Schneider, A. Dittmar, G. Georgi, J. Caro, The change of the unit cell dimension of different zeolite types by heating and its influence on supported membrane layers, Microporous and Mesoporous Materials, 117, (2009) 10.

[26] L. Gora, N. Nishiyama, J.C. Jansen, F. Kapteijn, V. Teplyakov, T. Maschmeyer, Highly reproducible high-flux silicalite-1 membranes: Optimization of silicalite-1 membrane preparation, Separation and Purification Technology, 22, (2001) 223.

[27] K. Sato, T. Nakane, A high reproducible fabrication method for industrial production of high flux NaA zeolite membrane, Journal of Membrane Science, 301, (2007) 151.

[28] W. Shon, D. Ryu, S.Oh, J. Koo, A study on the development of composite membranes for the separation of organic vapors, Journal of Membrane Science, 175, (2000), 163.

[29] T. Matsuura, Synthetic Membranes and Membrane Separation Processes, CRC Press, (1994) p. 420.

[30] M. Mulder, Basic Principles of Membrane Technology, 2de Edition, Springer, (1996), Chapter 5, p. 241.

[31] S. Choi, J. Kim, S.Lee, Sorption and permeation behaviours of a series of olefins and nitrogen through PDMS membranes, Journal of Membrane Science, 299, (2007) 54.

CHAPTER 5

CONCLUSION

5.1 General

In this thesis studies were conducted on the separation of nitrogen and fluorocarbon gases with membranes. The main sections of research conducted in this study were:

- the adsorption of tetrafluoromethane (CF_4) and hexafluoropropylene (C_3F_6) on MFI zeolites,
- the synthesis of composite ceramic based membranes for the single component separation of nitrogen, tetrafluoromethane and hexafluoropropylene,
- the composite (ceramic based) membrane binary mixture separation of nitrogen, tetrafluoromethane and hexafluoropropylene.

In this thesis each section was dealt with in a separate chapter and results were evaluated by correlating the results with relevant literature works and theories. The specific conclusions of each subject were discussed at the end of the respective chapters.

5.1.1 GAS ADSORPTION

The gas permeability through polymer membranes is a result of diffusivity and solubility of a gas. Although this is not entirely true for zeolite membranes, since activated gaseous diffusion is mainly dominant, the effect of gas adsorption does influence activated surface diffusion which in turn influences permeability through zeolite membranes.[1] The gas adsorption onto MFI zeolites can be used to help explain trends and results as obtained during membrane permeation. The study of hexafluoropropylene was an important aspect in this section, because no adsorption or permeation data on this gas is currently available in literature. The adsorption of nitrogen (N_2), tetrafluoromethane (CF_4) and hexafluoropropylene (C_3F_6) onto MFI zeolites (silicalite-1 and ZSM-5) was investigated by a gravimetrical method (**Chapter 2**). For both CF_4 and C_3F_6, adsorption data was obtained at temperatures between 303 K and 423 K under normal atmospheric conditions. It was possible to fit

the Langmuir isotherm for C_3F_6, while the CF_4 data did not fit any suitable isotherms, as the heat of adsorption in this study (≈ 110 kJ/mol) was not in the range (≈ -30 kJ/mol) indicated in literature.[2] For the C_3F_6 in this study, the adsorption onto silicalite-1 and ZSM-5 resulted in heat of adsorptions of -33 and -17 kJ/mol respectively. This is in the range -30 to -49 kJ/mol observed in literature for n-C_3 gases.[3,4,5]

5.1.2 SINGLE GAS PERMEATION

Having shown that differences in adsorption of CF_4 and C_3F_6 was possible using zeolites, this section of the research focused on the synthesis of inorganic membranes for separation of N_2, CF_4, and C_3F_6 (**Chapter 3**). A composite ceramic membrane consisting of a ceramic support structure, an MFI intermediate zeolite layer and a Teflon AF 2400 top layer was developed for separation of N_2, CF_4, and C_3F_6. The purpose of the Teflon® (PTFE) layer was aimed at the closure of possible defects present in the separation layer, forcing the gas molecules to follow the path through the zeolite pores. During characterization of zeolite membranes, it became apparent that the presence of non-zeolitic pores was a determining factor for selectivity performances of various membranes. By minimizing the contribution of non-zeolitic permeances, selectivities could be significantly improved. The added application of the Teflon AF 2400 sealing layer made it essential to investigate the adsorption of N_2, CF_4, and C_3F_6 onto this material. The adsorption was observed by means of a gravimetrical method similar to the gas adsorption study. A theoretical selectivity of 26 in favour of C_3F_6 was calculated in terms of the maximum molar amount of gas adsorbed for CF_4 and C_3F_6 onto Teflon AF 2400, with N_2 adsorption less than the detection limit of the instrument. For the composite ceramic membrane, ideal selectivities of 86 and 71 were obtained for N_2/CF_4 and N_2/C_3F_6 respectively, compared to 5.5 and 8 for the Teflon® coated ceramic, whilst ideal selectivities slightly higher than Knudsen selectivities were obtained for the MFI zeolite membrane. CF_4/C_3F_6 ideal selectivities ranged from 0.9 to 2, with C_3F_6 permeating faster though the composite ceramic membrane, a result of the higher adsorption of C_3F_6 on the Teflon® material.

5.1.3 BINARY MIXTURE SEPARATION

This section addressed the heart of the separation, by evaluating the available membranes for single and binary gases. Inorganic membranes (α-alumina support, NaA, NaY, hydroxysodalite, MFI) and composite membranes (Teflon® layered ceramic and composite ceramic membranes) were synthesized and characterized using the non-condensable gases N_2, CF_4, and C_3F_6. Single gas permeation studies indicated slightly lower than Knudsen selectivities for all the inorganic membranes due to non-zeolitic permeance, as a result of cracks and intercrystalline boundaries between individual zeolite crystals. As indicated in the single gas permeation studies (**Chapter 3**), the highest selectivities were obtained for the composite membranes, with ideal selectivities of 88 and 71 for N_2/CF_4 and N_2/C_3F_6 respectively. The hydroxysodalite (HS), MFI, Teflon® layered ceramic and the composite ceramic membranes (developed during single gas permeation studies) were chosen for binary gas mixture separation, due to their performances during single gas characterization.

The membranes exhibited binary mixture permeances in the order Teflon® layered ceramic > HS > MFI > composite ceramic (**Chapter 4**), similar to the single gas permeation results. N_2/CF_4 and N_2/C_3F_6 selectivities of 4 and 2.4 were obtained for the composite ceramic membrane, the highest for all membranes characterized. The CF_4/C_3F_6 selectivity was however only slightly higher than 1 due to adsorption of CF_4 and C_3F_6 on the Teflon AF 2400 polymer.

5.2 Evaluation

In this paragraph, the success of the research will be evaluated.

From the adsorption study, it became evident that the amount C_3F_6 adsorbed was considerably higher than the amount of CF_4 adsorbed, while the amount of N_2 adsorbed was practically negligible. The adsorption data indicated that separation of CF_4 and C_3F_6 would be possible by means of adsorption, with the highest ideal selectivities for separation of a binary gas mixture obtained at higher temperatures. If for instance other methods than membrane separations were considered for gas mixture separation, zeolites can assist in enhancing the mechanism. Currently, cryogenic distillation is used extensively in industry for fluorocarbon gas separation. As the separation of gases by distillation is achieved due to boiling point differences and the effective separation determined by the amount of each species present in the gas phase, the separation can be influenced by the addition of zeolite crystals with a specific Si/Al ratio. The formation of non-zeolitic pores (intercrystalline boundaries) experienced during zeolite membrane synthesis, especially for high aluminium content zeolites, is not an issue when considering adsorption as a separation method. When using zeolite crystals in cryogenic distillation, the presence of cracks might enhance the adsorption of gases onto the zeolite due to the higher surface area per crystal.

The membrane studies again emphasized the importance of defect-free membrane synthesis, especially when applied to the separation of non-condensable gases. Defect prevention, or defect repair of any kind, is advantageous for increased selectivity, but decreases permeability. Membrane separation at low temperatures, which could assist in increased adsorption or condensation of a specific gas in the intercrystalline pores, should not be excluded. Although the composite membrane was able to separate the binary mixtures N_2/CF_4 and N_2/C_3F_6, and the MFI membrane the CF_4/C_3F_6, effective separation would require a large number of cascade membranes. This study indicated that CF_4 and C_3F_6 separation from nitrogen could be achieved by means of an inorganic membrane when a sealing layer was used to eliminate defects.

5.3 Contribution to Knowledge

The following contributions to knowledge have been achieved as a result of this work:

- The Langmuir isotherm for the adsorption of C_3F_6 onto silicalite-1 and ZSM-5 zeolite has been determined using a gravimetrical method and the heats of adsorption was shown to be -33 and -17 kJ/mol for the silicalite-1 and ZSM-5 respectively.
- The need to develop a model for the adsorption of fluorocarbon gases onto zeolites has been identified.
- A composite inorganic-polymer membrane was synthesized for non-condensable gas separation.
- The inorganic membrane based separation of N_2, CF_4, and C_3F_6 was investigated and selectivities were improved by defect plugging.
- The contribution of non-zeolitic pores to permeation for zeolite based membranes, especially during non-condensable gas separation, has shown to be significant resulting in low gas mixture separations.

5.4 Recommendations

Recommendations can be made for the separation of fluorocarbons gases as presented in this study.

In terms of the membrane based separation studies the following recommendations are made:

- Develop or improve available adsorption models for the adsorption of fluorocarbon gases onto zeolites.
- Study the separation of N_2, CF_4, and C_3F_6 at temperatures below 273 K to see if improved selectivity can be obtained with inorganic membranes, due to observed increased adsorption of gases in zeolitic and non-zeolitic pores at lower temperatures.

- Develop alternative zeolite membrane synthesis to reduce or eliminate non-zeolitic pore formation.
- The addition of a condensable gas (for instance water or hexane) to the gas mixture (N_2, CF_4, and C_3F_6) which can adsorb in defects, to decrease permeance through non-zeolite pores.
- Treatment of zeolite membranes in a CF_4 inductive coupled plasma to alter the surface properties of the zeolite by fluorination of the zeolite. This might improve the adsorption of fluorocarbon gases and improve selectivity.
- The use of carbon based membranes can also be considered. Although carbon based membranes were not included in the scope of this study, various carbon based membranes with various specific pore sizes are available which might be used for possible fluorocarbon gas separation.
- Fluor based or partially fluorinated polymer membranes can be investigated for fluorocarbon gas separation. High solubilities of the fluorocarbon gases in these membranes are expected, which can result in high separation selectivities.
- Investigate a pressure swing process with zeolites, avoiding issues of cracks and defects of membranes, for the separation of fluorocarbon gases.

5.5 References

[1] J.G. Wiljmans, R.W. Baker, The solution-diffusion model: a review, Journal of Membrane Science, 107, (1995) 1.

[2] J. Peng, H. Ban, X. Zhang, L. Song, Z. Sun, Binary adsorption equilibrium of propylene and ethylene on silicalite-1: prediction and experiment, Chemical Physics Letters, 401, (2005) 94.

[3] J.F.M. Denayer, R.A. Ocakoglu, J. Thybaut, G. Marin, P.Jacobs, n- and Isoalkane Adsorption Mechanism on Zeolite MCM-22, Journal of Physical Chemistry B, 110, (2006) 8551.

[4] R.A. Ocakoglu, J.M.F. Denayer, G.B. Marin, J.A. Martens, G.V.J. Baron, Tracer Chromatographic Study of Pore and Pore Mouth Adsorption of Linear and Monobranched Alkanes on ZSM-22 Zeolite, Journal of Physical Chemistry B, 107, (2003) 398.

[5] F. Eder, M. Stockenhuber, J.A. Lercher, Sorption of light alkanes on H-ZSM 5 and H-mordenite, Studies in Surface Science and Catalysis, 97, (1995), 495.

ACKNOWLEDGEMENTS

"Whether you think you can, or that you can't, you are usually right."

- Henry Ford (1863-1947)

Very many people helped me during my studies, but many others assisted me on the road to where I am today. I not only want to give gratitude to individuals who enriched me in my work, but also those who gave me an opportunity to grow as a person. Firstly, I would like to give Lord Jesus all the credit, for without his compassion none of this would be possible.

I wish to thank the following people:

- My mother, Heila, for carrying me through live all these year, through easy and difficult times;
- My family, Renier, Corne, Corrie, Zola and Martin for all the support, emotional and financial. Without you this task would have been impossible;
- Prof. Henning Krieg, not only as my promoter, but as a friend and mentor. Thank you for all your support, motivation and understanding, especially the final few years;
- Prof. Philip Crouse from the University of Pretoria, for his assistance and input with the plasma synthesis of gases;
- Andrew, Lynette, Dr. L. Tiedt and Profs. Neomagus and Bruinsma for all their assistance;
- Oom Jan and Adrian, as well as the staff of the Instrumentation department for their contributions with experiments and experimental set-up preparations;

— Drs. J.T. Nel (co-promoter) and I.J. van der Walt (Jaco) at Necsa for their financial support; and their assistance during my study;

— My wife, Yvonne for her support during my Ph.D. study. Thank you for your unconditional love;

— My friend, Neels, his wife Villera and his family. For all your friendship, the good times on the golf course with you and Joos and all the funny jokes through the years, I thank you;

— My new family, the Willemse family for their support and for their friendship;

— All the friends I was privileged to have during my time in Potchefstroom, Jaco and Anel; Derik, Dawie, Frikkie, Hein and Kappie; Louis, Herman, Flip and Neil. Thank you for all the memories. You all made the time a joyful time in my live I will never forget;

— Profs. Breet (Ernst), Du Toit, Vosloo, Pienaar and Drs. Lachman, Read, Van Zyl and Van Sittert from the North-West University in Potchefstroom for your generous assistance whenever I needed it.

The financial assistance of the Innovation Fund (IF), South Africa, and the South African Nuclear Energy Corporation (Necsa), is hereby acknowledged.